UNIVERSITY
OF TASMANIA

Metal Catalysed Acetylene Oligomerisation

By

Samuel Stefan Karpiniec, BSc (Hons)

A thesis submitted in fulfilment of the requirements for the degree of

Doctor of Philosophy

School of Chemistry, University of Tasmania, September 2010

This thesis contains no material which has been accepted for the award of any other degree or diploma in any University, and contains no copy or paraphrase of material previously presented by another person, except where due reference is made in the text.

Samuel Stefan Karpiniec

September 2010

Acknowledgements

First and foremost, I would like to thank my primary supervisor Dr Dave McGuinness for inviting me to explore the realms of polymerisation catalysis. Dave has been a patient, helpful and extremely knowledgeable supervisor throughout this project. He has helped me to broaden my understanding of this area of chemistry, and to develop my research skills, both theoretical and practical. I would like to thank Dr Jim Patel, from CSIRO Australia, for his encouragement and helpful advice throughout the project. I am most grateful to Dr George Britovsek from Imperial College London for his friendly and enthusiastic supervision and support during my research visit in late 2008. I am especially grateful to A/Prof Noel Davies of the CSL for his help in product identification, and his remarkable knowledge of chromatographic techniques. Other members of the CSL have been of great help in analysis, and I am grateful to them all. I thank Prof Brian Yates for his help and advice regarding computational studies during this time. I thank Dr Michael Gardiner for his work acquiring crystal structures with the help of the Australian Synchrotron. I thank all the transient members of Lab 308 for their friendship and comradeship throughout this time. Likewise, I thank all the synthetic and computational group members, both students and academics, for their helpful discussions and comments.

I am grateful to the University of Tasmania, the School of Chemistry at UTAS, the Australian Research Council, CSIRO Australia and Imperial College London for support, both financially and otherwise.

Finally, I thank my family and friends for being there and surviving my curiosities, particularly throughout the last three years. I will always be here for you.

Abstract

The oligomerisation of acetylene by metal catalysts has been investigated as a potential route to liquid products, in the context of Gas-to-Liquid generation of petrochemicals. The catalysts trialled are known for their high activities in the polymerisation and oligomerisation of ethylene. Group III, IV and V metallocenes Cp_2MCl_n (M = Sc, Y, n = 1; M = Ti, Zr, Hf, V, n = 2), $Cp^*_2YCl{\cdot}THF$ and $[Cp^*_2CeCl]_n$ were activated with a range of alkyl aluminium cocatalysts, MAO and $AlEt_xCl_{3-x}$ (x = 2,3), and exposed to acetylene. Diimine complexes of nickel and palladium were also trialled, as were a small range of chromium complexes, in the presence of MAO. Activities were extremely low for all of these complexes, except in the presence of $AlEt_3$, where some light oligomers were produced (C_4, C_6). Further studies showed that growth occurred at $AlEt_3$ itself, and that the transition metals were ineffective. Elevated temperatures and extended run times produced a complex range of oligomeric and polymeric products, some of which were identified with the use of GC-FID and GC-MS. Oligomer growth is slow, and branching is introduced at an early stage; several proposals as to the mechanism of growth were suggested. The use of hydrogen gas and high metallocene concentrations failed to provide effective chain transfer activity. This system was explored theoretically using DFT methods, which showed that dimeric aluminium species impede product growth beyond the first insertion; crystallographic evidence also supported this claim. The use of $AlEtCl_2$ as an activator led to the copolymerisation of acetylene and aromatic solvents, and the nature of this process and the formed polymer were investigated in more detail. Bis(imino)pyridineiron(II) catalysts were trialled with acetylene, displaying high initial activity but quick deactivation. The catalyst containing

2,6-diisopropylphenyl substitution produces polyacetylene, as well as oligomers in the presence of the chain transfer agent $ZnEt_2$. The oligomer array is complex and was investigated by GC-FID and GC-MS; a mechanism is proposed for the formation of identified compounds. The use of more $ZnEt_2$ generates a higher proportion of oligomer, but slows catalyst activity. Catalyst deactivation was investigated by SEM and ICP-MS, and found to be due to encapsulation within the insoluble polyacetylene. The catalyst was not able to effective co-polymerise acetylene and ethylene. The *ortho*-tolyl substituted catalyst primarily forms benzene from acetylene (cyclotrimer). Deuterium labelling studies suggest cyclotrimerisation via a metallocyclic mechanism, which is interrupted in the presence of the $ZnEt_2$. Hydrogen was not effective as a chain transfer agent for the iron catalysts.

Table of Contents

Abbreviations

Ar	Aryl
Barg	Bar gauge of pressure
Bu	Butyl
COD	1,5-cyclooctadiene
Cp	Cyclopentadienyl
Cp^*	Pentamethylcyclopentadienyl
DCM	Dichloromethane
DFT	Density Functional Theory
DME	Dimethoxyethane
DMF	Dimethylformamide
DMSO	Dimethylsulfoxide
Et	Ethyl
GC	Gas Chromatography
GC-MS	Gas Chromatography-Mass Spectrometry
GTL	Gas-to-Liquid
ICP-MS	Inductively Coupled Plasma Mass Spectrometry
Me	Methyl
MS	Mass Spectrometry
NMR	Nuclear Magnetic Resonance
PA	Polyacetylene
PE	Polyethylene
Ph	Phenyl
PPA	Poly(phenylacetylene)
Pr	Propyl
SEM	Scanning Electon Microscopy
THF	Tetrahydrofuran
TMEDA	Tetramethylethylenediamine
TOF	Turn-over Frequency
TON	Turn-over Number

Chapter 1 Introduction

1.1 Acetylene and the Generation of Synfuels

Given our current high dependence on petroleum based fuels, there is an ever increasing need to make more effective use of available feedstocks. With the finite nature of crude oil reserves in the spotlight, alternatives such as natural gas are becoming more prominent as fuel sources. Hence, methods of effectively utilising natural gas are attracting much interest. Technologies such as the Fischer-Tropsch process have existed for many years, and form the basis of new large scale gas-to-liquid (GTL) synthetic fuel projects.[1] The Fischer-Tropsch process is able to utilise natural gas for the generation of petrochemical products via syngas (CO/H_2), leading to the production of a range of products including naphtha, diesel and waxes (Scheme 1-1). In this case the GTL process consists of two main steps: reforming (the reaction between O_2, H_2O, CO_2 and CH_4 to yield syngas) and the Fischer-Tropsch synthesis (reaction of syngas over Fe or Co catalysts).

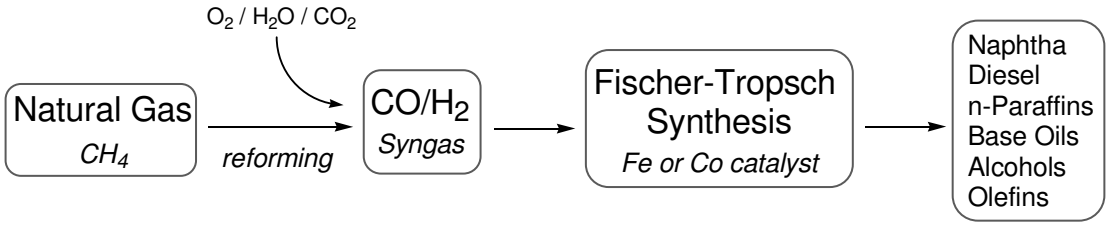

Scheme 1-1 Petrochemical products via Fischer-Tropsch Synthesis

The synthetic fuels produced from this process are advantageous in that they contain fewer impurities, such as sulphur and aromatics, than those refined from oil, and are thus cleaner burning. There are drawbacks, however, such as the large amount of CO_2 released in the reforming process, while the large plant footprint and capital costs associated with syngas production can also be prohibitive.

An alternative GTL process, patented by Hall and co-workers,[2,3] relies on the high-temperature pyrolysis of methane to produce acetylene gas and dihydrogen (Equation 1.1).

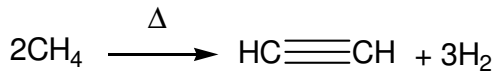

$$2CH_4 \xrightarrow{\Delta} HC{\equiv}CH + 3H_2 \qquad (1\text{-}1)$$

A closer look at this work reveals that acetylene was typically converted to ethylene by partial hydrogenation, and the ethylene then oligomerised to liquid products; little detail is given in these reports on the specific nature of the catalysts employed. Excess dihydrogen may be burned to help heat the system, or used for downstream product hydrogenation. A potential advantage of this system is that it can be performed on a small footprint, potentially making deployment to isolated natural gas reserves more feasible.[3] An alternative to hydrogenation and ethylene oligomerisation is the direct conversion of acetylene to liquid products. As such, an efficient and selective process for the oligomerisation of acetylene to fuel-length oligomers is of much interest. Herein, the development of homogeneous catalysts for this transformation is investigated.

There have been some reports of acetylene oligomerisation using heterogeneous catalyst systems. The reaction of an acetylene/methane stream over ZSM-5 zeolite catalysts loaded with nickel, platinum or palladium led to the formation of a large amount of linear and aromatic product. Palladium gave the largest proportion of higher oligomers, with 80% of C_5-C_8+ product.[4] Trimm and co-workers have recently reported on the linear oligomerisation of an acetylene/hydrogen mixture using Ni/ZSM5-Al_2O_3,[5] which gave a ~40% yield of C_4-C_{10} product. The use of Ni/SiO_2 catalysts by the same authors, [6] followed by downstream hydrogenation over Pt/SiO_2, allowed for the identification of a range of linear and branched oligomers up

to C_{10}. The majority of isolated product was in the C_2-C_6 region.

These recent contributions highlight the role that acetylene might play in the future production of hydrocarbon fuels, and that research in this area continues to be actively pursued. Against this backdrop, the current research project is focussed on the oligomerisation of acetylene to fuel-range liquid products (~C_4-C_{20}) using metal-based homogeneous catalysts, and fundamental investigations into the function of such catalysts.

1.2 A Brief History of Acetylene

As a prelude, it is useful to first touch on the nature of the monomer. The discovery of acetylene occurred almost 200 years ago. The gas was first identified by Edmund Davy in 1836, during his attempts to isolate potassium metal. By exposing potassium carbonate to very high temperatures in the presence of carbon, Davy produced a black solid (potassium acetylide, K_2C_2), which released acetylene on contact with water. Davy suggested that the gas might be useful for lighting, owing to the brightness with which it burned in air, but nothing was to come of this proposal for some years.[7] In 1860, Marcelin Berthelot, who in fact coined the term "acetylene," produced the gas by passing simple organic vapours through a red hot pipe. Later, in 1862, he produced acetylene by passing hydrogen gas through the poles of a carbon arc lamp.[8] Friedrich Wöhler discovered a method for preparing calcium carbide in 1862, by heating an alloy of zinc and calcium in the presence of carbon. He found that the hydrolysis of calcium carbide produced acetylene, much like the original observation of Davy (Equation 1-2).[9]

$$CaC_2 + 2H_2O \longrightarrow Ca(OH)_2 + HC{\equiv}CH \qquad (1\text{-}2)$$

The production of calcium carbide from lime and carbon, and from this acetylene, was reported by Thomas Wilson in 1889. Wilson is credited with the 1892 invention of large-scale acetylene production, based on this chemistry. The gas was widely used in lighting from the late 19th to early 20th centuries. Acetylene lamps were found in houses, street lamps, in mining sites and on cars, amongst numerous other places, needing only calcium carbide and water to function. Their use was gradually superseded by electric powered lights by around 1920.[10] Acetylene has been used as a reagent for metalwork since these early times, and is widely used today for applications such as the welding, cutting, coating and heat treating of metals. This is due to the extremely high temperatures (up to 3200 °C) attainable by the combustion of acetylene in the presence of oxygen.

Acetylene featured as an important feedstock for the chemical industry during the early 20th century, and a wide variety of chemistry was developed for the conversion of acetylene into important commodity chemicals. Generation from calcium carbide remained the basis of commercial production for many years. After 1940, other methods for the production of acetylene began to come into play, such as the thermal cracking, or pyrolysis, of methane and other hydrocarbons. This move toward the petrochemical-based production of commodity chemicals, however, has seen a large decrease in the use of acetylene as a feedstock, particularly in the early 1970s. The development of processes such as steam cracking have allowed for the large scale production of oil-derived olefins such as ethylene, propylene and butadiene. These more easily handled monomers have all but replaced acetylene in the production of many important products such as vinyl acetate and vinyl chloride. [11,12]

1.3 Acetylene Reactivity

Acetylene is the simplest hydrocarbon featuring a C≡C triple bond, and is an extremely reactive compound. Its highly unsaturated character, as well as high positive energy of formation (+227 kJ/mol at 298K), makes acetylene extremely reactive toward a number of chemical elements and compounds. Even in its pure form, acetylene needs to be handled with extreme caution. At pressures above 1.5 bar gauge (barg), acetylene is known to undergo spontaneous decomposition, leading to violent explosions. Liquid acetylene is also known to detonate (b.p. -84 °C), thus low temperature handling is not a recommended exercise. Acetylene can be transported in cylinders under pressure, dissolved in either acetone or dimethylformamide; the solvent is dispersed in a porous material that helps prevent any decomposition. Specialised pipelines can be used for the transport of acetylene under pressure, but this must necessarily be an expensive undertaking, due to the required safety mechanisms.[11]

A variety of chemical processes are possible due to the properties of acetylene. As the C≡C triple bond is very electron rich, acetylene readily forms π-complexes with a number of metal compounds. The acetylene C-H proton is reasonably acidic (pK_a = 25), which enables the formation of metal-acetylides, and participation in polymerisation processes such as chain transfer and termination (see Section 1.4.4).[13]

The reactions of acetylene in the presence of metal compounds are of particular relevance to the current research. There are a number of interesting processes of this type that have held industrially significant roles in the last century. Nieuwland reported on the reaction of acetylene with copper(I) chloride, in saturated ammonium chloride, to form vinylacetylene (Equation 1-3). Divinylacetylene and a tetramer

were also formed, thought to be further reaction products of vinylacetylene.[14]

(1-3)

This chemistry can be dangerous, as the reaction proceeds via copper acetylide intermediates, which are high explosives; silver acetylides are similarly dangerous. However, the method was significant to industry for many years, as vinylacetylene could be treated with hydrochloric acid to produce chloroprene (2-chloro-1,3-butadiene), and this polymerised to form Neoprene rubber (polychloroprene).[15]

1.3.1 Reppe Chemistry

A very important name in the field of acetylene chemistry is that of Walter Reppe. Driven by a shortage of raw materials such as rubber and oil in Germany during World War II, Reppe and co-workers found new approaches for generating needed products. Based on the calcium carbide process, Reppe used high pressure reactions of acetylene in the presence of heavy metal acetylides (particularly copper acetylides) or metal carbonyls to develop a number of important chemicals. He continued to work for BASF Ludwigshafen for many years after the war had ended, and made numerous contributions to this area.[12]

The reactions known as Reppe chemistry can be broadly grouped into four types: vinylation, ethynylation, carbonylation and cyclic/linear polymerisation; the first three are summarised in Scheme 1-2. Vinylation products include such compounds as vinyl chloride, acrylonitrile, acetaldehyde and vinyl acetate, and many other vinyl compounds that are important monomers for polymerisation (for example of vinyl

chloride to polyvinylchloride).[11] Ethynylation can produce products like propargyl alcohol and 1,4-butynediol, which are important starting materials in the manufacture of a range of polymers. The hydrogenation of 1,4-butynediol produces 1,4-butanediol, which is widely used in industry for the production of tetrahydrofuran and γ-butyrolactone. 1,4-butanediol is also used in the manufacture of the thermoplastic polybutylene terephthalate, polyurethanes, Spandex and plasticisers. Carbonylation proceeds by the metal-carbonyl catalysed addition of carbon monoxide and water to acetylene, forming carbonyl-containing compounds. Examples developed by Reppe are acrylic acid, hydroquinone and bifurandione, using nickel, iron and cobalt carbonyls respectively.[11,12,16]

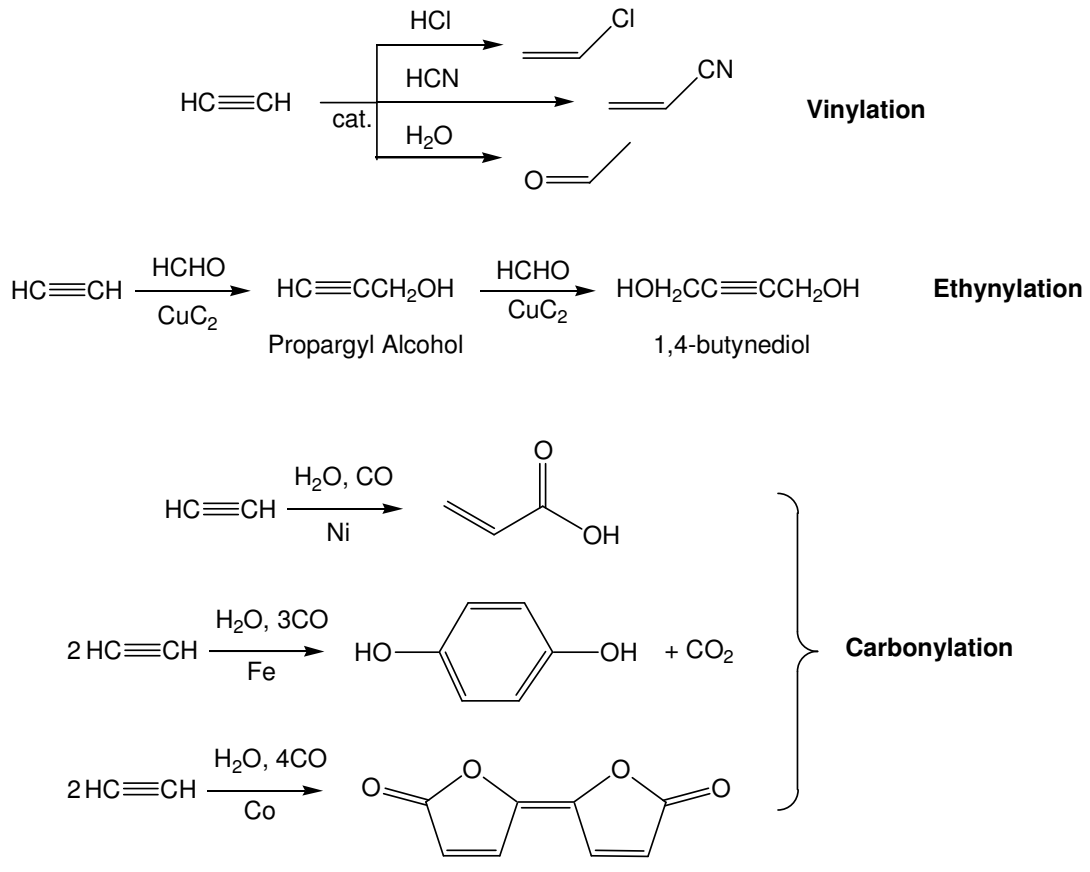

Scheme 1-2 Reppe Chemistry

The cyclisations of acetylene reported by Reppe are of particular interest, as they are a seminal work in the field of metal-catalysed acetylene oligomerisation

(Scheme 1-3). The reaction of acetylene under pressure, in the presence of a $Ni(CN)_2$ catalyst, produced primarily 1,3,5,7-cyclooctatetraene, amongst side-products including benzene, linear oligomers and a black mass. The use of $Ni(CO)_2(PPh_3)_2$ led primarily to benzene, as well as styrene.[17,18]

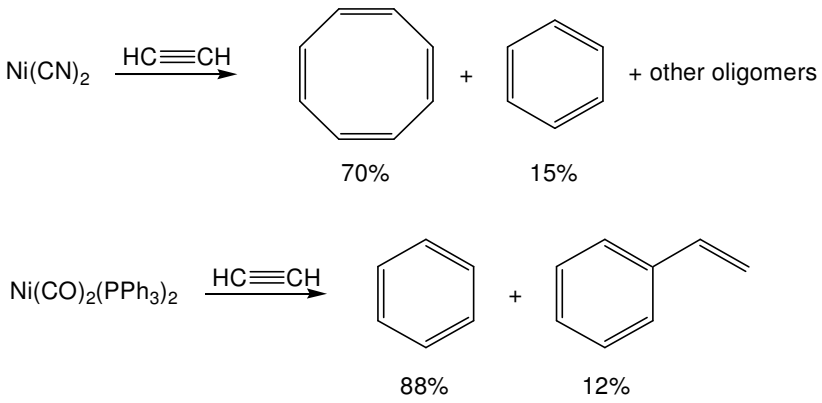

Scheme 1-3 Reppe cyclooligomerisation products

The difference in product output is curious, and there are various explanations. For example, it has been suggested that the products form via a concerted mechanism with the appropriate number of coordinated acetylenes simultaneously cyclising at the nickel centre. The presence of the strong phosphine donors in $Ni(CO)_2(PPh_3)_2$ makes the coordination of four acetylenes difficult, thus cyclotrimerisation is favoured in this case.[19] Overall, the work of Reppe, and particularly the cyclic oligomerisations, highlighted the possibility of using metal salts as catalysts to produce many products from acetylene, and indeed many more possibilities would follow.

1.3.2 Acetylene Polymerisation

Further to the discovery of low-pressure ethylene polymerisation by Ziegler, Natta first reported on the production of polyacetylene (PA) in 1958.[20] Using a $Ti(OPr)_4/AlEt_3$ system, acetylene was polymerised to a brittle and air-sensitive solid

– far from the workable, white product of ethylene polymerisation – which was disregarded for some years. Later, Shirakawa developed an improved synthesis of PA films.[21] Importantly, these materials were found to have the fascinating property of high electrical conductivity. When doped with oxidative reagents such as iodine and AsF_5, PA can achieve conductivity of 10^5 Ω^{-1} cm^{-1}, which is comparable to that of metallic platinum or lead; reductive dopants such as Na/NH_3 can also be effective in this process.[22,23] The polyconjugated backbone of the material gives way to this property, whereby a charge induced by the dopant is able to conduct current by movement along the polyene chain.

These discoveries spawned an interest in conjugated polymers, which are used in applications such as light-emitting diodes, and gas and chiral separation membranes. A drawback of polyacetylene is that, as well as being sensitive to air, it is extremely insoluble and cannot be melted, which makes analysis difficult by common techniques. However, research continues toward the preparation of more tractable materials. Shirakawa received the Nobel Prize in Chemistry in 2000 for his contributions to this discovery.[24]

1.4 Pathways to the Oligomerisation and Polymerisation of Acetylene

Compounds such as polyacetylene, benzene, and numerous commodity chemicals represent the wide range of products that can be derived from acetylene. Yet, while there are many established pathways, there remains scope for the development of acetylene-based chemistry. There appear to be relatively few accounts of systems for the sole production of linear oligomers of acetylene, which is relevant to the current research interest of generating synthetic fuels. Thus, it is prudent to document some of the known mechanisms for the oligomerisation and polymerisation of acetylene

(and its substituted derivates). The compounds that facilitate these processes are also important, and particular note will be made of those based on transition metals.

1.4.1 Ionic and Radical Pathways

There are several distinct ways in which alkynes can be polymerised, depending on the nature of the catalyst and the alkyne itself – this is evident in the variety of products available. Alkynes can polymerise by cationic, anionic and radical mechanisms (Scheme 1-4). Often this occurs in the presence of a chemical initiator, although thermal, radiation and photo initiated polymerisations have been observed for certain alkynes.[13,25]

Cationic polymerisation can be initiated by Lewis Acids such as SbF_5, H_2SO_4, $TiCl_4$ and $SnCl_4$, and occurs for alkynes such as phenylacetylene, 1-pentyne and 9-ethynylnapthalene. Anionic polymerisation occurs in the presence of nucleophiles; activated electrophilic alkynes such as acetylene dicarboxcylic acid and cyanoacetylenes are active even in the presence of weak nucleophiles. Alkali metals can be used to initiate anionic polymerisation. It has been noted that these mechanisms do not typically lead to high molecular weight polyacetylenes, and this is attributed to radical delocalisation over the conjugated polymer chain which interrupts propagation.[25] A similar process occurs in the ionic systems. In the anionic system, an electron transfer from the active centre to the polymer chain results in a delocalised radical anion and thus deactivation. The same occurs in cationic systems, but electron transfer is from the conjugated chain to the active site, forming a radical cation.

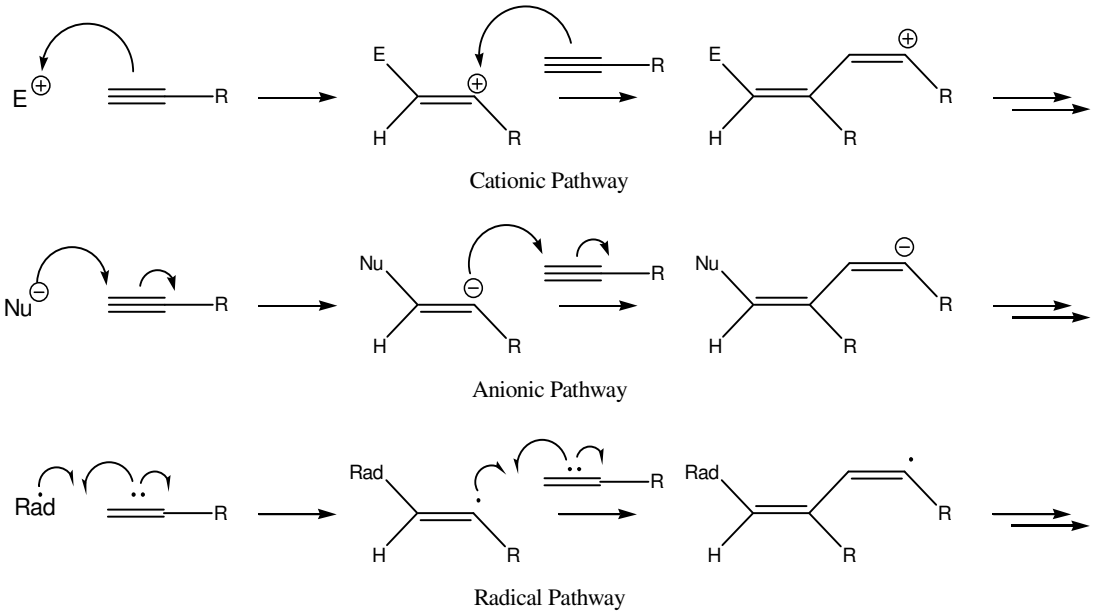

Scheme 1-4. Ionic and Radical Polymerisation

1.4.2 Carbene Mechanism

A carbene mediated process has been reported to occur for certain classes of catalyst, via metallacyclobutenes. Katz[26] reported on alkyne polymerisation by tungsten complexes (Ph)(R)C=W(CO)$_5$ (R = Ph, OMe). The carbene mechanism invoked (Scheme 1-5) is analogous to that for olefin metathesis, and involves four centre metallacyclobutene intermediates. These catalysts were active for the polymerisation of phenylacetylene, *n*- and *t*-butylacetylenes and propyne.

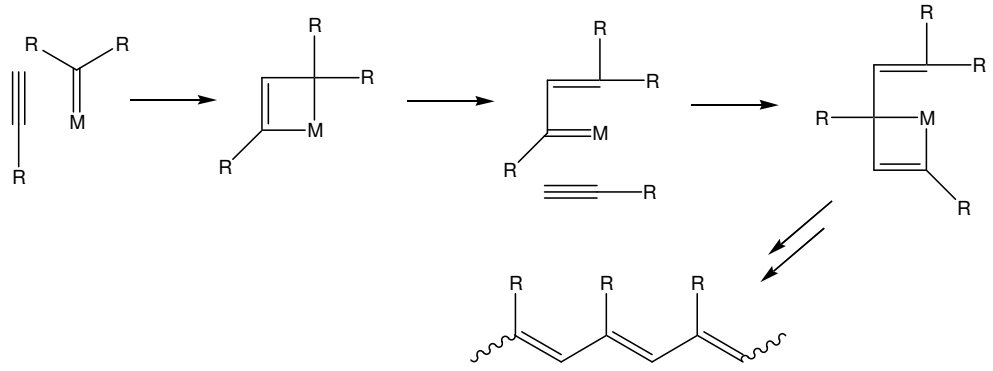

Scheme 1-5. Carbene mechanism for polymerisation of alkynes

The polymerisation of acetylene by the vinylcarbene complex $Cp_2Ti=CH-CH=CH_2Ph$ was documented by Takeda.[27] This was presumed to follow the carbene pathway, forming polyacetylene films. Polymerisation was also achieved using the complex $Cp_2Ti[P(OEt_3)]_2$, for which carbene intermediates were also proposed. Related to this, Rosenthal discussed the use of titanocene alkyne complexes, such as $[Cp_2Ti(Me_3SiC{\equiv}CSiMe_3)]$, as precatalysts.[28] It was proposed that the active species was a low valency "Cp_2Ti" species, formed via dissociation of the substituted acetylene. Subsequent acetylene coordination followed by a hydride shift and rearrangement could lead to a vinylidene complex "$Cp_2Ti=C=CH_2$" that was active for polymerisation via a carbene type pathway. Other carbene complexes have been found active for acetylene polymerisation by this mechanism, for example the Schrock carbene $W=CH\text{-}t\text{Bu}(N\text{-}2,6\text{-}C_6H_3\text{-}i\text{Pr}_2)(O\text{-}t\text{Bu})_2$.[29]

1.4.3 Metallocyclic Growth

Another well known pathway to the formation of acetylene oligomers (particularly cyclic) is via metallocyclic growth. The premise is that two coordinated acetylenes oxidatively add to a metal centre, forming a metallacyclopentadiene. Further acetylene addition grows the metallocycle, which can reductively eliminate the oligomeric product: the simplest case being benzene (Scheme 1-6).[30] This pathway also allows for the formation of cyclooctatetranene and higher cyclic products, via successive acetylene additions and metallocycle growth, prior to elimination. A similar pathway was proposed by Reppe to account for the formation of cyclooctatetraene in his initial observation.[17]

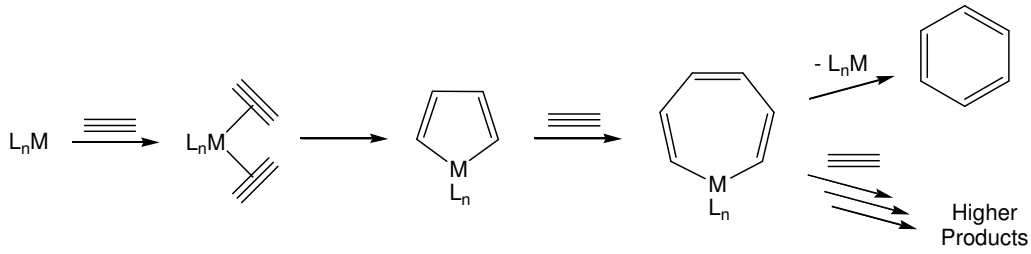

Scheme 1-6. Oligomerisation via Metallocyclic Growth

The nickel phosphine carbonyl $Ni(CO)_2(PPh_3)_2$ used by Reppe was investigated further by Meriwether,[31] who applied it to the oligomerisation of substituted acetylenes RC≡CH. For various R groups, esters, ethers and ketones were the most active, forming primarily cyclotrimer (1,2,4- and 1,3,5-substituted). Aryl, vinyl, alcoholic and higher alkyl (> C_3) acetylenes tended to form primarily cyclotrimers, with some traces of linear oligomer detected, while lower alkyl acetylenes (C_1-C_3) generated a larger amount of linear product. The steric bulk of the substituent was important, whereby bulky cyclohexylacetylene formed only a linear dimer, and *t*-butylacetylene was unreactive. Meriwether suggested the possibility of metallocyclic growth in these studies, alongside a linear growth mechanism (see Section 1.4.4), as the route to cyclotrimers.[32] He proposed metal-cyclobutadiene complexes as intermediates in the formation of metallacyclopentadienes – the metallocycle being thought to form via the cyclobutadiene complex – which then led to benzene and higher cyclics (Scheme1-7(a)).[19,25] Later studies are at odds with this suggested pathway. The isolation of cobalt-cyclobutadiene complexes from the $CpCo(CO)_2$ catalysed cyclotrimerisation of acetylenes has been reported.[33] These complexes were found to be inert toward further catalysis, which rather supports metallocyclic growth as the functional mechanism, with the cyclobutadiene complexes simply a byproduct of this reaction. A more likely pathway is thus shown Scheme 1-7(b).[19]

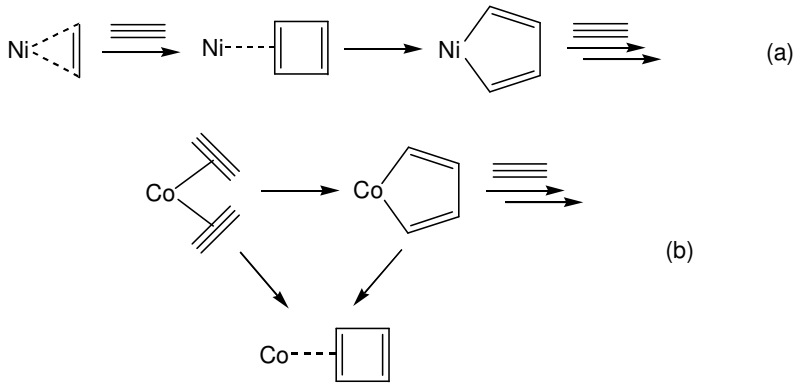

Scheme 1-7. Cyclobutenes or Metallocyclopentadienes?

A number of reports by Farona et al. discuss the use of early transition-metal metallocenes for the polymerisation of alkynes by metallocyclic pathways.[34-36] Several group IV metallocenes were investigated, in combination with ethylaluminiumdichloride, and found to be active toward both terminal and internal alkynes. Titanocene dichloride (Cp_2TiCl_2), in the presence of $EtAlCl_2$, reacts with phenylacetylene to produce both aromatic products (1,2,4- and 1,3,5- trisubstituted benzenes) and poly(phenylacetylene) (PPA).[34] At 80 ºC cyclotrimers were the sole products, whereas PPA comprised 70% of the total product at ambient temperature. Reaction at 12 ºC produced PPA and ladder complexes, which were found to be intermediates in the formation of PPA. The structure of fused cyclobutane rings in the ladder intermediates suggested that polymer growth might occur via [2+2] cycloadditions, and could occur via metal-cyclobutadiene complexes. Isomerisation could then lead to a polyconjugated structure (Scheme 1-8).[25]

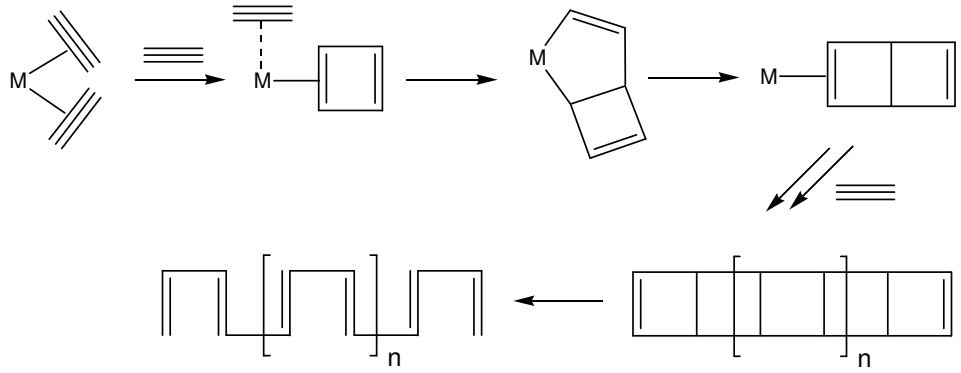

Scheme 1-8. Polymerisation via Ladder Intermediates
(Phenyl groups have been omitted for clarity)

The zirconocene based system $Cp_2ZrCl_2/EtAlCl_2$ was investigated by Farona and could polymerise phenylacetylene, as well as 1-hexyne, methylphenylacetylene and diphenylacetylene.[35] Spectroscopic and NMR analysis of the polymers formed suggested linear polyconjugation, in contrast to the ladder intermediates formed with titanocene. The use of 2-butyne produced a 1,2,3,4-tetramethylzirconacyclopentadiene complex (Scheme 1-9(a)), thereby providing evidence for a metallocyclic mechanism. Further mechanistic evidence was provided through the reactivity of a related zirconacyclopentadiene. In absence of the aluminium activator, this reacts with excess phenylacetylene to give PPA, or stoichiometrically to give the zirconacycloheptatriene (Scheme 1-9(b)). Successive phenylacetylene insertions into the zirconacycloheptatriene generate larger metallocycles which, followed by elimination, yield the final products. In later studies of both the titanocene and zirconocene systems, a variety of different sized metallocycles were isolated – rings with as many as 17 members – resulting from reactions with substituted acetylenes.[36] The reaction of alkyl-substituted metallocyclopentadienes with phenylacetylene led to the identification of cooligomers incorporating both alkyl and phenyl substituents: this confirmed the role of the metallocycle in oligomer growth. Trials performed using either the dicarbonyl

$Cp_2M(CO)_2$, or Cp_2MCl_2 reduced in the presence of magnesium metal, generated the same products as reactions using the $Cp_2MCl_2/EtAlCl_2$ system. This suggested that a low valency "Cp_2M" species was an intermediate in the catalytic cycle.

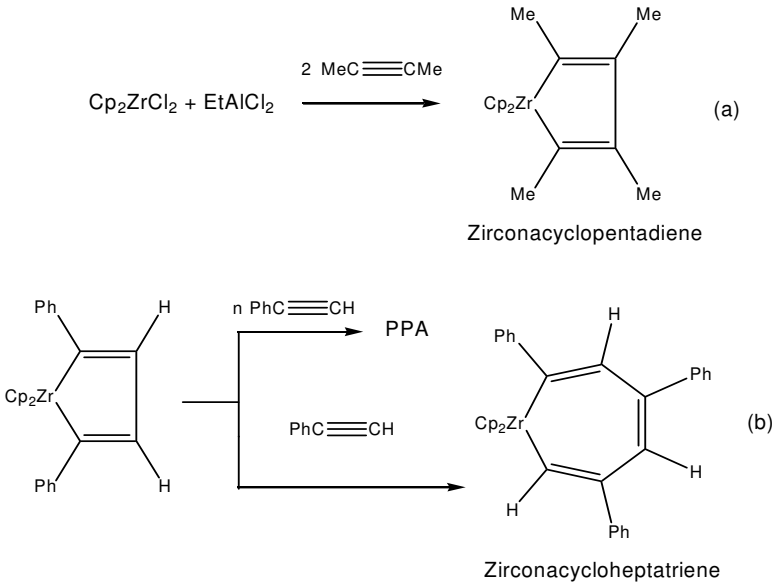

Scheme 1-9. Zirconacycles

There have been theoretical studies examining metallocyclic pathways to acetylene cyclotrimerisation in rhodium-based systems. Using DFT calculations, the authors examined cyclisation mechanisms via half-sandwich complexes "CpRh",[37] and $RhCl(PPh_3)_3$ (Wilkinson's Catalyst),[38] looking for the lowest energy pathway to arene formation. In the half-sandwich case, the active species "CpRh" is formed via dissociation of labile ligands from $CpRhL_2$ (eg L = CO, C_2H_4; L_2 = COD). In both reports, the already discussed mechanism of acetylene coordination followed by oxidative addition forms a metallacyclopentadiene (see Schemes 1-6, 1-7(b)). From here, a third acetylene unit can coordinate to rhodium, and might then proceed via several routes to cyclotrimerisation. One proposed option was a [4+2] cycloaddition, leading to an η^4-coordinated benzene, which was eliminated along with further acetylene coordination and recommencement of the cycle. Alternatively, acetylene

insertion could lead to an expanded metallacycloheptatriene, or by [2+2] cycloaddition to a metallabicyclo[3.2.0]heptatriene; either of these products would then reductively eliminate benzene (Scheme 1-10). The studies both found that the [4+2] cycloaddition was a barrierless pathway, and thus the lowest energy option. The expanded metallocycle and [2+2] cycloaddition both had much higher energy barriers to the same end point. As pointed out,[37] this is similar to findings for an analogous cobalt system,[39] however the cyclisation of acetylene using the ruthenium system CpRuCl was shown to involve a metallacycloheptatriene intermediate.[40]

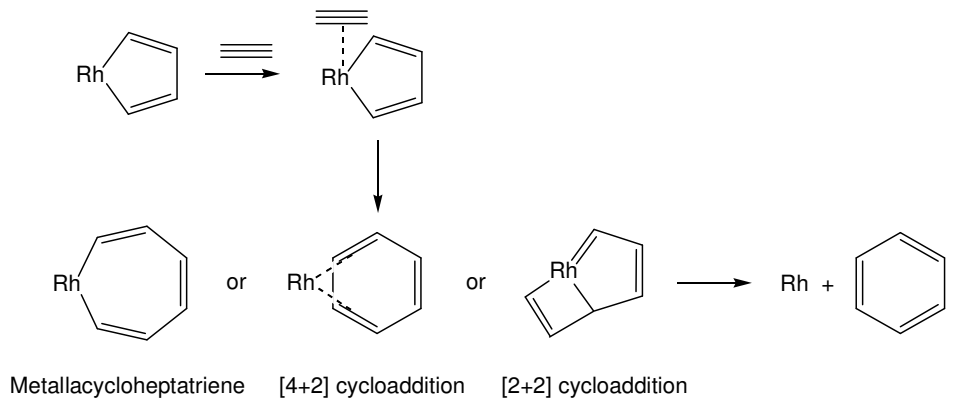

Scheme 1-10. Formation of benzene in rhodium systems

A number of other studies have reported on the formation of cyclic oligomers, which may be assumed to follow a metallocyclic route. Alkyne oligomerisation was reviewed by Keim,[30] who discussed a variety of metal carbonyls and other metal salts. The use of $Ni(PCl_3)_4$ forms tetrasubstituted cyclooctatetraenes from $HC{\equiv}CCO_2Et$, while $[NiX(\eta^3\text{-}C_3H_5)]_2$ (X = Cl, I) in the presence of HC≡CBu forms 1,3,5- and 1,2,4-tributylbenzenes from the chloride and iodide complexes respectively. The cyclotrimerisation of diphenylacetylene to hexaphenylbenzene is effected by $Co_4(CO)_{12}$ and $Rh_4(CO)_{12}$, while $PdCl_2(PhCN)_2$ forms hexasubstituted benzenes from methylphenylacetylene.

Higashimura investigated the reaction of Group V and VI metal halides with 1-hexyne[41] and phenylacetylene.[42] For 1-hexyne, selective cyclotrimerisation to 1,2,4- and 1,3,5- tributylbenzenes was achieved using $NbCl_5$ and $TaCl_5$; the niobium salt produced 70-80% of the 1,2,4- isomer, while tantalum yielded 55-70%. Phenylacetylene was reacted with NbX_5 (X = Br, Cl, F). The chlorides led solely to 1,2,4- and 1,3,5-triphenylbenzenes, though the bromides were less selective toward formation of the 1,2,4- isomer. The fluoride salts produced cyclotrimers but also linear oligomers – in fact no cyclotrimer was formed when TaF_5 was employed, using CCl_4 or dichloromethane as solvent.

Yur'eva[43] discussed several classes of transition metal catalysts, including di(cyclooctatetraene)iron for cyclotrimerisation of acetylene, and (1,5-cyclooctadiene)nickel halides for cyclotrimersation and polymerisation. The $TiCl_4/AlR_3$ Ziegler-Natta type systems can both cyclotrimerise and polymerise acetylenes, depending on the Al:Ti ratio employed; these systems can be applied to mono- and disubstituted acetylenes to produce more exotic cyclic products.

1.4.4 Growth via Linear Migratory Insertion

Transition metal assisted mechanisms are of particular relevance to the current research, especially those leading to linear products. A famous mechanism in olefin polymerisation is that proposed by Cossee in his investigations of Ziegler-Natta catalysts (Equation 1-4).[44] This mechanism involves the migration of a metal-alkyl group to a coordinated olefin, propagating chain growth. A number of reports of acetylene catalysis have been documented that are compatible with Cossee's original proposal.

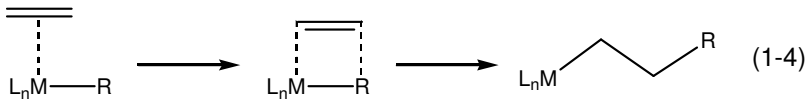

(1-4)

Daniels explored the use of Group IX and X transition metal phosphines $M(PPh_3)_2X_n$ (M = Ni, Pd, Co; X = Cl, Br, I).[45] Only the nickel catalysts were found to be active toward acetylenes, and of these the bromide and iodide complexes much more active than the chlorides. For $Ni(PPh_3)_2Br_2$, acetylene and phenylacetylene reacted to yield the respective polymers, 1-hexyne formed primarily cyclic and linear trimers, while propynol gave poly(propynol) and a large amount of cyclotrimer. Mechanistically, linear polymerisation was thought to proceed via a dissociative mechanism, with a relatively labile phosphine group making way for an incoming acetylene which could then insert (Scheme 1-11). Successive insertions could produce polymeric products, which were thought to possess nickel and bromine end groups; it should be noted that insertion into a bromine group seems unlikely in light of other studies (see below). The extent of polymerisation could be largely increased by using 10% THF in ethanol as solvent, rather than neat THF which, given the proposed mechanism, could be attributed to a lower coordinative ability of ethanol compared to THF. The possibility of a 5-coordinate associative mechanism was also not ruled out.

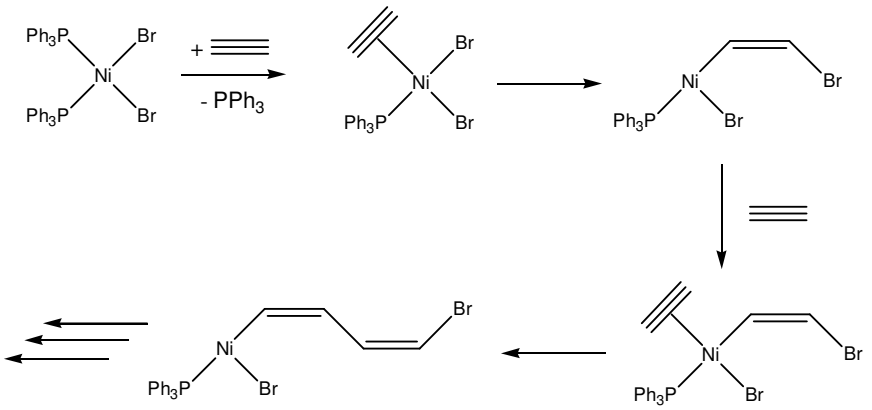

Scheme 1-11. Acetylene polymerisation via $Ni(PPh_3)_2Br_2$

The studies of Meriwether, on Reppe's $Ni(CO)_2(PPh_3)_2$ catalyst, proposed a linear growth mechanism, as mentioned earlier. [32] In this case, the active catalyst was suggested to form by reversible dissociation of the carbonyl groups, and then coordination of acetylene. An initial hydrogen transfer to the metal was thought to occur, forming a metal acetylide that was active toward further coordination and insertion (Scheme 1-12); consecutive insertions then lengthen the polymer chain until termination. It was proposed that chain termination could occur via hydrogen transfer from a coordinated acetylene monomer.

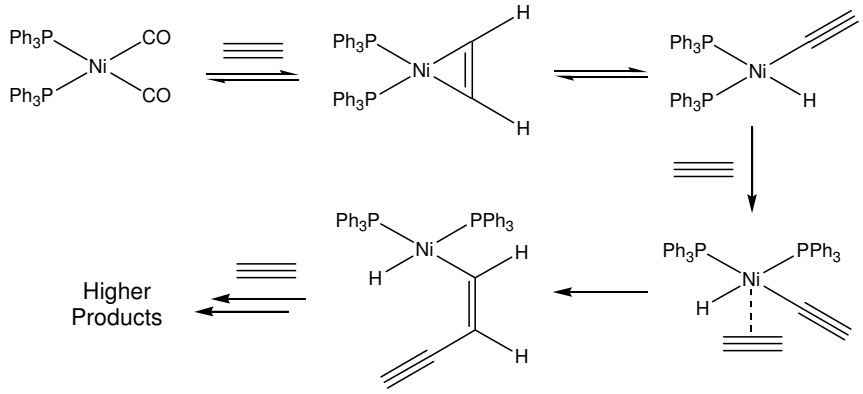

Scheme 1-12. Linear growth at Nickel

This mechanism also has the potential to generate cyclic products. Given a sequence of *cis*-insertions of acetylene into a nickel acetylide, the oligomer could "back-bite", involving a concerted hydrogen transfer and ring closure, releasing benzene and the nickel catalyst (Scheme 1-13).

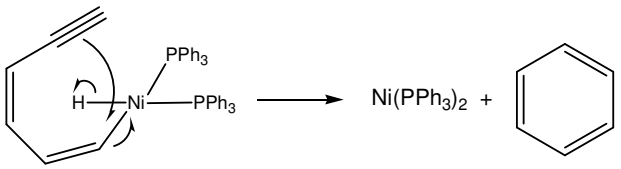

Scheme 1-13. Cyclisation following Linear Insertion

Katz[46] presented an important study aimed at clarifying the mechanism of Ziegler-Natta catalysis of acetylene, given the two options of a Cossee or carbene type mechanism. A mixture of ^{12}C-acetylene and ^{13}C-acetylene (24:1 ratio) was polymerised with $Ti(OBu)_4/AlEt_3$, and NMR techniques were used to measure the distance between the ^{13}C labelled carbon atoms in the polymer. Direct insertion via the Cossee mechanism would result in a double bond between the two labelled atoms, while the carbene mechanism leads to a single bond. This study supported the Cossee-type mechanism.

In targeting short oligomers grown from acetylene, mechanisms of controlling the chain length are extremely important. If there is no mechanism for chain termination or transfer, it may be difficult to avoid the formation of polymers. Sigma-bond metathesis is such a process, relevant to chain control in acetylene chemistry (Scheme 1-14).

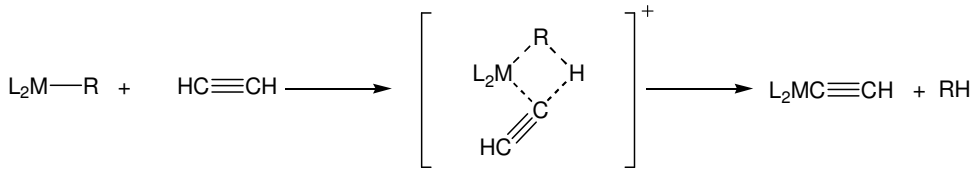

Scheme 1-14. σ-bond metathesis with acetylene

The use of lanthanide and actinide metallocene catalysts for the oligomerisation of alkynes has been explored by a number of groups, for example those of Eisen and Teuben. Eisen has documented the use of actinide metallocenes $Cp^*_2AnMe_2$ ($Cp^* = C_5Me_5$, An = U, Th) which form oligomeric products by reaction with terminal alkynes.[47,48] The initial function of the precatalyst is to allow activation of an alkyne C-H bond, which undergoes σ-bond metathesis with the metal-carbon bond to form an active metal-bis(acetylide). Subsequent insertion of further alkyne

molecules allows for chain growth; this process competes with further σ-bond metathesis, which releases the oligomeric product and regenerates the active metal acetylide (Scheme 1-15).

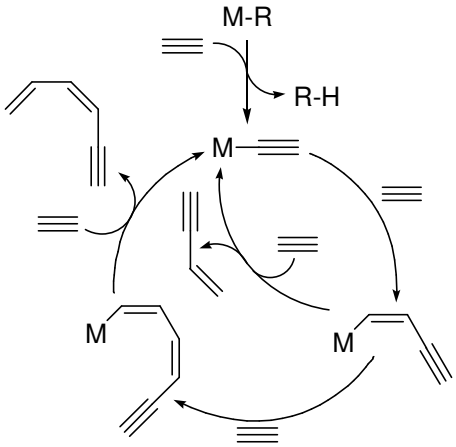

Scheme 1-15. Chain growth and termination via insertion and σ-bond metathesis

The use of various alkynes RC≡CH led to different product distributions. For *t*-BuC≡CH, a head-to-tail dimer was formed almost exclusively, whereas for $Me_3SiC{\equiv}CH$, a majority of head-tail-head trimer was produced (Figure 1-1). Using the trimethylsilyl monomer, Eisen was able to confirm the presence of several key catalytic species from the proposed cycle: the metal acetylide and the metal eneyne resulting from insertion.

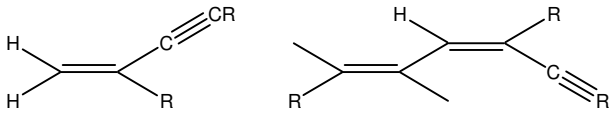

Figure 1-1. Head-tail dimer and Head-tail-head trimer

For R = *n*-Bu, Ph and cyclopentyl, a significant array of tetramers and pentamers was also found, while *i*-PrC≡CH produced a spread of oligomeric products including those with up to 7 monomer units. There was little difference in overall catalytic activity between the thorium and uranium complexes. Turnover numbers (TONs) of 100-400 were reported for the various systems tested, with turnover frequencies

(TOFs) ranging from 1-10 h^{-1}, while the use of different solvents did not have a significant effect on these rates. In terms of oligomer length, the more bulky substituted acetylenes favour dimer formation, while the less hindered substituents tend towards further growth. Mechanistically, a fine balance between the rates of alkyne insertion and σ-bond metathesis was considered to govern the relative amounts of dimer and higher oligomers formed.

Further work by Eisen considered other strategies to control chain length in these systems, by the addition of chain-transfer agents. The addition of primary or secondary amines to the thorium-based system described above allowed for the formation of a thorium-bis(amido) complex that participates in the catalytic cycle.[49] This can undergo σ -bond metathesis with an incoming acetylene to form the active species, then further insertion can occur. The free amine is able to protolytically release the unsaturated oligomer, regenerating the actinide-amide species (Scheme 1-16). This technique allowed for greater control over the oligomerisation process, and more selective production of dimers and trimers over higher oligomers, while substituent bulk on the acetylene and the amine both affected the product stereospecificity. The thorium complex showed TONs of 11-74 (TOFs of 0.15-3.7 h^{-1}), depending on the amine and the acetylene. Uranocene was trialled for all cases discussed in the paper, but did not exhibit the same extent of control as the thorium complex; in many cases no real effect was observed.

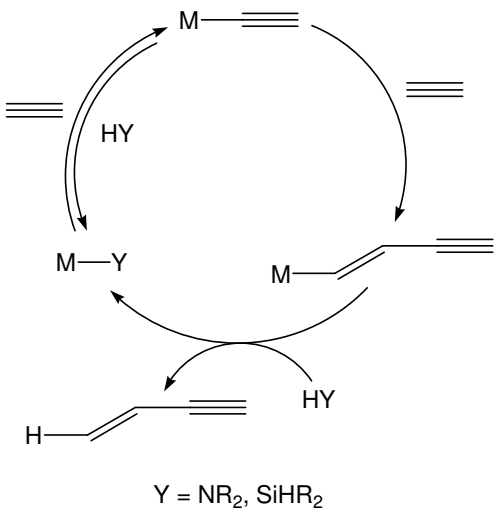

Scheme 1-16. Oligomer control by Protolytic Agents

Use of the secondary silane Et_2SiH_2 was, however, able to aid in the selective dimerisation of acetylenes in the uranocene system.[50] The proposed catalytic mechanism is similar to that for the amine controlled cycle, whereby an actinide-bis(acetylide) will first react with Et_2SiH_2 to form an actinide-acetylide-silyl complex, releasing the free acetylene. Insertion of a second acetylene grows the oligomer, and this product can be released protolytically by a free silane; the release by silane was thought to compete with σ-bond metathesis by a free acetylene. This system was also shown to yield a silylacetylene product ($Et_2HSiC{\equiv}CR$) and an alkene ($H_2C{=}CHR$). This suggested a different stereochemistry of reaction with the incoming silane, inferring an alternate pathway via a uranium hydride. These systems had TONs of 30-42.

Teuben has reported on the use lanthanide metallocenes for the oligomerisation of terminal alkynes.[51] The complexes $Cp_2LnCH(SiMe_3)_2$ (Cp = C_5H_5, Ln = Y, La, Ce) were shown to behave in a similar fashion to the Eisen actinide catalysts, where σ-bond metathesis with the acetylene monomer forms a metal (mono)acetylide which is active toward insertion. Once again, further growth by successive actylene

insertion then competes with chain releasing σ-bond metathesis. The extent and stereoselectivity of oligomerisation in this study was found to depend on the substitution at RC≡CH, as well as the metal in the catalyst. For the substituent R, bulky alkyl groups favoured dimerisation, while smaller groups tended towards higher oligomers; in the case of dimers, head-to-tail species were exclusively formed when less steric hindrance was present. Aryl and trimethylsilyl groups had an effect on chain length and regioselectivity, with a considerable amount of trimer formed as well as dimer. Of the dimer, a large amount of head-head product was identified alongside head-tail; electronic effects were cited as relevant in this case. The use of yttrium tended to favour production of dimers, while lanthanum and cerium showed a greater production of trimers and higher oligomers; all metals showed exothermic reactions in certain cases. The reactions of propyne with the lanthanum and cerium derivatives were exothermic, and showed TONs of 220-370 (TOF 73-123 h^{-1}).

Teuben also described the preparation of bis(trimethylsilyl)benzamidinate yttrium complexes $\{[C_6H_5C(NSiMe_3)_2]_2Y\text{-}\mu\text{-}R\}_2$ (R = H, C≡CH) as an alternative to the metallocene compounds.[52] These were found to be reactive toward terminal alkynes, producing primarily dimeric products. Use of phenyl- or *t*-butylacetylene, effected the formation of exclusively head-tail products, while trimethylsilylacetylene yielded only head-head coupled dimers; this contrasts to the mixtures of products seen for the lanthanide metallocenes. The complex was not active for the oligomerisation of acetylene itself, which notably seems to be the case for the majority of the systems discussed here; substituted acetylenes are typically the monomer of choice.

There do exist, however, examples of linear oligomer production from acetylene. One example is the use of scandium metallocenes $Cp^*_2Sc\text{-}R$ (R = H, alkyl, aryl,

amine), as investigated by Bercaw, which mechanistically behave in a similar fashion to Teuben and Eisen's systems. The active species here is a scandium acetylide, again formed by σ-bond metathesis with acetylene. The complex Cp^*_2Sc-Me was found to undergo this process with acetylene at -78 ºC, although insertion of acetylene was not observed until temperatures above 10 ºC.[53] This system allowed for the production of polyacetylene, as well as a range of linear oligomers identified by vinylic proton NMR signals; full characterisation of these products was not completed. Internal acetylenes did not react as for terminal acetylenes; these were found to react stoichiometrically, preferring insertion into Cp^*_2Sc-R over σ-bond metathesis, and did not form polymeric products.[54]

1.4.5 Other Examples of Alkyne Polymerisation and Oligomerisation

Many other examples of linear growth exist, however in a significant number of these cases the mechanism is not clear. Some of these studies are summarised below, and for each case it is possible to envisage carbene, metallocycle or linear growth mechanisms.

Tsonis and co-workers discussed the reactivity of Group VI metal carbonyls $M(CO)_n$ (M = Cr, Mo, W) toward acetylenes.[55] The use of terminal alkynes produced oligomeric and polymeric products. Molybdenum was found to be the most active metal tested, followed by tungesten then chromium. The activity of $Mo(CO)_6$ was increased in the presence of a Lewis base cocatalyst such as acetonitrile, and found to be optimal at temperatures above 75 ºC. Interestingly, the reaction of 2-heptyne in the presence of $Mo(CO)_6/CH_3CN$ led to the metathesis products butyne and decyne. Polymerisation of phenylacetylene was investigated by Higashimura and coworkers[56] using Group VI metal chlorides (WCl_6, $MoCl_5$). The tungsten salt was more active

than molybdenum chloride, and also produced a higher molecular weight polymer. For tungsten chloride, more polar solvents were found to decrease the extent of polymerisation, while the reaction rate was proportional to the concentrations of catalyst and monomer. The addition of acetic acid lowered both the reaction rate and polymer molecular weight, while the addition of water conversely increased both properties. The addition of $SnPh_4$ as a cocatalyst in the WCl_6 system drastically increased the rate of polymerisation of phenylacetylene to a high molecular weight product.[57] The tin complex was thought to reduce the tungsten centre, producing the active species. Low valency dicyclopentadienyl complexes of titanium[58] and vanadium[59] polymerise acetylene without the formation of oligomer, although the use of monoalkylacetylenes with the vanadium system led to the formation of cyclotrimer and other oligomers. $MoCl_5$ and WCl_6 were also reported to catalyse the polymerisation of 1-hexyne;[41] and this was benchmarked against Ziegler-type catalysts, being combinations of $TiCl_4$, VCl_4 or $VOCl_3$ with $AlEt_3$ or $AlEt_2Cl$. These systems produced cyclotrimer, but also linear oligomer – as much as 71% of the total yield for $VOCl_3/AlEt_3$ – which suggested that migratory insertion must be a prominent process. The use of $M(acac)_3$ (M = Fe, VO or Co) with $AlEt_3$ led to high molecular weight polymers of 1-hexyne.

1.5 Aims

The overall goal of this project is to investigate new catalytic systems for the oligomerisation of acetylene. As one step in a potential pathway toward Synfuels, efficient and selective catalysis is essential to the overall process. This introduction has covered some of the broad range of complexes available for alkyne polymerisation, including metals from most transition groups, and a variety of

mechanisms by which they function. However, while there is a wide range of acetylene based chemistry in the literature, as discussed, there is not an abundance of methods that lead to selective production of linear oligomers. Hence, there is indeed scope for further development of this chemistry.

Since Ziegler's initial discovery, a wealth of chemistry has developed regarding the metal-catalysed polymerisation and oligomerisation of ethylene. There are also many cases where acetylene and ethylene behave in a similar fashion, and it was considered that many ethylene polymerisation catalysts may be ideal candidates to trial for their reactivity toward acetylene. Thus, it was proposed to survey a broad range of transition metal based ethylene polymerisation catalysts. This would involve the use of transition metal catalysts, activated in the appropriate fashion, and their exposure to acetylene gas. Any activity would be noted, and any output products identified and quantified. This would follow on to system optimisation, with the ideal target of liquid oligomers in mind. Further to this, the undertaking of mechanistic studies would help to gain insight into the function of any active systems, and could aid in the further optimisation of said systems. Finally, given a system producing soluble oligomers, the ideal target would be chains lengths such as those present in diesel fuel, being in the range of C_{10}-C_{20}.

This work is comprised of several sections. Firstly, the use of Group III, IV and V metallocenes was investigated, in combination with a number of alkyl aluminium activators; a number of other non-metallocene catalysts based on nickel, palladium and chromium were also trialled. This early work led to extensive exploration of the reactivity of triethylaluminium with acetylene, both experimentally and computationally, as this reaction was found to have potential for the growth of

acetylene oligomers. The metallocene work also led to the brief investigation of acetylene/arene copolymerisation by Lewis-acidic aluminium species. The use of bis(imino)pyridineiron catalysts forms another line of investigation, as does the effect of diethylzinc as a chain transfer agent in these systems. This research led to further oligomerisation/polymerisation studies, and examination of the reasons behind a rapid and unexpected catalyst deactivation.

Chapter 2 A Survey of Transition Metal Complexes

2.1 Introduction

The low-pressure polymerisation of ethylene by a heterogeneous $TiCl_4/AlEt_2Cl$ system was discovered by Ziegler in 1953. A multitude of research has followed in the 50 years since this discovery, both in optimising the original system and exploring its mechanistic function.[60] Further to these lines of investigation, there have been great advances in developing better catalysts for ethylene polymerisation. One well known class of catalyst in this context are the metallocenes; transition metal complexes featuring cyclopentadienyl ligands. A variety of metallocene complexes have been developed, most notably those based on the Group IV metals titanium, zirconium and hafnium, featuring simple, substituted and constrained-geometry cyclopentadiene groups (Figure 2-1). The zirconocene complexes are known to have particularly high activities in the polymerisation of olefins, and the variety of geometries available allows for the fine-tuning of polymer properties such as structure, tacticity and molecular weight.[61]

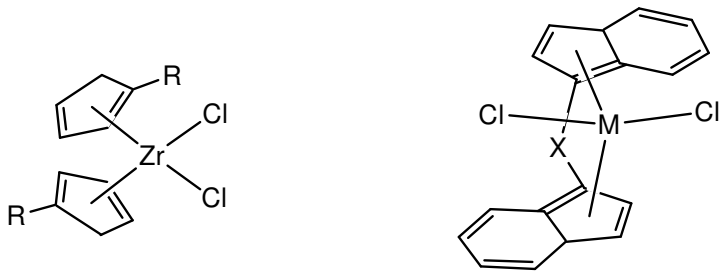

Metallocene
R = H, alkyl

Constrained Geometry Metallocene
M = Zr, Hf; X = CH_2, Me_2Si

Figure 2-1. Examples of Metallocene Complexes

The metal complexes alone do not typically provide catalytic activity, so these "precatalysts" must be activated by a suitable process. This is usually achieved using

alkyl aluminiums such as $AlR_nCl_{(3-n)}$ (R = alkyl, n = 1-3), MAO [{MeAlO}$_n$], or other main-group compounds. Broadly speaking, activation in this way involves alkylation of the transition metal and the formation of an electron-deficient metal cation. A vacant site at the transition metal allows for the coordination of an olefin, followed by migration of the alkyl group, propagating chain growth (Scheme 2-1). Factors like the Lewis acidity of the activator and structural compatibility with the transition metal complex govern how suitable an activator is for a certain precatalyst; this can have a great effect on the overall activity.[62]

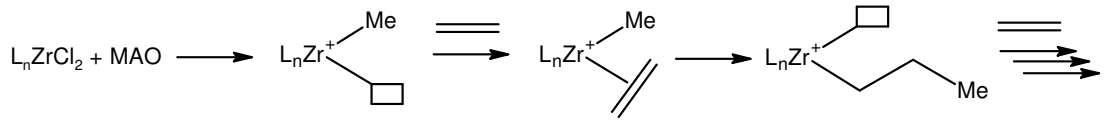

Scheme 2-1. Activation by Aluminium Alkyls

More recent developments have further expanded this field, moving away from Group IV metallocenes.[63,64] One approach is the use of other metals; neutral Group III metallocene alkyls $[Cp_2MR]_n$ (M = Sc, Y), for example, are isoelectronic with cationic zirconcene $[Cp_2ZrR]^+$, and provide reasonable polymerisation activity without the use of a cocatalyst. A myriad of catalysts featuring non-metallocene ligands have also been explored, including those based on diamides, diimines, iminopyridines, iminopyrrolides, N-heterocyclic carbenes, and other mixed heteroatom donor (PO, NO chelates) ligands.

Given the high ethylene polymerisation activity of many of these catalysts, including the metallocenes, there would be appear to be a great many targets to trial for acetylene oligomerisation activity. The early transition metal metallocenes were an obvious choice, and evaluation of these is the subject of this chapter; several mid-late

transition metal non-metallocenes are also discussed here. As part of this survey, two bis(imino)pyridineiron(II) catalysts were investigated, which displayed promising reactivity towards acetylene. The iron catalysts were thus studied extensively, and are discussed separately in Chapter 6. The metallocene trials documented in this chapter have been published as part of a recent journal article.[65]

2.2 Synthesis of Metallocenes

The early transition metal complexes considered for testing feature metals from Groups III-V. A number of these precatalysts, such as the Group IV and V metallocene dichlorides Cp_2MCl_n (Cp = C_5H_5), were able to be purchased directly from chemical suppliers. However, those featuring substituted cyclopentadiene ligands, or Group III and lanthanide metals, required some assembly in the laboratory.

The Group III metallocenes $[Cp_2MCl]_n$ (M = Sc, Y) are fairly easily prepared via a salt metathesis route. A general preparation for rare earth complexes of this form was reported in 1963,[66] and proceeds by reaction of sodium cyclopentadienide with the anhydrous transition metal salt at room temperature (Reaction 2-1). The complexes are oligomeric in nature, commonly existing as chloride-bridged dimers.

$$MCl_3 + 2NaCp \xrightarrow{THF} 1/n[(Cp)_2MCl]_n + 2NaCl \qquad (2\text{-}1)$$

A modified procedure was later reported,[67] which uses slightly less than 2 equivalents of the sodium salt; presumably this avoids the formation of $(Cp)_3M$ complexes. Workup via toluene extraction yields the products, more easily than by sublimation as was used in the original preparation. The newer procedure was followed, and the desired complexes were successfully prepared.

Synthesis of the other desired metallocenes has been reported by several groups, and typically follows a similar pathway to that described above.[68] The pentamethylcyclopentadienyl (Cp^*) Group III and lanthanide complexes are often isostructural to the Cp complexes, but can also be prepared in a monomeric form, with a THF moiety occupying the final coordination site; either form was considered acceptable for catalytic testing. These preparations often require longer reaction times and the addition of heat, depending on the metal being used; the bulkiness of the Cp* ligand likely has a large effect on this. The insolubility of the transition metal salt is often an issue, which can be partially overcome by the preformation of a THF adduct (MCl_3·nTHF). This approach was used to prepare YCl_3·nTHF (n = 3.25 by microanalysis), by soxhlet extraction of anhydrous YCl_3 in THF overnight. The adduct was reacted with $NaCp^*$, then the resulting mixture extracted with toluene cooled to -20 °C. This yielded fine needles of Cp^*_2YCl·THF.[69]

In contrast to the yttrium complex, the scandium analogue must be prepared by a slightly different route. The THF adduct of $ScCl_3$ was prepared, but following a different path as only a hydrated scandium salt was available at this stage. This was overcome by reaction with thionyl chloride, which both dries the hydrate and produces $ScCl_3$·nTHF (n = 2.8 by microanalysis) in one pot (Reaction 2-2).

$$ScCl_3{\bullet}6H_2O + 6\ SOCl_2 \xrightarrow{THF} ScCl_3{\bullet}3THF + 6\ SO_2 + 12\ HCl \qquad (2\text{-}2)$$

An attempted synthesis using the scandium salt and $NaCp^*$ failed to produce Cp^*_2ScCl·THF, despite the successful use of NaCp in the preparation of $[Cp_2ScCl]_n$. It was subsequently found that the Cp^* derivative must be prepared using the lithium salt, $LiCp^*$, according to a literature report.[54] The target cannot be attained by solvent

extraction, and must be sublimed from the reaction mixture after 3 days under reflux. Unfortunately, successive attempts to synthesise this compound were unsuccessful. Sublimation failed to yield any product at the appropriate temperature of 120 °C, and while some solid did sublime above 300 °C, NMR could not confirm this to be the desired product.

Mixed success was achieved in the preparation of lanthanide Cp^* derivatives. The cerium and lanthanum complexes are formed by reaction with $LiCp^*$, as for the scandium analogue. Here, the metal has a significant effect on reaction time, whereby $LaCl_3 \cdot 0.3THF$ is reported to react within 6 hours at reflux, while $CeCl_3$ is said to take 3 days.[70] The lanthanum preparation had initially been attempted using anhydrous $LaCl_3$, but was unsuccessful despite refluxing for 3 days to compensate for not using the THF-coordinated salt. After preparing $LaCl_3 \cdot nTHF$ (n = 1.3 by microanalysis) for a second attempt, the reaction was still unsuccessful, with only a trace of product sublimed that could not be confirmed as the desired complex. The cerium analogue, however, was produced in a good yield, with the expected yellow-brown solid collected after sublimation at 300 °C, between 10^{-5} and 10^{-4} mmHg.

2.3 Oligomerisation of Acetylene with Metallocenes

The metallocenes tested for acetylene reactivity were the complexes Cp_2MCl_2 (M = Ti, Zr, Hf, V) and $[Cp_2MCl]_n$ (M = Sc, Y); also tested were $Cp^*_2YCl \cdot THF$ ($Cp^* = C_5Me_5$) and the lanthanide complex $[Cp^*_2CeCl]_n$. Each metallocene was trialled with each of the alkyl aluminium activators $AlEt_nCl_{(3-n)}$ (n = 2,3) and MAO. In the initial set of trials (as described in Section 8.9), 50 μmol of the metal complex was dissolved in 50 mL of toluene ([M] = 1.0 mM) along with 300 equivalents of

activator. After stirring under 1 bar gauge of acetylene for 30 minutes, the reaction mixtures were quenched with dilute acid, and an internal standard added. Product analysis was performed by GC-FID and GC-MS.

It was somewhat surprising to find that the catalysts trialled were, on the whole, quite unreactive. Analysis showed only the smallest traces of oligomeric product when using MAO or $AlEt_2Cl$ as activator, and no solid polymer was collected. A trial using zirconocene dichloride confirmed the lack of reactivity of the metallocene in the absence of activator. The use of $AlEtCl_2$ as activator caused a rapid exotherm and the formation of large amounts of a dark solid. However, a blank run using the aluminium alkyl showed this not to be an effect of the transition metal, but of $AlEtCl_2$ itself; this observation is discussed separately in Chapter 5. When triethylaluminium was employed as the activator a significant quantity of 1-butene was identified by GC-MS – a likely product of acetylene insertion into an ethyl group. A trace amount of 1,3-hexadiene was also detected, hinting at a second insertion, along with a small amount of 1-hexene; the latter can be explained by acetylene insertion into butyl groups present in $AlEt_3$ (around 5% by NMR). Only trace amounts of dark solid were collected in each case, with the exception of titanocene dichloride/$AlEt_3$ which produced somewhat more solid product than the other catalysts. Reduced titanocene derivatives are known to polymerize acetylene from previous work.[28,71]

All of the runs activated with $AlEt_3$ were repeated at 60 °C to see if the product output might be improved. Indeed, a greatly increased production of 1,3-hexadiene was observed, as were traces of some higher oligomers; the output of dark polymer remained only a trace. A comparison of the quantified oligomer yields, based on the

C_4 and C_6 products, suggested that there was no outstanding metallocene catalyst, but that the generation of these oligomers was quite consistent. Surprisingly, when a blank run was performed using $AlEt_3$ alone, this yielded a similar oligomer output, both at room temperature and at 60 °C, as the runs with transition metals (Figure 2-2). This result suggested that the transition metal complexes were not significant in facilitating oligomer growth under these conditions, and that this chemistry should be pursued in terms of chain growth at the aluminium alkyl. Further studies confirmed this possibility, and are the subject of Chapter 3.

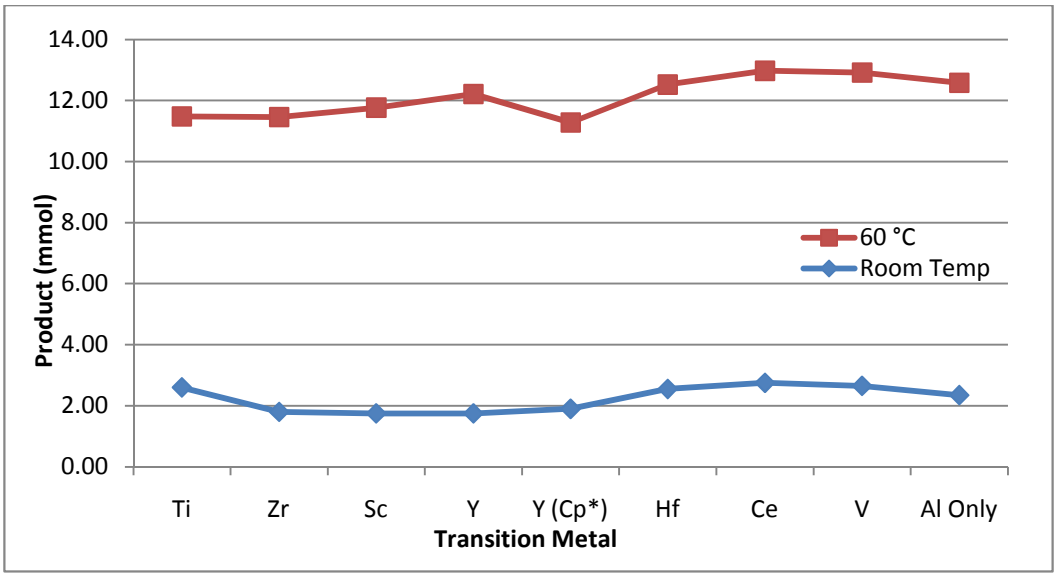

Figure 2-2. C_4 and C_6 oligomeric product yield for different metallocenes and $AlEt_3$

2.4 Synthesis of Pd and Ni Diimine Complexes

Several Group 10 complexes featuring bulky diimine ligands were developed by Brookhart,[72] and were found to exhibit good activity in the polymerisation of ethylene and α-olefins. Nickel and palladium complexes were prepared as cationic methyl complexes and used directly for catalysis, while dibromonickel analogues were tested after activation with MAO. The MAO-activated halide complexes were considered ideal targets to trial with acetylene. The 2,6-dimethylphenyl substituted

analogues were chosen (Figure 2-3), as Brookhart's trials showed a tendency towards low molecular weight products in this case.

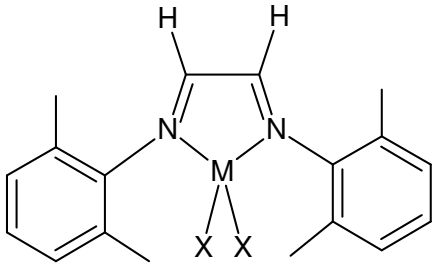

M = Pd, X = Cl

M = Ni, X = Br

Figure 2-3. Targeted Diimine Complexes

The nickel complex was prepared according to Brookhart's method, which is a modified version of earlier reports,[73,74] and essentially involves ligand displacement from $(DME)NiBr_2$ by the diimine ligand. The resulting dark brown complex precipitated from DCM, and was completely insoluble in most other solvents. The literature reports no NMR data, however on addition to DMSO-d_6, the complex quickly changed to a bright yellow. NMR signals matching those of the free ligand were now visible, suggesting the complex had indeed formed, but that preferential coordination of DMSO had displaced the diimine ligand. The targeted dichloropalladium complex has not been reported, but analogous complexes varying in N-aryl substitution have been, following the same premise of ligand displacement. Two attempts were made by adding the ligand to both $(COD)PdCl_2$ and $(PhCN)_2PdCl_2$ precursors in DCM, but neither resulted in the obvious precipitation of an insoluble product as seen for the nickel system. Cooling with the addition of hexanes or ether yielded only a small amount of orange solid, which was not soluble in $CDCl_3$, but would dissolve in DMSO-d_6. The NMR signals of this were analogous but not identical to the free ligand, suggesting that the correct complex had been

formed. The compound remained stable in air for several weeks, and it was possible to gain a crystal structure of this complex following slow evaporation of a nitromethane solution to yield orange rods. Figure 2-4 shows three ORTEP representations of the crystal –a general view, one directly onto the chelate ring plane and one along the N-N vector – which show the square planar geometry of the complex. The asymmetric unit was found to have two independent molecules, with no obvious significant differences between them, and three well ordered nitromethane solvent molecules. The molecules have approximate, non-crystallographic, C_{2v} symmetry. The ORTEP representations exclude all but the chelate ring backbone hydrogens for the sake of clarity, and thermal ellipsoids of all non-hydrogen atoms are shown at the 50% probability level. An analogous structure featuring 2,6-diisopropyl substitution at the N-aryl rings has been published, and the core bond distances and angles around the palladium centre are very similar.[75] Some selected bond distances and angles are given in Table 2-1 for comparison to the published analogue. The structures vary obviously in the angles between the chelate ring plane and the aryl rings. In the 2,6-dimethyl substituted structure, the aryl ring planes sit at 85.99º and 85.10º relative to the chelate plane, while in the 2,6-diisopropyl structure they are further from perpendicular at 80.66º and 82.73º. This is likely explained by increased steric bulk in the 2,6-diisopropyl analogue pushing the aryl rings further toward the chelate plane.

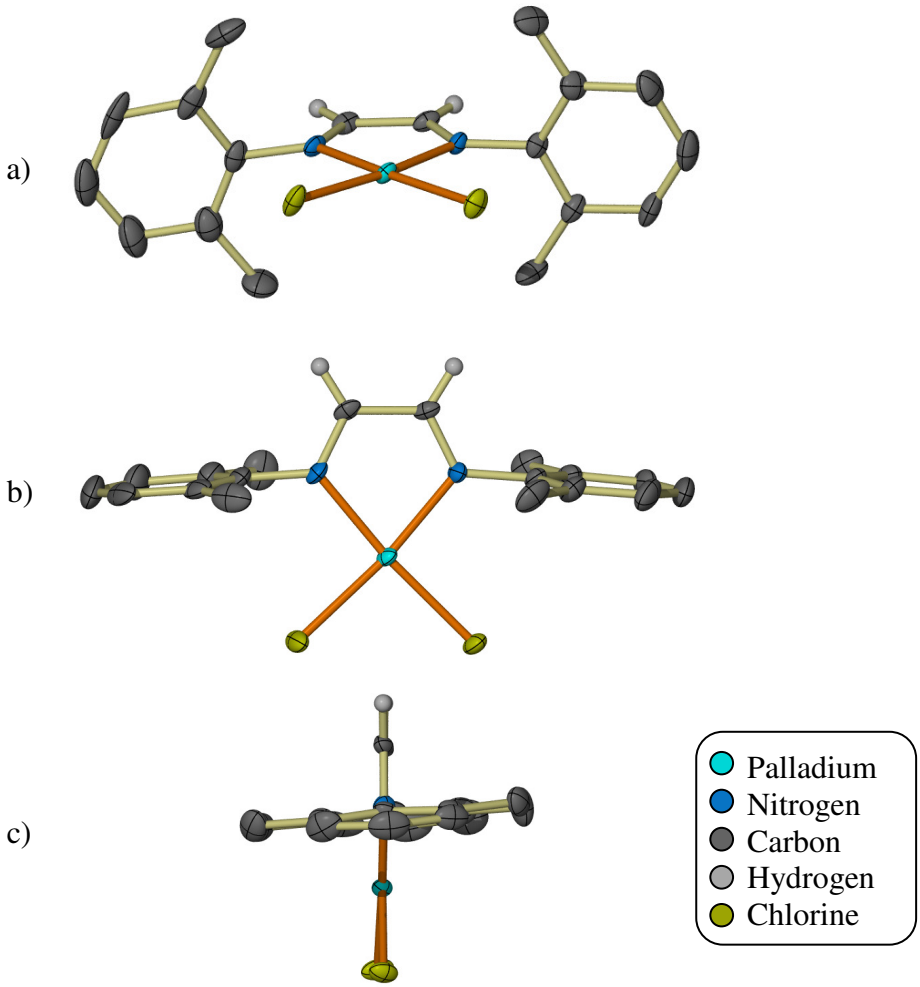

Figure 2-4. Crystal Structure of the Palladium Complex
a) General View b) Chelate Ring Plane c) Along N-N vector

Table 2-1. Selected Bond Angles and Distances (Å) for Palladium Complexes

	Palladium Complex	2,6-diisopropyl Analogue
Pd-N1	2.027(4)	2.0248(14)
Pd-N2	2.018(4)	2.0142(15)
Pd-Cl1	2.2812(11)	2.2799(5)
Pd-Cl2	2.2725(13)	2.2834(5)
N1-C1	1.279(6)	1.282(2)
C1-C2	1.462(7)	1.460(3)
C2-N2	1.279(7)	1.280(2)
Cl1-Pd-Cl2	91.95(5)	91.963(17)
N1-Pd-Cl1	94.86(11)	95.17(4)
N2-Pd-Cl2	93.67(13)	93.66(4)
N1-Pd-N2	79.55(16)	79.29(6)

2.5 Oligomerisation of Acetylene with Other Transition Metal Systems

The complexes trialled in this section feature metals from Groups VI and X. The diimine compounds were synthesised as discussed above, while the other complexes were donated by research colleagues, and are shown in Figure 2-5. Two bis(imino)pyridineiron(II) catalysts, as already mentioned, are discussed separately in Chapter 6. The chromium complexes have all been trialled and found to be active in ethylene oligomerisation[76,77] and polymerisation.[78]

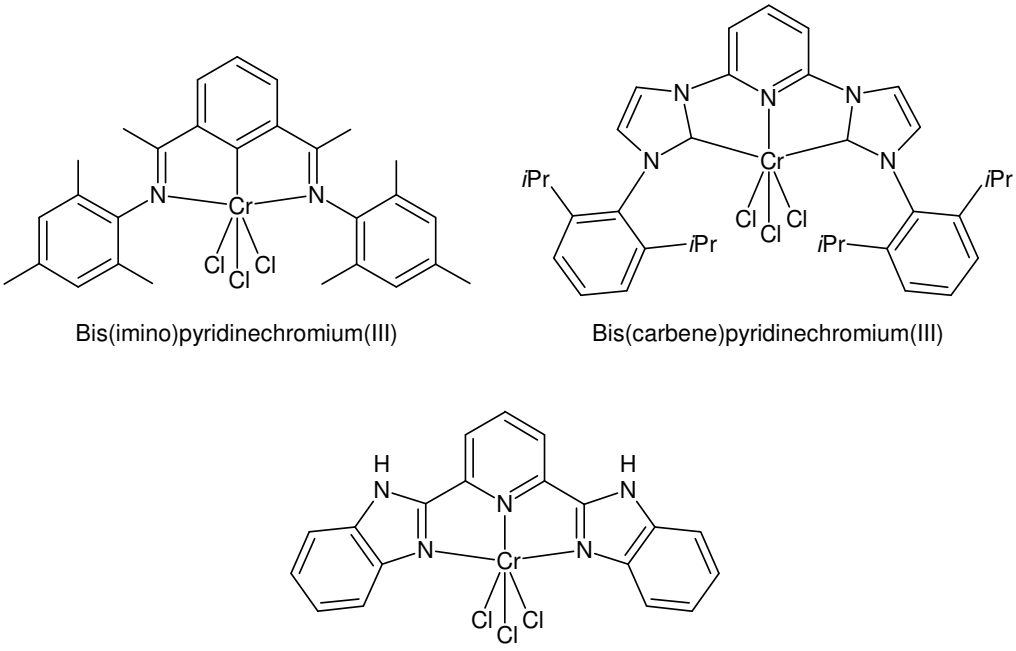

Figure 2-5. Chromium complexes investigated in this study

Catalytic trials were performed under similar conditions to those used for the metallocene complexes (Section 2.3), and are summarised in Table 2-2. MAO was employed as the activator for all. The use of less than 50 μmol for two of the chromium complexes is due to only a limited amount of these donated complexes being available.

Table 2-2. Reaction Conditions for Trialled Complexes

Complex	Amount (μmol)	MAO (Equiv.)
Palladium Diimine	50	100
Nickel Diimine	50	100
Chromium Bis(Benzimidazole)pyridine	10	500
Chromium Bis(imino)pyridine	10	500
Chromium Bis(carbene)pyridine	50	500

Overall, none of these complexes were very active for acetylene oligomerisation or polymerisation. The palladium and nickel diimine complexes did not qualitatively appear active during testing. Both showed a darkening of solution upon acetylene exposure, but no exotherm. No solid product was collected, and analysis of the organic phase showed a small amount of benzene to be the only substantial oligomeric product. The nickel catalyst produced 0.11 mmol of benzene over 30 minutes (TON = 2.2), while the palladium catalyst produced 0.25 mmol (TON = 5); the minor abundance of benzene in the toluene solvent (1:13000) was taken into consideration.

The chromium bis(carbene)pyridine complex, a yellow solution after MAO activation, did show a rapid colour change to a dark blue/red upon acetylene exposure. This quick visual change was the only noticeable activity, however, as no exotherm or acetylene uptake was seen over the remainder of the run. Presumably, a complex was formed by reaction with acetylene, which remained inactive thereafter. GC-MS showed evidence for several aromatic compounds with mass spectra suggesting disubstituted benzenes, which may have formed as adducts between acetylene and the toluene solvent. Trial of the bis(benzimidazolyl)pyridine chromium complex showed a slow initial reaction (ca. 1 minute) to develop a purple colour, but no further activity was apparent over 30 minutes. Only trace solid product was collected post-quench; GC-MS showed a trace of aromatic product but no linear

oligomers. The bis(imino)pyridine chromium complex also developed a purple colour over around 1 minute, but activity again seemed to cease after this time. Work-up yielded a small amount of unquantifiable solid, and a yellow organic solution. There was GC-MS evidence for several linear oligomers including pentadienes (MW 68), C_7 (MW 94), C_9 (MW 120), C_{11} (MW 146) and C_{13} (MW 172). A total of 1.67 mmol of oligomer was produced (TON = 167), however 48% of this amount was benzene. The odd carbon numbers presumably arise from acetylene insertion into a methyl group, obtained from either free trimethylaluminium in the MAO activator, or MAO itself. The use of metal alkyls is known to promote chain transfer in some catalytic systems (this is discussed in some depth in Chapter 6), and it was considered that such a process might be occurring here involving free trimethylaluminium in the MAO, which would explain the odd-numbered oligomers observed. As such, the run was repeated including 500 equivalents of diethylzinc to test for potential chain transfer with this reagent. Unfortunately, the zinc seemed to further inhibit catalyst activity, as only trace amounts of the expected even-numbered oligomers were detectable.

2.6 Summary and Conclusions

A variety of early to late transition metal complexes were tested for acetylene oligomerisation in combination with alkyl aluminium activators. These complexes were chosen on the basis of their known high activities for ethylene oligomerisation and polymerisation. In all cases, however, acetylene oligomerisation was low to absent. Given that some evidence was observed for chain growth at $AlEt_3$ it was prudent to focus more closely on this reaction, which is the subject of the next chapter.

Chapter 3 Acetylene Oligomerisation with Triethylaluminium

3.1 Introduction

In the previous chapter (Section 2.3), evidence for limited chain growth at $AlEt_3$ was observed. The reaction of acetylene with triethylaluminium was in fact reported by Wilke[79] in 1960, following on from Ziegler's studies of the Aufbau reaction (ethylene insertion into $AlEt_3$).[80] Wilke documented the single insertion of acetylene to form $Et_2Al\text{-}CH{=}CHCH_2CH_3$. The growth to higher products via further insertion was thought not to occur, but the formation of higher branched species was suggested, due to the condensation of unsaturated organoaluminium species. So, while the formation of chains longer than C_4 is not ruled out in the original paper, the observation of 1,3-hexadiene – suggesting a second acetylene insertion – infers that further chain growth at aluminium is occurring under the conditions used in the current study. This has been studied in considerable depth in this chapter, and the majority of this work has been published as a communication and a full paper.[65,81]

3.2 Oligomerisation Experiments

Further trials using triethylaluminium alone were performed, and are summarised in Table 3-1. As the temperature was increased and trials run for longer, there was a darkening of the reaction solution towards almost black. Workup yielded a bright yellow oligomer solution and a dark polymer. While the visible formation of polymer increased with these runs, on workup the solid was found to be a very fine powder, and difficult to separate. A quantifiable amount could not be collected until the run time was extended to 4 hours at 100 °C. For shorter runs (1-2 hours) the solid had a dark green colour and waxy appearance, perhaps hinting at a lower molecular weight

product on the edge of solubility. The generation of solid product was greatly increased, however, when the experiment was run at 130 °C.

Table 3-1. Product output for $AlEt_3$ experiments[a]

Run	[$AlEt_3$] (M)	Temp (°C)	Time (h)	Polymer Yield (g)	Oligomer Yield (g)	Oligomer (mmol)
1	0.3	30	0.5	Trace	0.13	2.4
2	0.3	60	0.5	Trace	0.60	10.2
3	0.3	100	0.5	Trace	1.72	20.8
4	0.3	100	1	Trace	1.46	13.5
5	0.3	100	2	Trace	1.76	15.0
6	0.3	100	4	0.95	2.21	15.8
7[b]	0.3	130	4	5.43	1.94	14.3
8	0.6	100	2	Trace	4.35	30.7
9	1.0	100	2	Trace	6.40	60.0

[a]All runs performed in 50 mL of toluene except where noted. [b]Using 50 mL xylene.

Accordingly, increases in temperature also allowed for the observation of oligomers beyond the butene and hexadiene seen up to 60 °C. GC analysis of oligomer samples revealed a forest of peaks eluting well after 1,3-hexadiene, for runs performed at 100 °C. A typical chromatogram is shown in Figure 3-1.

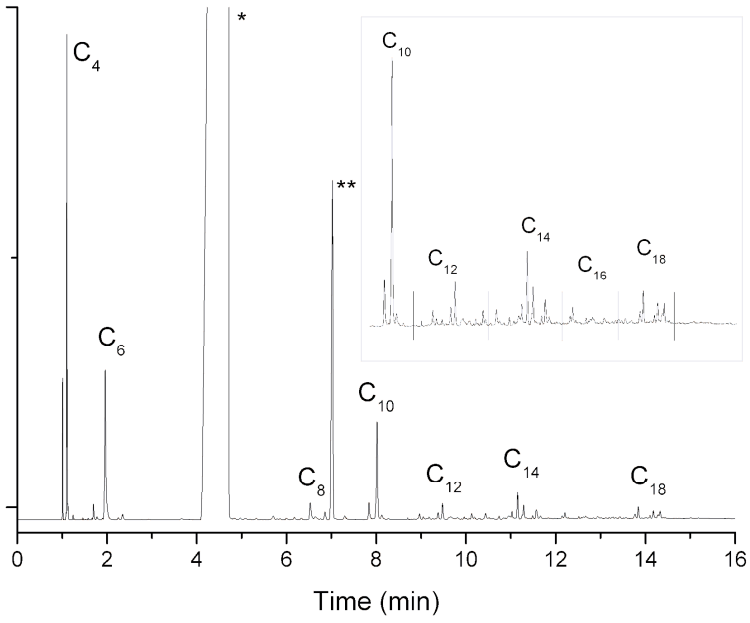

Figure 3-1. GC trace of oligomers produced with $AlEt_3$ (2 h, 100°C).
* Toluene (solvent); ** *n*-nonane (internal standard).

3.2.1 Oligomer Quantification

Quantification of the oligomeric products was not a straightforward task, due to the complex array of peaks. Identification of any single component after 1,3-hexadiene was challenging, as many peaks overlapped and showed the same molecular weight by GC-MS, suggesting *cis*/*trans* isomers and/or branching of the growth products. Mass spectra were often quite similar, and no reference spectra for likely compounds were available, confounding the issue. Thus, quantification was performed by integrating regions containing peaks of the same molecular weight, with reference to an internal standard. The molecular weights used in this quantification represent polyunsaturated products formed by multiple insertions of acetylene into an ethyl group, being 56 (butene), 82 (hexadiene), 108 (C_8), 134 (C_{10}), and so on. This could only be an approximate representation, of course, but was able to serve as a guide to product output.

Broadly speaking, oligomer production rose with an increase in temperature up to 100 °C. This remained fairly constant on a molar basis as run time was increased at 100 °C. For the majority of runs with 15 mmol of $AlEt_3$, the oligomer yield was around 15 mmol, seemingly representing 1 growth product per aluminium atom. Wilke[79] noted that, in the formation of Et_2Al-butenyl, acetylene insertion occurred only at one ethyl group, and did not then proceed at the remaining two sites; the quantified yields found here seem to broadly support this. Run 3 (30 minutes) seems to be an exception, however, with 20.8 mmol of product oligomer recorded. This is most likely a result of the difficulties in quantifying the complex array of higher oligomers (and also possibly due to the progression of oligomers into insoluble polymers in longer runs, see below). The lower oligomers are more easily quantified,

thus run 3 is probably a more accurate representation of the molar output. This suggests that insertion into a second ethyl group is possible at higher temperatures.

Another experiment gave more weight to this argument. The 30 minute run was repeated, and the end solution quenched with O_2 (5% in N_2), followed by dilute acid. The quantity of ethanol present in solution would represent the number of Al-Et groups that *did not* undergo acetylene insertion (Reaction 3-1). This was found to be 19 mmol – almost the same as the quantified oligomer output. Allowing for apparent errors in quantification in either analysis, this suggests that insertion occurs at approximately 1.3-1.6 ethyl groups per aluminium at 100 ºC, 30 min (given 45 mmol of Al-Et groups initially present); certainly more than a single insertion. Additionally, this figure is probably higher for the longer runs (4 hr, entries 6 and 7): polymer formation, which is significant in these runs, cannot be quantified on a molar basis, but does result from insertion into Al-ethyl groups. The polymer therefore represents additional insertions into the Al-ethyl bond beyond those which can be quantified from the oligomer output.

$$Et_xAlR_{(3-x)} \xrightarrow{O_2} (EtO)_xAl(OR)_{3-x} \xrightarrow{H^+} x\ EtOH + (3-x)\ ROH \quad (3\text{-}1)$$

The quantified oligomeric yield at 130 °C is similar to the 4 hour run at 100 °C (entries 6 and 7). This may seem counterintuitive, given the large increase in polymer production. However, the oligomer distribution at 130 °C is skewed toward higher molecular weight chains, which agrees with a greater overall progression toward solid polymer.

The use of twice the concentration of $AlEt_3$ in run 8 (0.6 M) showed an approximate doubling of oligomer output, both in mass and moles, compared to run 5

([$AlEt_3$] = 0.3 M). Run 9 ([$AlEt_3$] = 1.0 M) also shows an appropriate increase in product mass, based on [$AlEt_3$], but not in terms of molar output which is higher than expected. On increasing the $AlEt_3$ concentration, the oligomer distribution tends towards the lower molecular weight end, and the amount of oligomers suggests around 1.3 growth products per aluminium. This may provide further support for acetylene insertion at a second ethyl group, which may in this case be favoured by the higher concentration of Al-ethyl groups.

3.2.2 Product Distribution

Analysis of the oligomer molecular weight distribution revealed an interesting phenomenon. While a distinct lack of C_8 products was found, there were at least two prominent C_{10} compounds present. Attempts to locate the missing C_8 compounds were fruitless. Different solvents (benzene, cyclohexane) and internal standards (*n*-heptane, *n*-nonane) were employed, as it was suspected these may have obscured some C_8 peaks on the GC trace. However this only confirmed the presence of a very small amount of these products: there was a "hole" in the distribution where C_8 should have been. This pattern appeared to repeat itself in the higher oligomer regions, albeit to a lesser extent, such that every *second* growth product (ie every increase of C_4H_4) was more prominent that its predecessor. As such, after C_6, the major species are C_{10}, C_{14}, C_{18}, and so forth, with lower yields observed for C_8, C_{12}, C_{16} (see Figures 3-1 and 3-2). This unusual observation suggested that simple linear insertion was not the only growth process occurring in this system.

As such, identification of the major products was of interest, as an aid to elucidation of the mechanism of higher oligomer formation. It is worth noting that the 4 hour run does not fit this trend so well, with more C_{12} observed than C_{10}; this can perhaps be

explained by greater overall progression of the initially formed distribution toward higher chain lengths and solid polymer. Similarly, an increase in C_8 peaks (with molecular weight 108) was seen in the 4 hour runs, however the total amount still appears to be lower than expected.

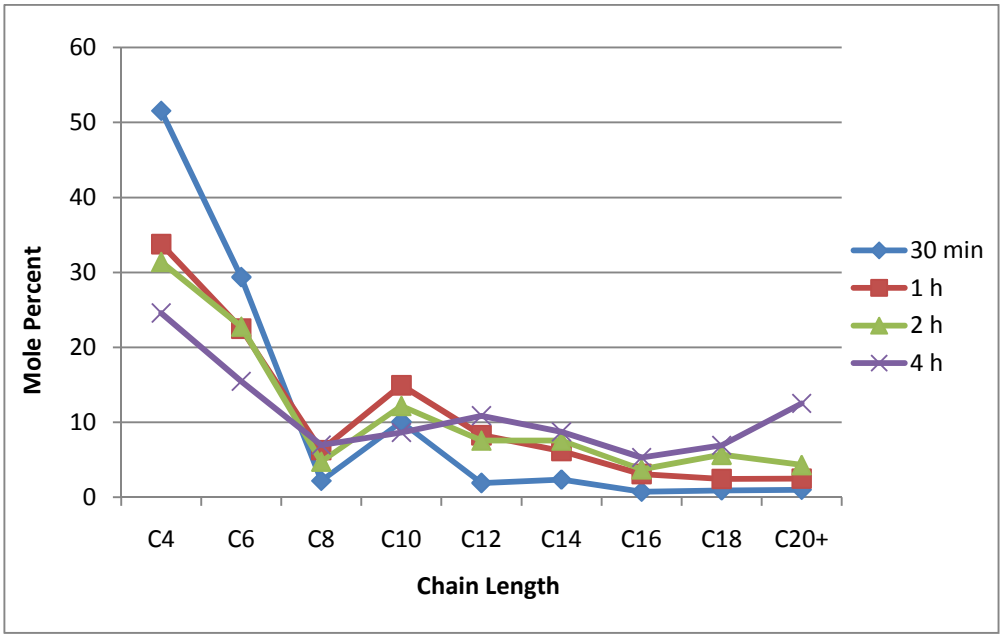

Figure 3-2. Oligomer distribution (mol %) resulting from growth at $AlEt_3$ (toluene, T = 100ºC, [Al] = 0.3M, 1 barg acetylene)

3.2.3 Hydrogenation and Identification of Oligomers

With the aim of simplifying the chromatogram, several oligomer samples (prepared using $AlEt_3$, 4 hours, 100 °C) were hydrogenated. By removal of unsaturation from the oligomers, any *cis*/*trans* isomers would condense to the parent alkane, making identification and quantification by GC-MS more straightforward. The resulting GC traces were indeed simplified, but still showed a large number of products. The degree of saturation, according to GC-MS, decreased with an increase in molecular weight, pointing to less successful hydrogenation of the longer oligomers. The first hydrogenations were performed using Pd/C under H_2, and it was thought that perhaps

this hydrogenation catalyst was not performing adequately. Rylander[82] discusses a variety of mid-transition metals for the hydrogenation of alkenes, and suggests that palladium binds relatively weakly to the double bond being hydrogenated. This can allow for double-bond migration into an inaccessible position on the oligomer, where hydrogenation is not possible, which is of particular relevance if there is branching present. Platinum was said to be the metal least likely to encourage double-bond migration in this fashion, so PtO_2 (Adam's Catalyst) was also trialled for hydrogenation. Unfortunately, the platinum species was no more effective at hydrogenating the oligomers beyond around C_{12}, and an increasing degree of unsaturation remained present. During this time the use of an H-Cube hydrogenation apparatus was also possible. This device allows for on-line generation of hydrogen at high temperatures and pressures, while the sample is passed through a catalyst cartridge via an HPLC pump. The sample was run using 80 bars of hydrogen at 80 ºC, which easily hydrogenated the early oligomers, but unfortunately was no more successful than the Pd or Pt catalysts above C_{12}.

Despite troubles with the higher oligomers, the C_{10} compounds were fully hydrogenated, and resolved into four saturated species (Figure 3-3). The major peak was identified, by mass spectra comparison and co-elution with a commercial standard, to be 3-ethyloctane, comprising around 90% of the C_{10} product in hydrogenated samples. Also identified in this manner was 4-ethyloctane (around 5%). The two other peaks were *n*-decane (around 4%) and a branched species (initially unidentified). Two saturated C_8 oligomers were observed post-hydrogenation; *n*-octane and a minor unidentified compound; these were present in small quantities compared to the C_{10} products. A hydrogenated sample from a run at higher aluminium concentration ($AlEt_3$ 0.6 M, 3 hours, 100 °C) revealed a larger

quantity of the unknown C_{10} compound (now 24% of the total C_{10} product), as well as an increase to 13% for *n*-decane. The branched product was able to be identified as 3-methylnonane using mass spectra and co-elution.

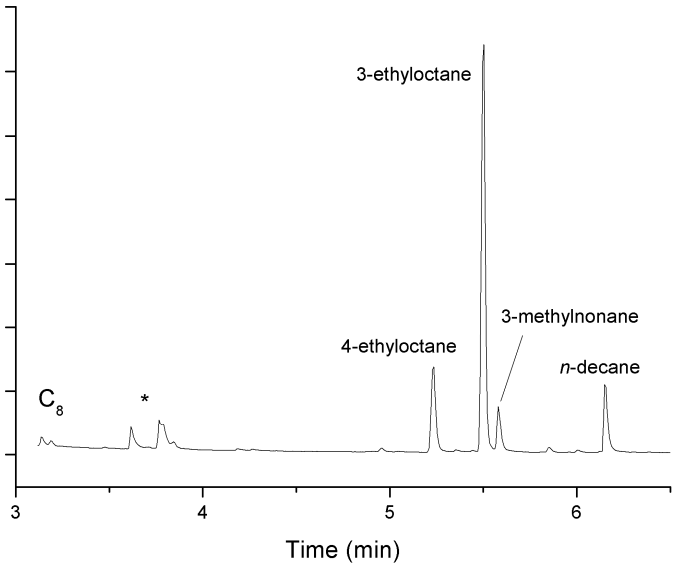

Figure 3-3. Hydrogenated C_{10} oligomers.
*Trace xylenes from the toluene solvent.

3.3 Mechanistic Investigations

3.3.1 Pathways to Branching

The observation that branching is introduced from an early stage of growth suggests that linear chain growth (migratory insertion of acetylene) is not the only process occurring in this system. The condensation of organoaluminium species, as suggested by Wilke, might provide a reasonable explanation of the formation of branches in these products (Scheme 3-1, top). The species formed by the first two acetylene insertions at $AlEt_3$ contain Al-butenyl and Al-hexadienyl motifs. The combination of these species can hence form C_8, C_{10} and C_{12} branched products and could explain the preferred growth by 4 carbons at a time, although it does not explain why C_{10} is preferred over C_8. There are further indications that such a route is not responsible

for the major products. The position of ethyl branching seen in the major C_{10} peak (3-ethyloctane post hydrogenation) cannot be formed by the condensation of Al-butenyl and Al-hexadienyl. A related reaction which could lead to all of the C_{10} skeletal structures observed is the condensation of Al-ethyl and Al-octatrienyl groups (for example Scheme 3-1, bottom). In both cases however, the reactions depicted in Scheme 3-1 would lead to products with a molecular weight of 138 g/mol (after quenching but prior to hydrogenation). In contrast, the major C_{10} compounds observed have a molecular weight of 134 g/mol. This molecular weight represents the equivalent of four double bonds, suggesting that the addition of four acetylene units was necessary to form these structures. In the case of the 0.6M $AlEt_3$ trial mentioned above, several peaks with a molecular weight of 138 g/mol could be identified in the pre-hydrogenation GC/MS. In addition, this run showed increased amounts of 3-methylnonane post hydrogenation. This suggests that the condensation pathway is perhaps more favourable at higher concentrations of $AlEt_3$, as would be expected for such an intermolecular reaction; this is consistent with the findings of Wilke,[79] whose reactions were carried out with neat $AlEt_3$. However, the ethyl-branched compounds still make up 63% of the product in this case, the major C_{10} molecular weight being 134 g/mol (pre-hydrogenation).

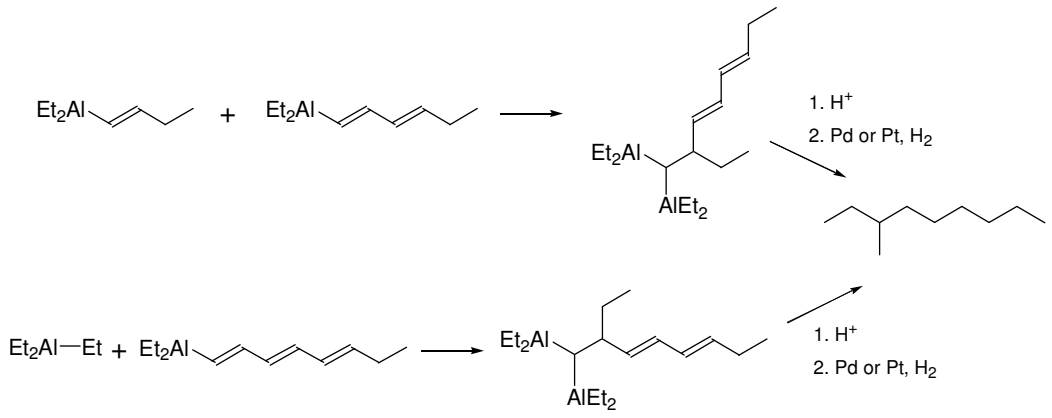

Scheme 3-1. Condensation of unsaturated oligoalanes as a possible route to branching

Another option considered was that, at a certain chain length, the unsaturated oligomer chain could back-bite, with the furthest olefin inserting into another ethyl group at aluminium (Scheme 3-2). This could explain the reduced amount of C_8 product, if C_8 was the ideal chain length to undergo such a process to form a C_{10} species, and would explain the introduction of ethyl branching into the oligomer structure. However, the product molecular weight (138 g/mol) would again be too high to explain the major peaks at 134 g/mol.

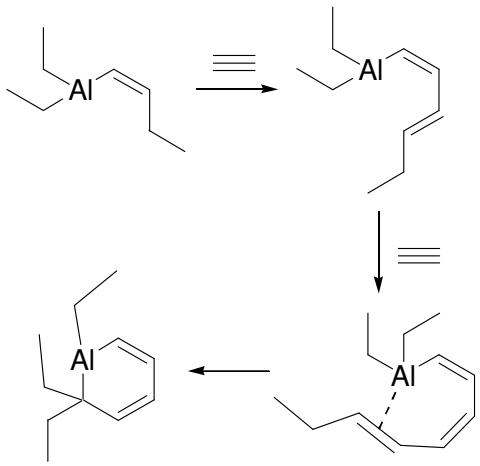

Scheme 3-2. Back-biting mechanism as a possible route to oligomer branching

Several other experiments also rule out these suggestions as the major pathway. A reaction solution was quenched with D_2O, and showed only [D_1]oligomers by GC-MS. This confirms that only one point of oligomer attachment to metal was present prior to quench, which is not the case for the back-biting or condensation mechanisms. This result also demonstrates that chain transfer is not occurring to any observable extent in this system. An attempt to grow higher products by heating a solution of the lower Al-oligomer products (primarily Al-butenyl and Al-hexadienyl) in the absence of acetylene produced only a trace of higher product. This again shows that a pathway of product condensation is not significant for the standard [Al] concentration of 0.3 M, and underlines the role of acetylene in product growth. It

should be noted that, at higher concentrations of $AlEt_3$ (0.6 M and above), quenching of the solution with D_2O did produce some $[D_2]$-C_{10} oligomer of molecular weight 140 g mol^{-1} (MW 138 g/mol with H_2O quench). This again suggests that secondary condensation reactions do become significant, but only at higher aluminium concentrations.

A model experiment was run, under the same conditions, but using $AlMe_3$ in place of $AlEt_3$, and the oligomeric products were analysed. The first two compounds, propene and 1,3-pentadiene, are analogous to the growth seen with $AlEt_3$, suggesting direct insertion. While a small number of even-numbered carbon chains were present, the odd-numbered products were very much predominant – this again suggests that the condensation pathway is not favoured, as the major growth products would then be even-numbered. Also notable in the higher products was the same peculiar growth mode; there was a distinct lack of C_7 (analogous to C_8 in the $AlEt_3$ system), but a significant quantity of C_9 compounds; the higher oligomers were, again, most prominent every 4 carbons (C_{13}, C_{17}). The oligomer solution, a complex array of products as seen for $AlEt_3$, was hydrogenated to try to identify any specific components. By comparison with reference spectra, the major saturated C_9 product was identified as 3-ethylheptane. The presence of ethyl branching in oligomers produced by both $AlMe_3$ and $AlEt_3$ confirms that branching must involve acetylene addition, and is not the product of addition of the Al-alkyl group. This experiment further confirmed that the major products do not arise from condensation of lower Al-oligomers, as addition of these would not lead to the carbon-number distribution observed.

After oligomerisation with $AlEt_3$, removal of the volatiles under vacuum left the

higher C_{10+} fractions as a yellow liquid. ^{1}H NMR spectroscopy of this liquid provides some insight into the functionality present prior to hydrogenation. One end group of the oligomers may be represented by a multiplet at 5.0 ppm corresponding to two terminal olefinic protons. The remaining olefinic resonances from 5.2–6.5 ppm are consistent with internal olefin protons, including conjugation (>6 ppm). The methylene protons of the other end group, the initiating ethyl group, could be accounted for by a peak at 1.60 ppm. This shift is inconsistent with a methylene group hydrogen α to the double bond and suggests that, for the most part, unsaturation adjacent to the ethyl end group has been removed in the C_{10+} oligomers. A broad peak centred at 2.0 ppm is consistent with terminal-alkyne unsaturation, and functional-group tests confirm the presence of acetylide functionality.[81] Finally, a series of multiplets between 2.4–3.0 ppm are consistent with a methine proton α to the alkyne. These observations suggest that the major C_{10+} oligomers might be formed according to Reaction 3-2. Additionally, this process is consistent with the identity of the branched C_{10} products, 3- and 4-ethyloctane, following hydrogenation. It should be noted, however, that the ^{1}H NMR spectrum of this product mix is very complex, and alternate interpretations are possible.

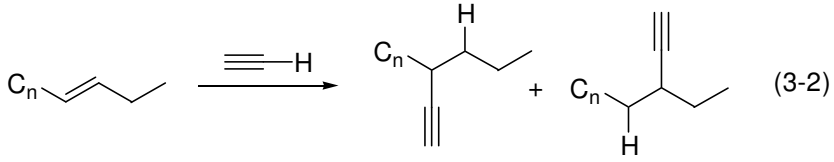

(3-2)

The results of this study have not provided overwhelming evidence for any particular mechanism. Clearly normal migratory insertion of acetylene cannot produce the branching suggested above, and as such, a second mode of acetylene addition has been considered. One possible mechanism which fits the experimental data is based upon the relative rates of two different growth processes (Scheme 3-3).

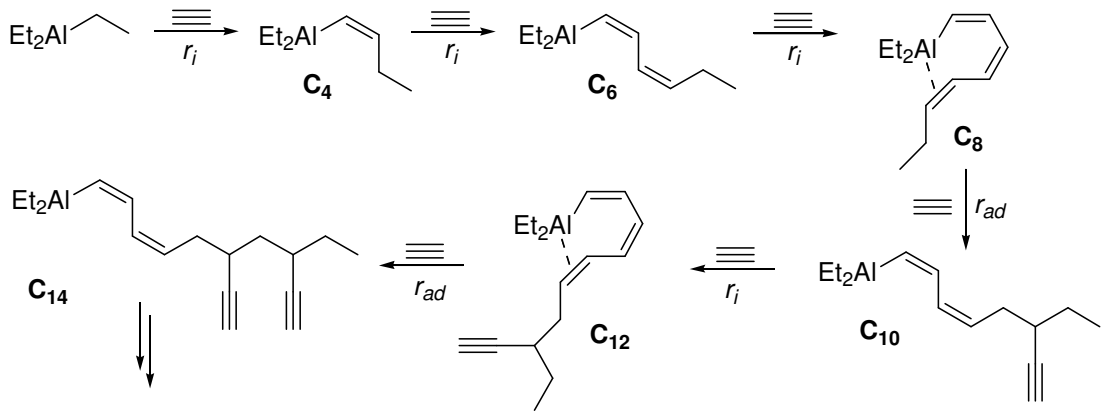

Scheme 3-3. Proposed mechanism of acetylene chain growth at $AlEt_3$

According to this mechanism, conventional migratory insertion sequentially produces butenyl-Al, hexadienyl-Al and octatrienyl-Al. Once the octatriene moiety forms, the chain can back-bite such that a double bond can interact with the fourth coordination site of monomeric trialkyaluminium. This is not possible with the shorter chains, whereas simple models show that two *cis* double bonds closest to the Al would leave the third in an ideal position to interact with a vacant coordination site of Al. This interaction may activate the double bond enough to facilitate acetylene addition across it, producing the branched C_{10} oligomers. Once the third double bond is removed, the next acetylene unit must insert to give Al-C_{12}, before another addition across the double bond can occur. The distribution of oligomers observed can be explained by a model whereby the rate of addition across the double bond, r_{ad}, is significantly greater than that for insertion, r_i. This would lead to a situation whereby oligomeric chains with a favourable double bond interaction with Al (Al-C_8, Al-C_{12}…) would rapidly react, resulting in the observed depletion of these chain lengths.

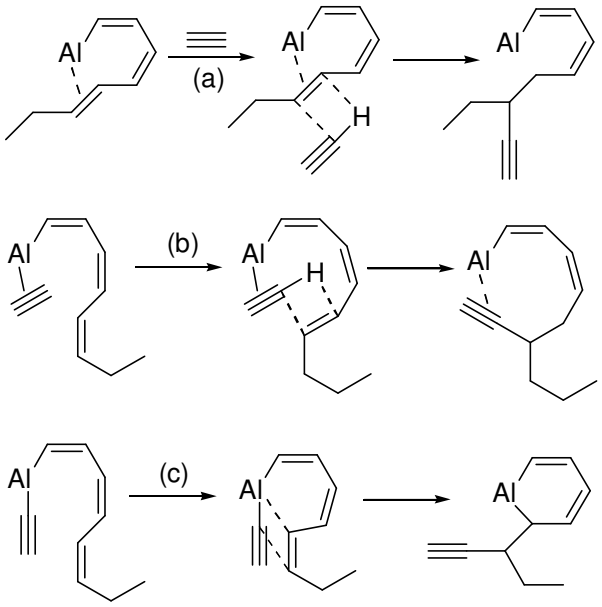

Scheme 3-4. Possible mechanisms of chain branching

Some possible intermediates for acetylene addition across the double bond are shown in Scheme 3-4. The first of these (a) involves interaction of the oligomer double bond with the Al, followed by addition of acetylene across this bond. The second possibility is that shown in Scheme 3-4(b), whereby the acetylene unit coordinates to Al, activating it towards addition across unsaturation in the oligomeric chain. The Al-acetylene complex precursor in Scheme 3-4(b) would also be the precursor to insertion into the Al-$C_{oligomer}$ bond, and as such its presence during catalysis is likely. A third possibility (Scheme 3-4(c)) can be discounted as this would lead to doubly deuterated C_{10} compounds upon quenching with D_2O, which is at odds with experimental observations. Additionally, there is no evidence for the formation of Al-acetylides (in the absence of transition metals, see Section 3.5). Also considered was the involvement of aluminium dimer structures, however this seems unlikely at this stage as the production of branched C_{10} compounds appears to be approximately first order in aluminium concentration.

A further route to chain branching involves intramolecular σ-bond metathesis which could occur once the oligomer chain becomes long enough. A representation is shown in Scheme 3-5. This could be considered a highly plausible possibility, as it explains the formation of both major branched products, though it does not clearly explain the peculiar carbon-number distribution. The aforementioned NMR data neither fits so well with the pre-hydrogenation oligomers that would be formed in such a process, as they feature no acetylide moieties.

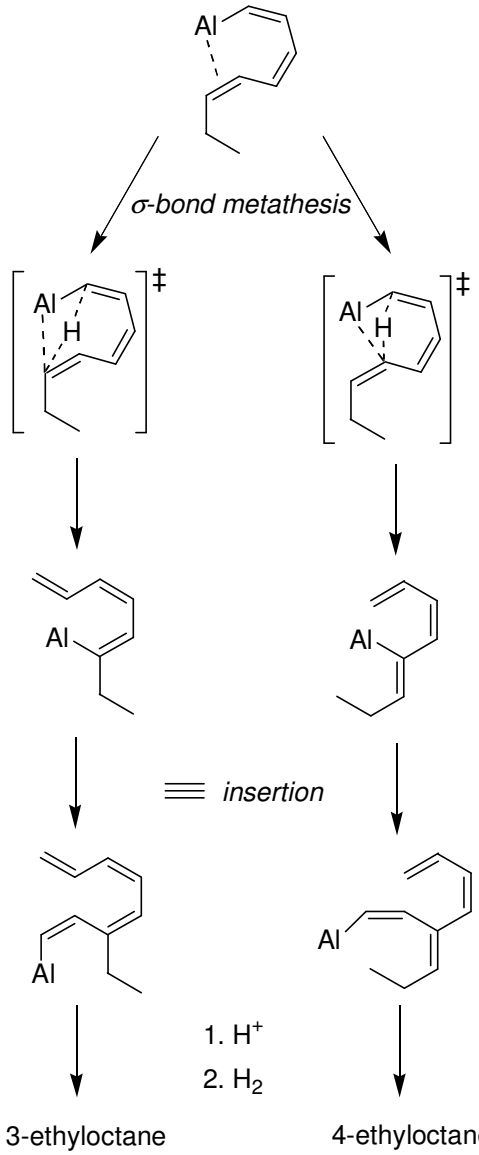

Scheme 3-5. Branching via intramolecular σ-bond metathesis

Overall, there are a number of mechanistic proposals that adequately address the method of oligomer growth in this system, however they all have their shortcomings and do not fully explain the observations of this experimental work. Further investigations are therefore required to fully understand the processes occurring during acetylene chain growth at triethylaluminium. It is clear, however, that this process is more complex than one of simple migratory insertion of acetylene.

3.3.2 Structural Investigations

The results as discussed thus far follow a curious pattern: while the first insertion of acetylene to yield Et_2Al-CH=CHCH_2CH_3 is reasonably facile, subsequent insertions into the Al-alkenyl bond occur only under more forcing conditions. Likewise, insertion at a second ethyl group is more difficult, although it does appear to occur at higher temperatures. The exact reasons why subsequent insertions at aluminium are more difficult were not particularly clear. One theory was that, following a first insertion, the aluminium may become locked up as a tightly bridged dimer. Triethylaluminium is known to exist in equilibrium between its monomeric and dimeric forms, energetically preferring the dimer.[83] Presumably, a butenyl moiety would be a stronger bridging group than ethyl, thus further favouring dimer formation (Reaction 3-3).

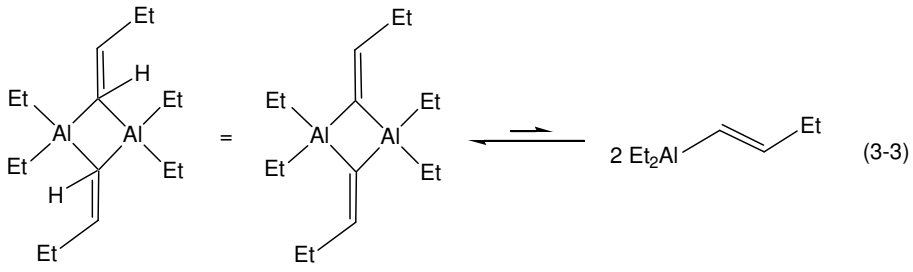

(3-3)

This makes sense in the context of electron-deficient bonding between the bridging carbon and the aluminium centres (3 centre, 2 electron), whereby the sp^2 character of

an alkene bridge is able to donate more electron density to these bonds than the sp^3 carbon of an alkyl group. The same rationale can explain the preference for phenyl bridging seen in the dimeric structure of $Me_2Al(\mu\text{-}Ph)_2AlMe_2$.[84] The relative strength of dimers in the current system has been investigated computationally and is discussed in Chapter 4.

It was of interest to pursue structural evidence relating to chain growth in this system. Given this interesting reactivity under mild conditions – the rapid first insertion of acetylene and subsequent slow progress – it was possible to isolate a pure sample of $Et_2Al\text{-}CH{=}CHCH_2CH_3$, by exposing $AlEt_3$ (1.9M in toluene) at 50 °C to acetylene for 1 hour. The product is a pyrophoric liquid and was identified by NMR spectroscopy (^1H, ^{13}C, COSY, HSQC, see Section 8.6). An interesting feature was seen in the ^1H NMR spectrum: the peak for the alkene β-proton occurred at 7.45 ppm, which is a very high frequency for an alkene proton, especially compared to the α-proton at 5.54 ppm. This can be explained in the context of the dimeric structure mentioned above, whereby polarisation of the double bond could have a deshielding effect on the β-proton (Figure 3-4). Wilke mentioned the possibility of Al-C bond polarisation in his original studies on this system.[79]

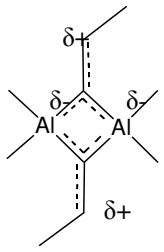

Figure 3-4. Double-bond polarisation

With a pure liquid sample as a good starting point, the next goal was the attainment of crystallographic evidence. As techniques suitable for crystallising liquids were not

available, the addition of a number of reagents was tried, with the aim of forming a less soluble derivative of the organoaluminium. The first approach was the addition of a nucleophilic reagent to form a coordination complex. If the aluminium compound indeed existed in equilibrium between dimer and monomer, a bulky electron donor might trap the monomer in a four-coordinate state, forming a solid product (Reaction 3-4). There is some precedent for this kind of reaction, such as the work of Takeda, who discussed the preparation of a number of alkylaluminium-ether complexes, and the characterisation of these liquid products by infrared spectroscopy.[85] It would seem that the relatively small ethers used (Me_2O, Et_2O, MeOEt, THF) were not adequate to induce precipitation. An earlier report by Davidson examined the reaction of trimethylaluminium with amines, phosphines, alcohols and thiols.[86] Many of these donors lead to adducts with the alkyl aluminium while the use of trimethylamine, importantly, led to the formation of a solid product in $Me_3N \rightarrow AlMe_3$.

Two attempts were thus made, separately adding triethylamine and diphenylether to the neat organoaluminium compound. The amine failed to produce any solid product, even after cooling below -20 °C, so was not pursued further. The reaction with bulky diphenylether did yield a white solid after cooling, however ^1H NMR showed this to be the unreacted ether.

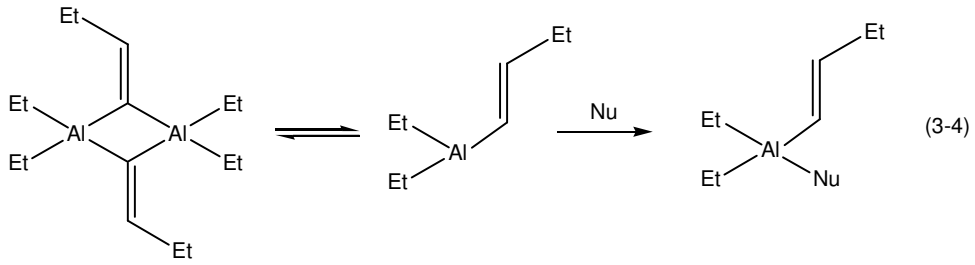

(3-4)

Another approach was the attempted formation of a lithium salt by reaction with phenyllithium, both with and without the presence of tetramethylethylenediamine

(TMEDA) (Scheme 3-6). The theory behind this approach is two-fold. On one hand, the added bulk of a phenyl substituent at aluminium might aid in crystallisation, while on the other, TMEDA is known to bind to lithium ions, further aiding in crystallisation. This has been reported by Gardiner in the reaction of $Al\{[N(t\text{-}Bu)CH_2]_2\}_2$ with *n*-butyllithium, which forms a lithium adduct of the aluminium species.[87] The addition of 2 equivalents of TMEDA to the system allowed the formation of a crystalline ionic product, with cationic lithium coordinated by two TMEDA molecules.

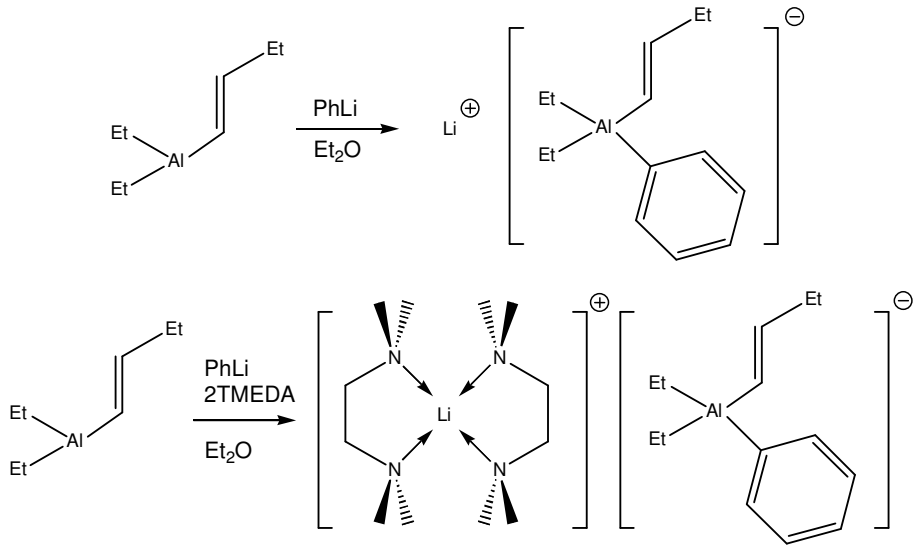

Scheme 3-6. Proposed formation of Ionic Aluminium Complexes

In this case, however, these reactions did not yield the desired products. In the presence of TMEDA, a bright red liquid was formed that was insoluble in the diethylether solvent, and easily separated on cessation of stirring. Kept under argon, the red colour faded to pale yellow over time and a fine white crystalline solid precipitated. The crystals were, unfortunately, not of adequate quality to obtain structural data. The reaction without TMEDA proceeded smoothly, forming a fine, white, ether soluble solid. Attempts to recrystallise this compound were not effective, however, and it was not pursued further in light of the ensuing results.

A third approach was the selective alcoholysis of the aluminium species. Given the proposed dimeric structure of the Al-butenyl complex and the apparent strength of these bridging groups, it was thought that stoichiometric quenching of the compound with a bulky alcohol might yield a solid product with these bridging groups intact. Thus, the Al-butenyl was reacted with 4 equivalents of phenol (per dimer); this reaction yielded a white crystalline solid upon cooling to -20 °C. A crystal structure was obtained using facilities at the Australian Synchrotron, which unfortunately showed no trace of the desired butenyl bridge. Instead, it would appear that the butenyl groups were quenched away from the metal, leaving a multinuclear structure with bridging phenols (Scheme 3-7). Evidently oxygen is a far stronger bridging group than the butenyl. Interestingly, GC analysis of a quenched sample of the crystal showed a butene to ethane of ratio of 1:30 (as opposed to 1:2 in the Al-butenyl compound) – this almost suggests that the alkenyl groups were selectively quenched during alcoholysis.

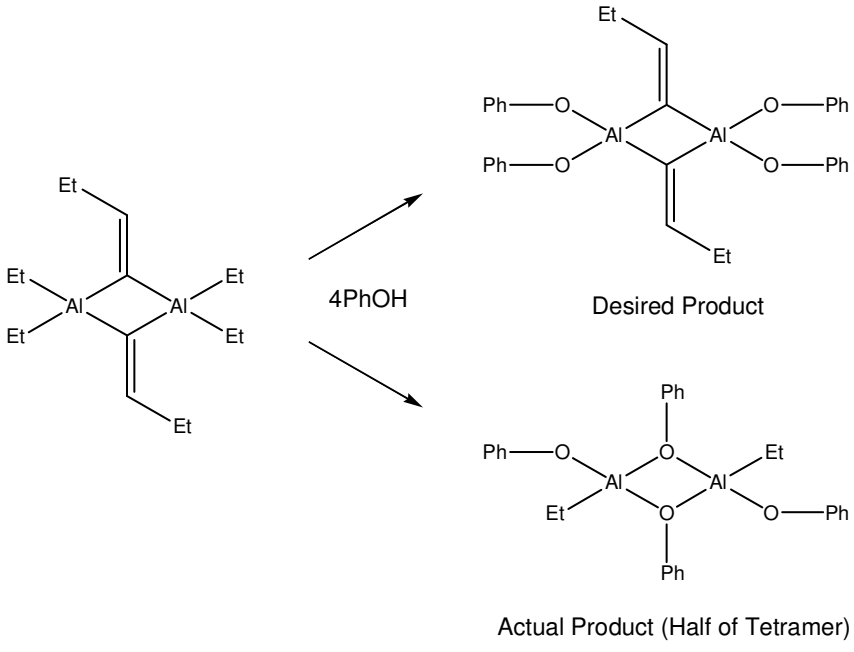

Scheme 3-7. Proposed and Actual Products of Alcoholysis with PhOH

The crystal structure itself is shown in Figure 3-5, and is tetrameric in form, featuring two oxygen bridges between each four-centre dimeric core, while one ethyl group remains per aluminium, leading to two 5-coordinate centres at the inner aluminium atoms. The view along the central O-O vector (Figure 3-5(b)) shows the two rings of the bridging groups to be parallel to each other and perpendicular to the dimeric plane. The aryl rings at the outer bridging positions, however, are significantly splayed away from the centre of the molecule. It is suspected that this added steric bulk shrouding the outer 4-centre aluminium atoms prevents further polymerisation beyond the tetrameric species observed here.

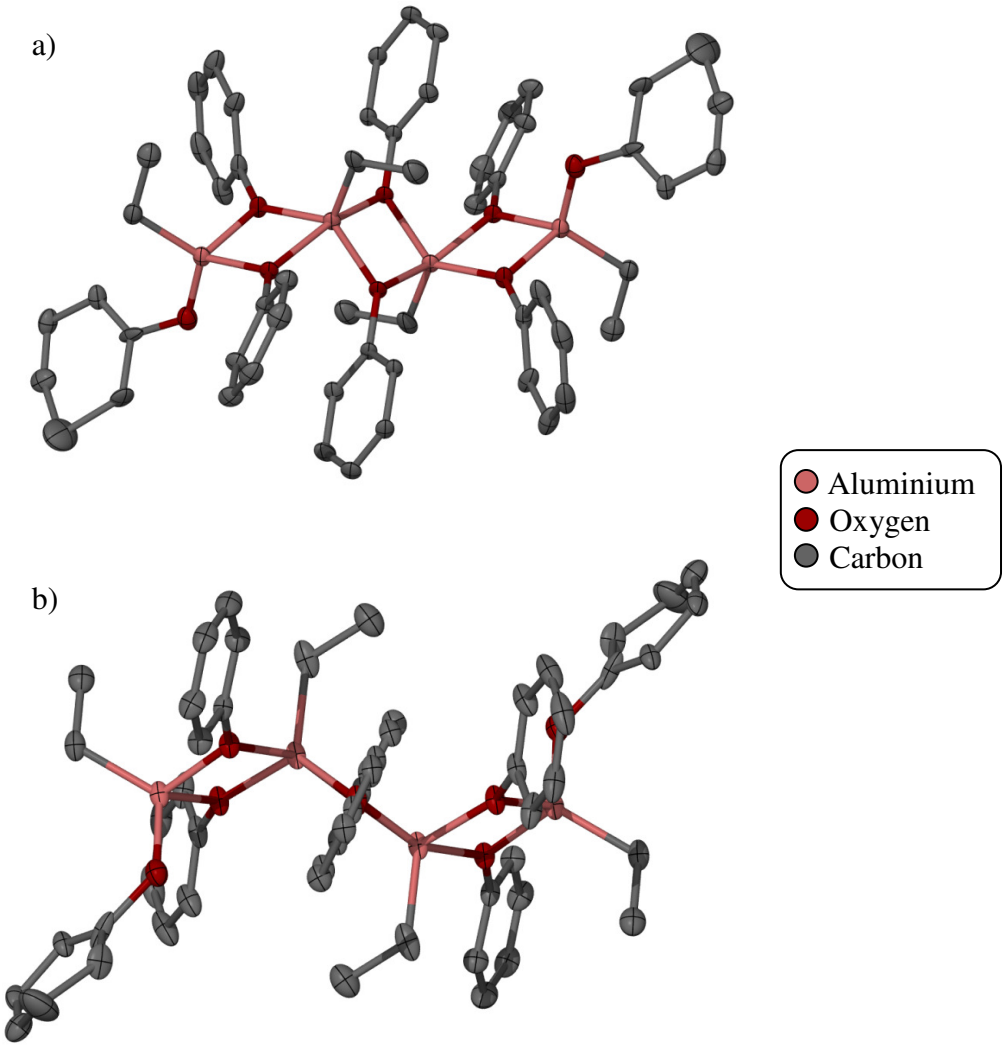

Figure 3-5. Crystal Structure of $Al_4Et_4(OPh)_8$
a) General View b) View along central O-O vector

Given this promising result in terms of obtaining a crystalline product, it was mused that an even more bulky alcohol might be the key to preserving the butenyl bridge. Employing 2,6-diphenylphenol, the reaction was repeated, this time using only two equivalents per dimer. If one phenol unit made its way into a bridging position, it was thought, the bulky rings flanking the oxygen might make it very difficult to accommodate a second phenol unit in the other bridging position. Additionally, by using less equivalents of alcohol than the phenol experiment, the chance of a butenyl moiety surviving the alcoholysis would be higher. This reaction, as for the phenol, produced a white crystalline solid on concentration and cooling. Acid quench of this product now showed a butene:ethane ratio of around 1:3, which was much more promising. Crystal data was again collected at the Australian Synchrotron, and this time confirmed the presence of a butenyl bridged dimer. One butenyl bridge was intact, with the other bridging position occupied by a substituted phenol. Interestingly, the crystalline product features 3 phenol groups, even though only 2 equivalents of the reagent were added (Scheme 3-8). Presumably some disproportionation occurs in solution to produce the solid product.

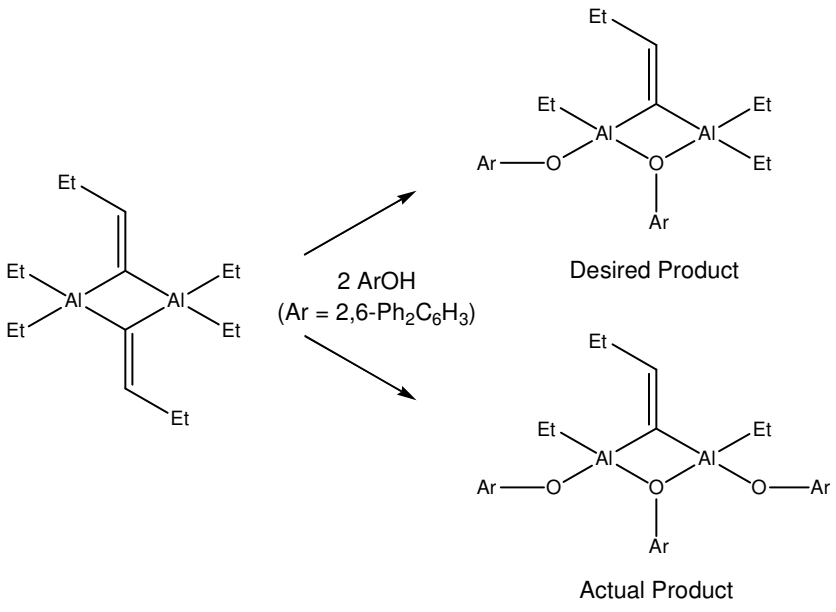

Scheme 3-8. Reaction with 2,6-diphenylphenol

The crystal structure for this compound is shown in Figure 3-6, with the core featuring approximate, non-crystallographic, C_s symmetry. The hydrid stick/ORTEP representation (Figure 3-6(a)) shows the basic structure, featuring the bridging butenyl group. Importantly, the double-bond of this group shows the protons to be arranged in a *cis* fashion, which is consistent with the computationally predicted geometry resulting from insertion via a four-centre transition state (see Chapter 4). The bulky 2,6-diphenylphenol groups clearly shroud access to the bridging alkene, preventing further hydrolysis and preserving this important structural feature. This steric shrouding is also depicted in the partial space filling model in Figure 3-6(b).

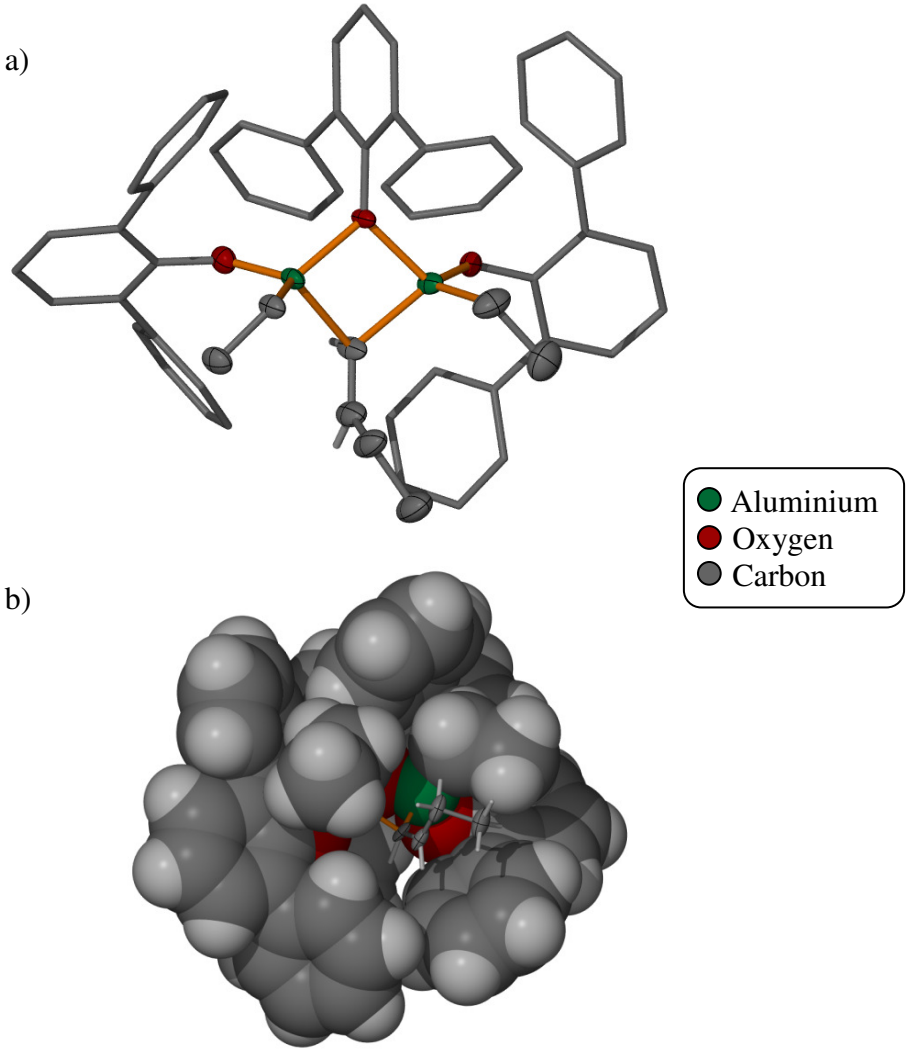

Figure 3-6. Crystal Structure of $Al_2Et_2(C_4H_7)(OC_6H_3Ph_2)_3$
a) Hydrid Stick/ORTEP View b) Partial Space-Filling Model

The bond lengths around the structural core serve as an indication of bonding strength in this dimer. The distances from the bridging oxygen to the aluminium atoms are roughly equivalent at 1.868(2) and 1.874(2) Å, and are shorter than the respective Al-$O_{terminal}$ bonds of 1.732(2) and 1.734(2) Å, which is to be expected given the 3-centre bonding arrangement at the bimetallic core. The Al-C bond lengths are much longer at 2.098(3) and 2.077(4) Å, which again serves as a guide to the relative bridging strength of the aryloxy group. The Al-C bonds to terminal ethyl groups, in comparison, are 1.945(3) and 1.947(4) Å respectively. The fact that one Al-C bond is shorter by 0.021 Å suggests an asymmetrical distribution of electron density around this 3-centre Al-C-Al moiety, and probably points to the aluminium with the shorter Al-C distance as that to which the butenyl group was attached prior to dimerisation.

This result has provided some structural evidence that the butenyl group formed in this reaction sits in a bridging position between two aluminium atoms. This corroborates the theory that tightly bound aluminium dimers are responsible for the sudden drop in reactivity after the first acetylene insertion into triethylaluminium, and agrees with the experimental observation that progress past these early growth products is more hindered at higher aluminium concentrations. As mentioned earlier, the growth process has been examined computationally and is discussed in Chapter 4.

3.4 The Effect of Hydrogen

While oligomer chain growth at aluminium is evidently occurring, in the process discussed thus far the production of oligomers is stoichiometric in aluminium; the oligomers are only released upon quenching the solution. Thus, it was of interest to

investigate methods that promote chain termination or chain transfer, rendering the process catalytic. Hydrogenative chain termination (Reaction 3-5) is used widely for molecular weight control in ethylene polymerisation with transition metals, although the reactivity of aluminium alkyls towards hydrogen was unknown at the time of this investigation. A further reason for considering hydrogen is that it is a co-product of the pyrolysis of natural gas to produce acetylene, and as such mixed acetylene/hydrogen streams would be available from such a process.

$$M{-}R + H_2 \longrightarrow M{-}H + RH \quad (3\text{-}5)$$

Trials were performed using a standard amount of $AlEt_3$ in toluene (0.3 M), with mixtures of acetylene and hydrogen (Table 3-2). The acetylene partial pressure was kept constant at 2 bar, in line with earlier experiments. Using 2 bar of hydrogen in the mix, the production of solid polymer was greatly suppressed, particularly in longer runs; the organic phase appeared much clearer than runs without H_2, with none of the waxy green residue or black polyacetylene characteristically seen. An increase to 9.5 bar of hydrogen completely stopped the production of polymer.

Table 3-2. Oligomer and Polymer Yields for H_2/acetylene mixtures[a]

H_2 Pressure (bar)	**Time (h)**	**Polymer Mass (g)**	**Oligomer Mass (g)**	**Oligomer (mmol)**
2	1	Trace	1.15	15.5
2	4	0.125	1.41	13.6
9.5	4	None	0.98	9.7

[a]All runs at 100 °C, 2 bar absolute acetylene pressure, [Al] = 0.3M

Inspection of the GC chromatograms for the runs using 2 bar of hydrogen showed a normal spread of oligomers, when compared to experiments in the absence of hydrogen. The quantified oligomer output was comparable on a molar basis, although the oligomer mass was reduced. This decrease in productivity seems to

suggest that some inhibition of oligomerisation results from the presence of hydrogen – this observation is further discussed below. A run quenched with D_2O revealed some deuteration of the known peaks observed by GC-MS. However, there was a significant proportion of [D_0]-oligomer present. The proportions of [D_0]- and [D_1]-oligomer (Table 3-3) were calculated by inspection of the mass spectra of known compounds, allowing for both natural isotopic abundances and fragmentations involving loss of protons. These results all suggest that some degree of chain termination is occurring in the presence of hydrogen; the reduction in polymer production for these runs would support this notion.

Table 3-3. [D_0]-oligomer percentages in D_2O quenched C_2H_2/H_2 run[a]

Oligomer	Percentage [D_0]
1-butene	27%
1,3-hexadiene	42%
C_{10}	46%

[a] 2 bar H_2, 2 bar C_2H_2, 4 h, 100ºC, [Al] = 0.3M

The run using 9.5 bars of hydrogen was more drastically affected in terms of product output. The C_4 and C_6 regions showed a fairly normal yield, however the actual compounds present showed a change from normal growth patterns. There appeared to be a large increase in the amount of *n*-butane in this run, with the ratio of butane to butene 12 times higher than a comparable run with no hydrogen (recalling from Chapter 2 that some *n*-butane is detected in a standard run, resulting from Al-^{n}Bu impurities in the $AlEt_3$). It was not considered that direct hydrogenation across the double bond of Al-CH=CHCH$_2$CH$_3$ was very likely, as this kind of process is typically catalysed by transition metal compounds (eg Pd, Pt, Ni, Rh).[82] The most likely explanation seems to be that 1-butene, formed through chain termination with hydrogen, inserts into the Al-hydride formed in the process to yield an Al-Bu species

(Scheme 3-9(a)). Such a sequence is expected to be more favourable under elevated hydrogen pressure.

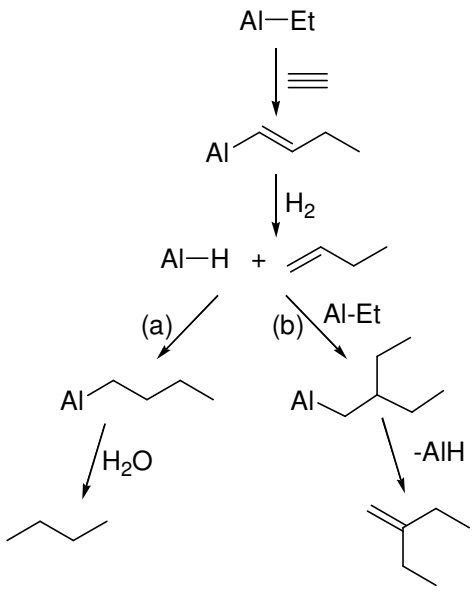

Scheme 3-9. Possible formation of Branched C_6 oligomers

The C_6 fraction featured no 1-hexene or 1,3-hexadiene, but a single peak which was identified as 3-methylenepentane by GC-MS and co-elution. This can again be explained by the presence of 1-butene; 1,2-insertion in $AlEt_3$ followed by β-hydride elimination (or direct β-hydrogen transfer to more 1-butene)[88] to produce 3-methylenepentane seems possible (Scheme 3-9(b)). β-Hydride elimination from a β-branched Al-alkyl is known to be more facile.[88] None of the oligomers expected from C_8 and above were observed, and an approximate quantification of the minor products formed showed the yield in this area to be greatly reduced. Taken together, the above observations suggest that at high partial pressures of hydrogen, chain termination occurs more rapidly than further insertion into Al-CH=CHCH$_2$CH$_3$, generating 1-butene as the primary product. Insertion of this into an Al-hydride bond can lead to butane, whereas insertion into Al-Et leads to 3-methylenepentane. All of this suggests a controlling effect of dihydrogen toward oligomer growth in this

system, especially under higher pressure. At the same time, unfortunately, the presence of hydrogen seems to greatly inhibit the productivity; as such the reaction does not appear to become catalytic. At this stage it is unclear why the presence of hydrogen hinders further acetylene insertion. One possibility is that the formation of Al-hydrides results in strongly bound μ-H dimers,[88] which do not readily take up acetylene (Reaction 3-6). The nature of such likely species has been investigated computationally, and is discussed in Chapter 4.

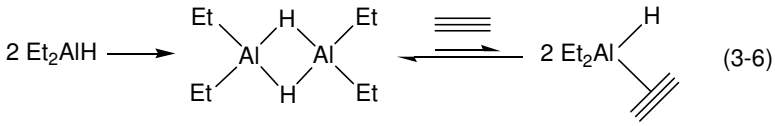

(3-6)

3.5 The Effect of High Concentrations of Cp_2ZrCl_2

A second possible strategy to promote chain termination that was explored was the effect of Cp_2MCl_2 (M = Zr, Hf) under more forcing conditions and at higher concentrations. Early transition metal, lanthanide, and actinide alkyl (or alkenyl) complexes are known to undergo facile σ-bond metathesis with primary alkynes (Reaction 3-7),[47-49,51,53,89] whereby the oligomeric chain is released and further insertion at the metal-acetylide can begin (see Scheme 1-15 in Section 1.4.4). Oligomer chain exchange (transmetallation) between Al and Zr/Hf might thus lead to chain termination, as illustrated in Scheme 3-10.

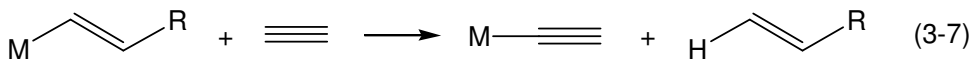

(3-7)

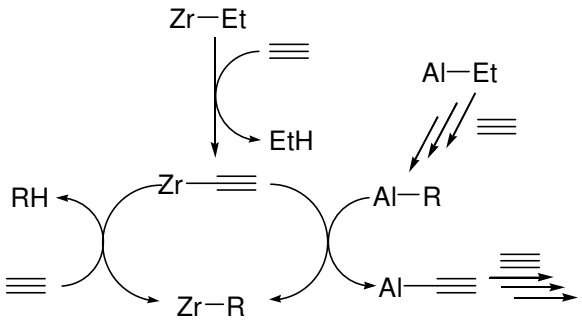

Scheme 3-10. Chain transfer and termination with Zr

Although the metallocene complexes had little effect in the first series of tests, it was reasoned that their role might become apparent under more forcing conditions. Hence, further experiments were performed using triethylaluminium and either hafnocene or zirconocene dichloride (Table 3-4).

Table 3-4. Acetylene oligomerization in the presence of Cp_2MCl_2 (M = Zr, Hf)[a]

Entry	Metallocene (mM)	Temp (°C)	Time (h)	Poylmer Yield (g)	Oligomer Yield (g)	Oligomer (mmol)
1	Zr (1.0)	60	4	Trace	1.28	16.8
2	Hf (1.0)	60	4	Trace	1.09	15.1
3	Zr (1.0)	100	0.5	0.02	1.77	18.3
4	Hf (1.0)	100	4	1.95	2.74	19.5
5	Zr (1.0)	100	4	0.94	1.57	12.2
6	Zr (2.0)	100	4	0.90	1.41	12.5
7	Zr (10.0)	100	4	0.24	0.88	7.8
8[b]	-	100	4	0.95	2.21	15.8

[a] All trials used 0.3M $AlEt_3$ in 50 mL toluene, 1 barg acetylene.
[b] No Cp_2MCl_2 was used in entry 8 (blank $AlEt_3$ run).

The first experiments were conducted with a Cp_2MCl_2:$AlEt_3$ ratio of 1:300 (Entries 1 to 5). As with the experiments in the absence of Zr or Hf, it was found that greater yields of combined oligomeric and polymeric products were attained as the run times were extended. The yield of oligomeric product increased significantly for the 100 °C runs, and solid product was collected only at this temperature. The 60 °C runs showed an oligomer distribution skewed towards the lighter (C_4 and C_6) products, and little difference was observed between hafnocene and zirconocene

dichloride runs at this temperature. These results at low temperature or short run times are very similar to those using only $AlEt_3$, and unfortunately there seemed to be no trend away from the generation of solid polymer, which would be an ideal result. After 4 hours at 100°C however, some influence of the metallocenes became apparent (Entries 4 and 5). Hafnocene dichloride led to an increase in the amount of polymer (Entry 4) relative to oligomerization in the absence of transition metal (Entry 8). This result is clearly counter to the desired effect, and perhaps suggests that acetylene polymerisation is being catalyzed at the Hf centre. In the presence of Cp_2ZrCl_2 (Entry 5) polymer output was similar to that in the absence of this complex, although the oligomer yield curiously dropped somewhat. The use of 2 mM Cp_2ZrCl_2 (Entry 6, Zr:Al = 1:150) did not cause much deviation from the trial with less Zr. An increase to 10 mM of Cp_2ZrCl_2 (Zr:Al = 1:30), however, effected a marked reduction in polymer production, as well as a further drop in oligomer. Closer inspection of the chromatogram for this experiment revealed a different range of oligomeric products. Two previously unseen peaks were now visible in the C_6 region, alongside 1,3-hexadiene and 1-hexene. These were identified as 3-methylpentane and 3-methylenepentane. It is interesting that the system produces these previously unseen C_6 products, and implies that the Cp_2ZrCl_2 is playing some role in catalysis at higher concentrations. While 3-methylpentane can conceivably be formed via condensation of Al-ethyl and Al-butenyl species in solution, this has not been observed in the absence of zirconocene. The formation of 3-methylenepentane is difficult to imagine by condensation pathways, given the available reagents. A quench with D_2O was able to shed some further light on the nature of the new C_6 compounds, and the system as a whole (Table 3-5).

Table 3-5. Deuteration of C_6 oligomers[a]

Compound	MW: H_2O quench	MW: D_2O quench	D_n
3-methylpentane	86	89	D_3
1-hexene	84	85	D_1
3-methylenepentane	84	86	D_2
1,3-hexadiene	82	82/83	D_0/D_1

[a] Run conditions according to Table 3-4, entry 7.

The $[D_1]$-1-hexene confirms the attachment of this oligomer to one metal, prior to quench, consistent with a single insertion of acetylene into an Al-butyl group. Approximately 20% of the 1,3-hexadiene present was also $[D_1]$-oligomer, consistent with a single metal attachment, however the remainder was $[D_0]$. This suggests that a chain transfer process may now be taking place, at least to some extent, which releases hexadiene from the metal centre prior to quenching. The mass spectra for 1-butene, compared to a non-deuterated sample, also showed a mixture of $[D_0]$ and $[D_1]$ product. In this case the $[D_1]$ comprised around 60% of the total, and it is unclear why this proportion should differ from that seen for 1,3-hexadiene. The result, however, certainly supports the notion of chain transfer facilitated by zirconocene.

Yet more interesting are the observations of $[D_2]$ and $[D_3]$ isotopomers for the branched compounds. These results imply multiple points of attachment to a metal, prior to quench, and hence a different mechanism in operation. One possible pathway is that shown in Scheme 3-11, and assumes the prior formation of metal-acetylide species (M = Al, Zr) according to the chain transfer mechanism postulated above (Scheme 3-10). Two additions of M-Et across the triple bond in a M-acetylide would produce the observed backbone. Quenching would yield 3-methylpentane, or the $[D_3]$ isotopomer if D_2O was used. Alternatively, release of M-H by β-hydrogen

elimination, followed by quenching, would yield 3-methylenepentane (the [D_2] isotopomer in the case of a D_2O quench). The formation of metal-acetylides is supported by the observation above of chain termination prior to quenching. The Zr-catalysed addition of aluminium alkyls across alkynes (carboalumination) has been reported in some detail by Negishi,[90] and a similar process seems to be in operation here.

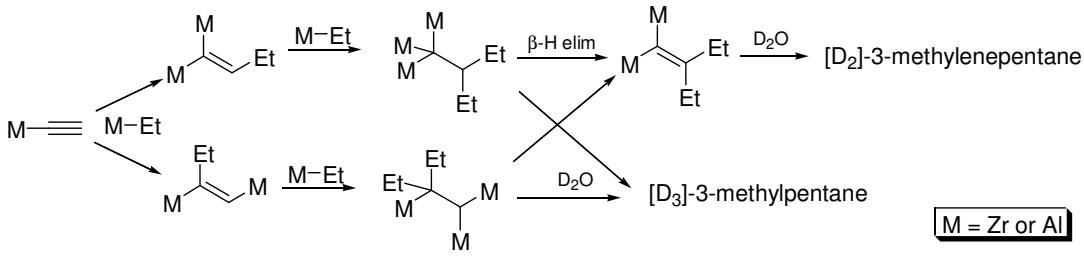

Scheme 3-11. Growth via metal acetylides

It has been suggested that such metal acetylides would most likely exists as dimers; $M_2(\mu\text{-}C{\equiv}CH)(\mu\text{-}R)$, R = alkyl, alkenyl, alkynyl. For simplicity these species are not shown in Schemes 3-10 and 3-11, but are likely intermediates (and may facilitate the reactivity suggested in Scheme 3-11). The possibility of M-C≡C-M has also been suggested, formed by a second reaction of M-C≡CH; the formation of $L_nZr\text{-}C{\equiv}C\text{-}ZrL_n$, for example, has been reported.[91] Such species seem quite possible and are not ruled out, however no evidence has been found in this work.

It is not easy to explain why these processes should lead to a decrease in the yield (in mass and moles) of oligomer; normally the opposite would be expected. The formation of M-hydrides is implicated in Scheme 3-11, and could retard further insertion as was postulated in Reaction 3-6. Another related possibility is that acetylide-bridged species retard further insertion, due to the likely strength of such dimers. The compound $Ph_2Al(PhC{\equiv}C)_2AlPh_2$ has been shown to exist as an

acetylide-bridged dimer that invokes two bridging modes, with the acetylide moiety forming a σ-bond to one Al centre while undergoing π-donation to the other Al, leading to a highly stable complex.[92] Again, this possibility has been considered as part of theoretical investigations (Chapter 4).

Interestingly, the oligomers above C_6 were less pronounced in the gas chromatogram for this run. The hydrogenated sample, however, revealed more prominent peaks. There appears to be a larger range of products present for each carbon number, each present in a small quantity and eluting over a wide range, prior to hydrogenation. This is borne out in the C_{10} region which shows a large number of compounds of molecular weight 138 and 140. This amount was several times larger than the compounds of molecular weight 134 seen, which are attributed to the standard mode of growth by $AlEt_3$ (Section 3.2); in a standard run there are almost no compounds of molecular weight 138 or 140 visible in this area. This again supports Zr-catalysed addition of M-Et across unsaturation in the growing chain. Post-hydrogenation, 3-ethyloctane was no longer the primary structure, as previously seen. Relative increases were seen in all of 4-ethyloctane, 3-methylnonane and *n*-decane, and all four of these C_{10} compounds were present in similar quantities. A new C_{10} peak was also present, eluting earlier and around 2.5 times larger than the other compounds. It was not possible to fully identify this structure, however the mass spectrum suggested multiple branching points.

Further to these experiments, a small-scale reaction was performed, using a Zr:Al ratio of 1:3.5 ([$AlEt_3$] = 0.3 M, total volume 10 mL). In contrast to previous trials, the solution darkened significantly on exposure to acetylene, within 1-2 minutes. After 2 hours at 100 °C a significant amount of solid product was collected; after

drying, this amount (0.98 g) was comparable to the 4 hour experiments with the lowest loadings of Zr, or none at all. Given the scaling factor, this represents 5 times the production of polymer with respect to the amount of Al, in a shorter timeframe. The result is interesting, as the increases in Zr:Al ratio explored previously (from 1:300 to 1:30) effected a *reduction* in polymer production. It may suggest that, under these conditions, different growth mechanisms are becoming more prominent. Growth at the Zr centre has hitherto not been considered to occur to any great extent, but at such a high concentration may be significant; it should be noted in this context that earlier benchmark trials with Cp_2ZrMe_2 alone did not display any reactivity toward acetylene. The dark orange liquid phase from this reaction appeared to contain only a small amount of oligomer by GC. A number of overlapping C_6 products were visible by GC-MS, more than were seen for the Zr:Al ratio of 1:30. Compounds of molecular weights of 80, 82 and 84 were observed, representing different degrees of unsaturation. Compounds of 80 g/mol had not previously been observed in this investigation, and must represent an isomer of hexatriene; this compound was minor, however. A hydrogenated sample revealed 3-methylpentane and *n*-hexane as the two skeletal structures, with the branched species now representing 60% of the fraction. This further supports the notion of a role of the Cp_2ZrCl_2 in the formation of these branched species, as this proportion is increased with the higher Zr loading.

As the results with higher zirconium loadings had effected some change in the oligomeric output, the scandium complex $[Cp_2ScCl]_n$ was trialled at high concentration (Sc:Al = 1:30; 100 °C; 4 h). This seemed a good potential candidate in light of the proposed mechanisms involving Cp_2ZrCl_2, owing to reports of σ-bond metathesis reactions of acetylene at permethylscandocene complexes.[53] The use of

scandocene effected only a small change, however, in comparison to runs using only $AlEt_3$. The yield of polymer (1.52 g) and oligomer (2.44 g) were similar to a standard $AlEt_3$ run, and the oligomer distribution much the same. The major C_6 products detected by GC-MS were 1-hexene and 1,3-hexadiene, indicating that the branched products formed with Cp_2ZrCl_2 were not produced in this system.

Oligomer growth was finally attempted using both a high loading of Cp_2ZrCl_2 and a mix of acetylene and hydrogen. As both the use of hydrogen and an increase in zirconocene had shown some positive effect toward regulating chain growth, it was considered that they may work more effectively in tandem. A 4 hour run (100 °C, 2 bars each of H_2 and acetylene, [Zr] = 10 mM, [Al] = 0.3M) yielded a yellow oligomer solution, but only trace solid product. GC-MS showed a multitude of C_6 products, as seen for the other runs with high zirconium loadings, which condensed to 3-methylpentane and *n*-hexane after hydrogenation; the branched isomer comprised around 40% of the total. The higher oligomers were an extremely complicated array which appeared different to previous runs. Interestingly, the usual prominent C_{10} peaks with molecular weight of 134 g/mol were not obvious by GC-MS. In this region, the most common molecular weights were 138 and 140 g/mol. Both compound types have been seen in the experiment using Zr/Al and no hydrogen, however the 140 g/mol products were more prominent when hydrogen was used. These observations suggest partial hydrogenation and/or addition of M-Et across unsaturation in the oligomeric chains, as expected. The hydrogenated sample showed the same array of C_{10} skeletal structures as in a comparable run in the absence of hydrogen. Some branched C_{12} structures were also clear in the chromatogram, however reference spectra and other data were insufficient to fully characterize these.

In summary, while high concentrations of Cp_2ZrCl_2 showed some evidence of promoting chain transfer, this was insufficient to make the process catalytic in $AlEt_3$. The transition metal seemed to inhibit acetylene insertion at moderate concentrations, and at very high concentration led to increased polymer production.

3.6 Summary and Conclusions

Investigations into the reaction between acetylene and $AlEt_3$ have revealed that chain growth occurs at the aluminium centre, akin to the Aufbau reaction of ethylene with $AlEt_3$. Following the first insertion, the course of the reaction depends upon the concentration of aluminium. At high concentrations there is some evidence for condensation reactions (insertion of oligomer chain unsaturation into Al-alkyl groups), as was reported by Wilke.[79] At low aluminium concentrations a hitherto unprecedented mode of chain growth occurs which i) introduces branching into the chain, and ii) leads to an unexpected carbon-number distribution of oligomers. A variety of possible mechanisms by which this could occur have been discussed, but these remain speculative and further work is necessary. Computational studies that add some further insight into the nature of this process are presented in the next chapter. The introduction of hydrogen and high concentrations of Cp_2ZrCl_2 does appear to lead to chain termination reactions, however this is accompanied by inhibition of acetylene oligomerisation. As such, it has not been possible to render the process catalytic in aluminium.

Chapter 4 Computational Studies of Triethylaluminium Reactions

4.1 Introduction

The work involving the reactions of acetylene with early transition metal catalysts and aluminium activators has been fascinating, as for the most part the transition metal complexes have not shown significant activity towards acetylene (Chapter 2), however growth was found to be possible using triethylaluminium. While further investigations showed that a large amount of zirconocene dichloride could be made to alter product growth in the aluminium system (Chapter 3), it was the reactions with triethylaluminium itself that were the most interesting. There were a number of experimental observations that at first appeared to be at odds with previously published results; particularly those of Wilke, who reported on the reactions of acetylene with triethylaluminium in 1960.[79] Of particular note are the following observations made in the present study:

1. The insertion of acetylene into $AlEt_3$ occurs repeatedly to grow long chain oligomeric and polymeric products (particularly at high temperatures)
2. For a variety of oligomerisation runs, insertion occurs at (on average) 1.3-1.6 ethyl groups at aluminium
3. Branching is introduced early in the growth process, which infers a growth mechanism other than simple linear insertion

Wilke found that acetylene insertion occurred just once, forming a butenyl group at aluminium (Al-CH=CH-CH_2-CH_3), and that this occurred at only one ethyl group per aluminium. It should be pointed out that Wilke's experiments were conducted under milder conditions than those employed in this work. Even at the elevated

temperatures used presently, the major products on a molar basis are Al-butenyl species. As such, the differences between the two studies can likely be attributed to reaction conditions. Wilke also suggested that branching can occur by the condensation of unsaturated organoalanes, however the major products we have observed by GC cannot form by this pathway. As the observations of the current work have been consistent and repeatable, it was considered that computational chemistry may be a useful tool to both reinforce and further explain these results. The relative stability of aluminium dimers has been found to be of great importance to the systems studied, and several pertinent examples including alkenyl, alkynyl, hydride and chloride-bridged complexes will also be discussed.

4.2 Theoretical Methods

All calculations were performed using Gaussian03[93] or Gaussian09,[94] utilising hardware from the Australian Partnership for Advanced Computing Program (APAC), or National Computational Infrastructure. Geometry optimisations were performed using the B3LYP[95-98] functional, using the 6-31G(d) basis set. [99] [100]Single point energies were calculated using 6-311+G(2d,p).[101,102] These levels of theory were considered adequate for the molecules being studied; while a larger basis set is often used for the modelling of transition metal atoms, the relative simplicity of the electronic structure of aluminium did not warrant this approach. Gibbs Free Energy corrections were not applied to the final energies for these structures. Gas-phase calculations provide a poor estimate of the true free energy changes in solution, and this is accentuated when the number of molecules changes, as is the case in the first three steps of the reaction pathway. The Gibbs corrections were therefore excluded; thermal corrections for enthalpy were instead applied to the single point energies. It

has been noted that in the computational modelling of certain systems, for example olefin polymerisation, density functionals often do not accurately describe a number of mid-long range interactions. This effect was considered relevant to the system being studied currently. There are several approaches that are used to address this shortcoming, and a number have been compared recently for the description of hydrocarbons.[103] Thus, a dispersion correction described by Grimme was applied to the B3LYP single point energies, with a scaling factor of 1.05, to yield the final B3LYP-D values.[104] Grimme's method has been found to more accurately describe long-range van der Waals forces in many systems.

4.3 First Insertion of Acetylene

The model reaction considered in this study was the first reaction of acetylene with triethylaluminium. To generate a comparative energy surface, the likely reaction species need to be determined and modelled (Scheme 4-1). The obvious species in the reaction are monomeric triethylaluminium, acetylene, and the product diethyl(butenyl)aluminium. The likely reaction intermediates considered were a coordination complex of triethylaluminium and acetylene, and a transition state of the insertion of acetylene into an Al—Et bond. These structures would be determined with the aid of modelling software. Also considered was the monomer-dimer equilibria of triethylaluminium. The dimeric species is known to be more energetically favourable than the monomer, hence the energy required to break the dimer into the monomeric form is relevant to the overall process.[105] The calculations performed thus far assume that coordination and insertion do not occur while aluminium is in its dimeric form; attempts to model the coordination of acetylene to the Al_2Et_6 dimer showed this process to be too high in energy.

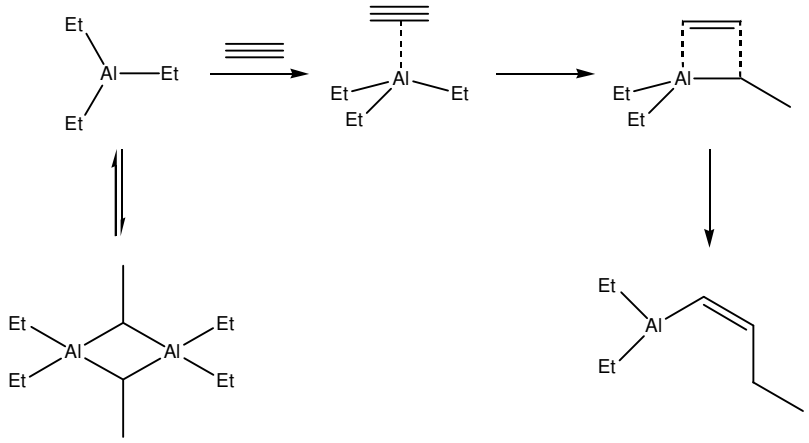

Scheme 4-1. First insertion of acetylene into $AlEt_3$

This reaction was modelled as described above, with all energies compared to the free monomers (the sum of triethylaluminium and acetylene) on a per-Al basis. The optimised coordination complex $AlEt\cdots C_2H_2$ showed acetylene bound at around 2.7Å from planar triethylaluminium. The transition structure for insertion was discovered by shortening the distance between the α-carbon of an Al-Et group and the nearest carbon of coordinated acetylene until a transition state was found. The transition state involves a four-centre structure as shown in Scheme 4-1. The structure of this transition state is similar to that in a previous computational study, where direct insertion of acetylene into AlH_3 was found to be considerably more facile than a metathesis pathway.[106] Optimisation after this point led to the diethyl(butenyl)aluminium product. The energy surface for this reaction can be seen in Scheme 4-2, with the free $AlEt_3$ monomer and acetylene at 0 kJ/mol (**F**). There is first a 38 kJ/mol barrier to the dissociation of the triethylaluminium dimer (**D**) to form the free monomer (the value used for **D** represents half of the total dimer energy, plus free acetylene). The transition state (**TS**) lies at a peak of 35.1 kJ/mol: a 65.7 kJ/mol barrier from the preceding complex **C**, or a total of 73.1 kJ/mol from the dimer **D**. This latter value represents the effective activation enthalpy for the

reaction. The final product (**P**) is extremely energetically favourable, sitting 171.9 kJ/mol below zero, or 207 kJ/mol below the **TS**. Hence, some energy is necessary for dissociation of the dimer to form the reactive monomer, and while the formation of the coordination complex **C** is mildly endothermic, it is only unfavourable relative to the dimer by 7.4 kJ/mol. The major barrier is hence the formation of the transition state **TS**, which precedes acetylene insertion into Al-Et. These results seem to broadly support experimental observations, which see formation of some insertion product at room temperature, but much more once the reaction temperature is increased, providing the energy needed to reach the transition state **TS**. The energy pathway also agrees with the results of Sakai, for the insertion of acetylene into H_2Al-H and H_2Al-CH_3, although the energy of dimer dissociation was not mentioned in that study.[106]

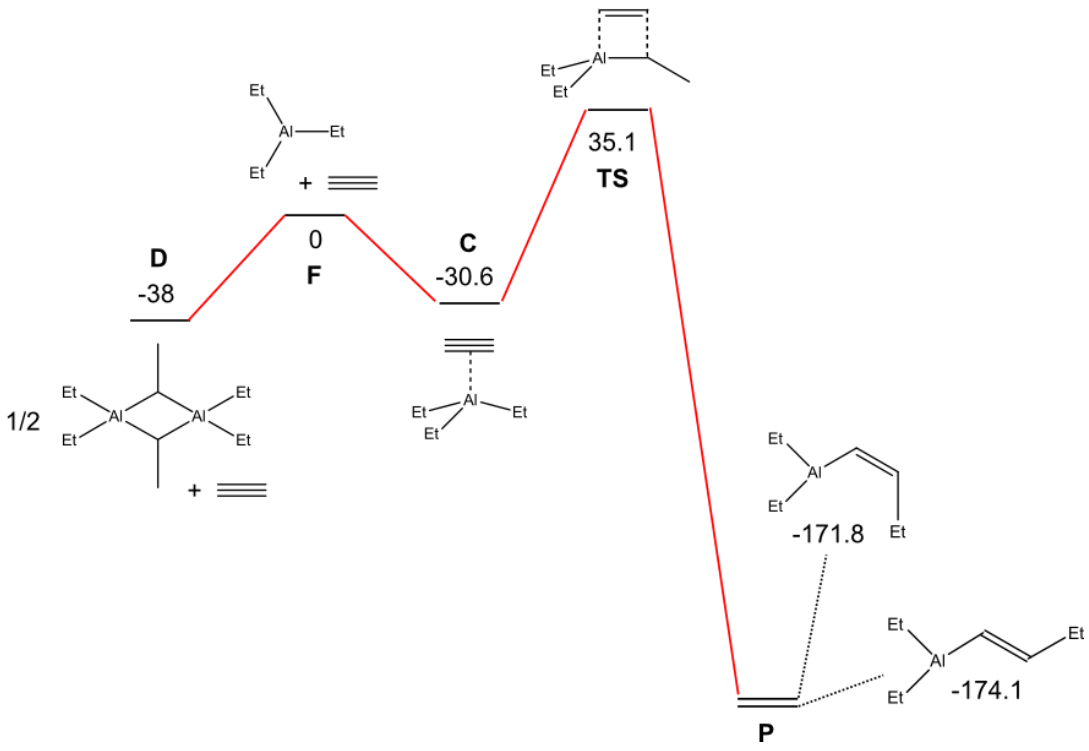

Scheme 4-2. Potential energy surface for the First Insertion of Acetylene into $AlEt_3$ (kJ/mol)

It should be noted that the end product arrived at by geometry optimisation features a *cis*-butenyl moiety at aluminium, which is the correct geometry given the four-centred transition state. The *trans* structure was also modelled for comparison, but found to be only 2.3 kJ/mol more stable than the *cis* isomer.

4.4 Second Insertion of Acetylene

The reactions discussed here were modelled in the same fashion as the first: by coordinating acetylene to the organoaluminium monomer, then pulling acetylene towards the desired position for insertion, to find a transition state; finally optimising this structure to the end product. Several permutations of this reaction were considered here, and will be discussed in turn. As mentioned earlier, Wilke found that acetylene insertion occurred only once, and into one ethyl group. Thus, here will be compared the difference between a second insertion into the Al-butenyl group, and insertion into a second Al-Et group. Both of *cis*- and *trans*-butenyl isomers of diethyl(butenyl)aluminium were used as starting monomers, and both insertion pathways were followed for each isomer. Dimers of diethyl(butenyl)aluminium, featuring *cis*- or *trans*-bridging butenyl groups, were modelled for consideration of the dissociation to monomer; these will be discussed in more detail later.

At a glance, the overall energy surface of the *cis* isomer (Scheme 4-3) does not vary a great deal from that for the first insertion of acetylene. There is a mild energy barrier from the free monomers **F** to the transition state **TS** of 26.2 kJ/mol, or 52.3 kJ/mol if compared to the coordination complex **C** – if anything this is more easily achieved than the first insertion. The product **P** is once again the most stable species in the pathway.

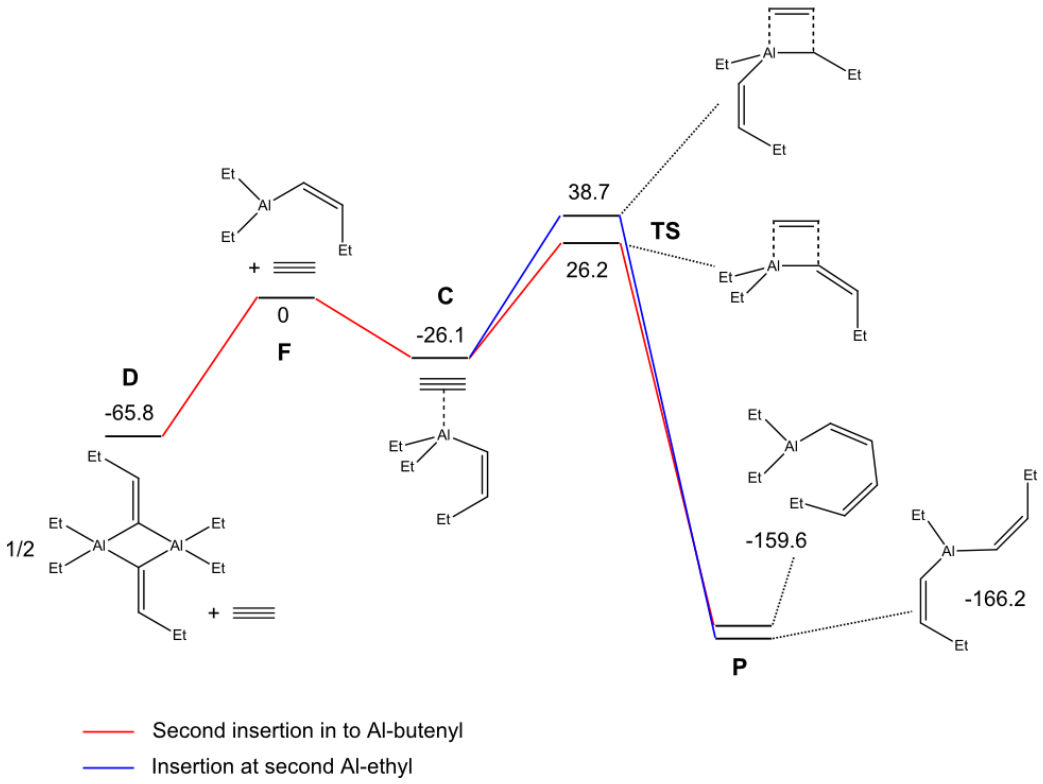

Scheme 4-3. Energy surface for the Second Insertion of Acetylene into *cis*-$AlEt_2$(butenyl) (kJ/mol)

Insertion into a second ethyl group follows an almost identical pathway, except that the barrier to the transition state is 12.5 kJ/mol higher (38.7 kJ/mol) than that for a second insertion into the same group. This agrees with the experimental results that suggest some insertion occurs beyond the first ethyl group, especially in longer experiments, however the major kinetic product would come from a second insertion at Al-butenyl. The end products resulting from the two pathways are similar in energy, though the dibutenyl(ethyl)aluminium product is 6.6 kJ/mol more stable than the diethyl(hexadienyl)aluminium species. It is interesting to compare the second insertion into Al-butenyl with the first into Al-ethyl. The barrier from **C** to the **TS** for the second insertion (52.3 kJ/mol) is somewhat lower than that for the first insertion (65.7 kJ/mol). However, the overall barrier from the dimer to **TS** is 18.9 kJ/mol higher for the second insertion (92 kJ/mol) than for the first (73.1 kJ/mol). This suggests that the second reaction with acetylene, via any pathway, is indeed more

difficult than the first, and that the large increase in required energy relates to the dissociation of the aluminium dimer.

The story is much the same for the *trans* isomer (Scheme 4-4) as for the *cis*. Dimer dissociation rules the overall barrier to insertion, and the individual steps differ by only a few kJ/mol. The relative energies for **C** and **D** vary by less than 1 kJ/mol from the *cis* scheme, though the *trans* monomer is around 2.3 kJ/mol more stable than the *cis*. The energy barrier for insertion into Al-butenyl is 54.5 kJ/mol from **C**, or 94.1 kJ/mol from the dimer **D**. This makes the transition from **C** to **TS** 2.2 kJ/mol more difficult for the *trans* pathway, while that from **D** is 2.1 kJ/mol more difficult. Insertion into a second ethyl group is again less favourable, this time by 12 kJ/mol. The end products resulting from the two insertion pathways are practically identical in energy, varying by about 1 kJ/mol. Overall, there is practically no difference between the energetic pathways for the two geometries.

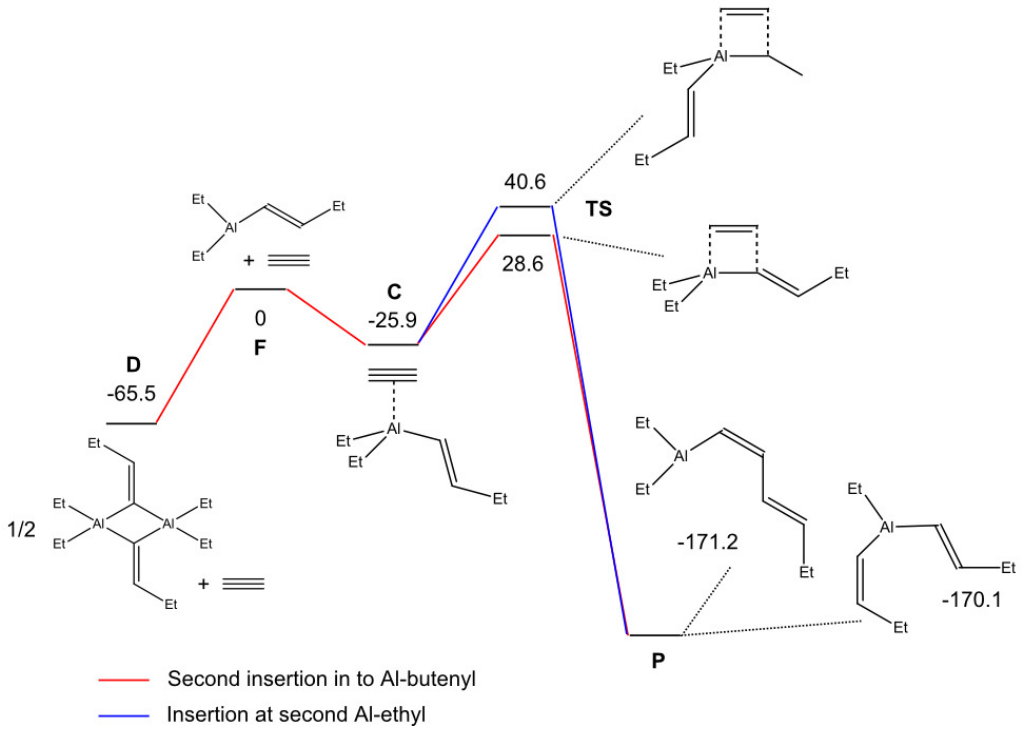

Scheme 4-4. Energy Surface for the Second Insertion of Acetylene into *trans*-$AlEt_2$(butenyl) (kJ/mol)

4.5 Third Insertion of Acetylene

The third insertion of acetylene, into Al-hexadienyl, was modelled, beginning from *cis,cis*-$AlEt_2$(hexadienyl) and proceeding to the end product *cis,cis,cis*-$AlEt_2$(octatrienyl). A dimer for comparison to the free monomers was also modelled to compare dissociation energies, featuring *cis,cis*-hexadienyl bridges. The reaction surface is again analogous to the previous insertions (Scheme 4-5).

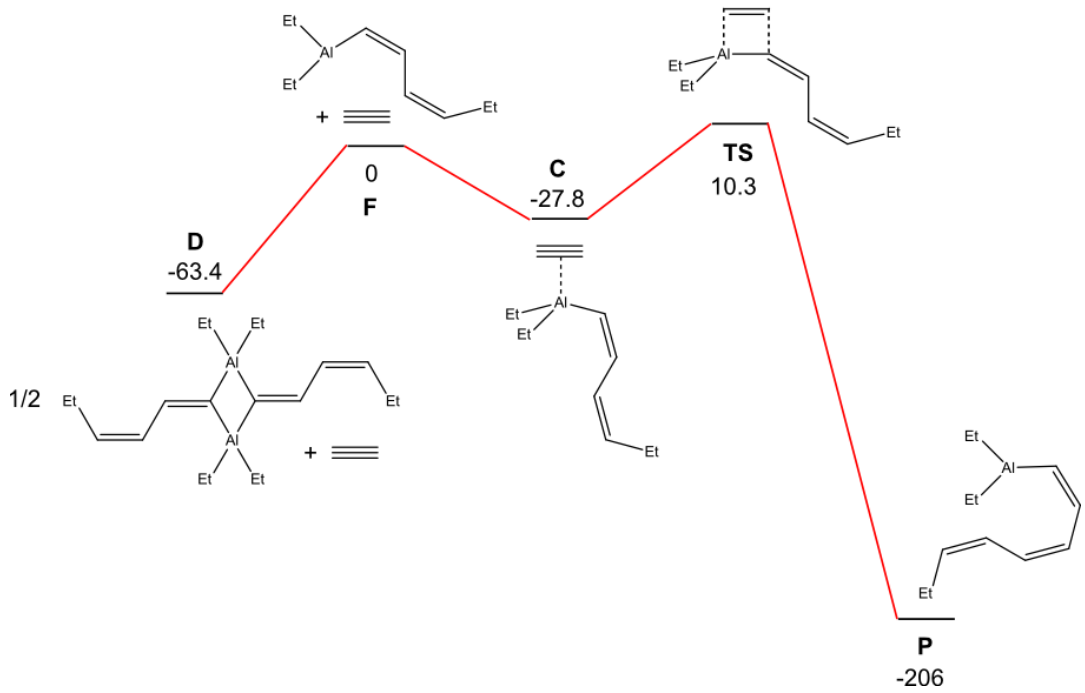

Scheme 4-5. Energy Surface for the Third Insertion of Acetylene (kJ/mol)

The coordination complex **C** lies at a similar position to the previous alkene-bridged reactions, if just a few kJ/mol more stable. The barrier from **C** to **TS** is reduced, at 38.1 kJ/mol, compared to ca. 50-65 kJ/mol for the first and second insertions of acetylene. The aluminium dimer featuring hexadienyl bridges is of similar energy to those with butenyl bridges. So, given the lower overall barrier to the transition state, it may be a fair prediction that insertion at this stage is more facile than the previous insertion; indeed, the total barrier from **D** to **TS** of 73.7 kJ/mol is almost indentical to that for the first insertion into Al-Et (73.1 kJ/mol). However, the high dimer

dissociation energy is still expected to impede overall growth, and this effect is likely to persist in all ensuing growth stages. In light of the previous results, the *trans* pathway was not modelled for the third insertion, as the geometry changes had negligible effect on the overall energy surface.

4.6 Aluminium Dimers

The energy requirement for the dissociation of aluminium dimers, as mentioned earlier, is relevant to obtaining the free monomer that participates in this reaction. For triethylaluminium, the dimer is certainly known to be more stable than the monomer.[105] During the experimental investigations of this project, it became apparent that this factor greatly influences the progression of chain growth after the initial insertion: while the formation of 1-butene was observed at room temperature (albeit a small amount), more than a trace of 1,3-hexadiene was not observed until the reaction was performed at 60 °C. The idea developed that a dimer featuring butenyl bridges would be more stable than one with alkyl bridges, as the π-orbitals in the double bond could contribute electron density to the bridging bonds, strengthening them; thus more energy would be required to dissociate such a dimer for further reaction. It was also noted that a higher initial concentration of $AlEt_3$ (0.6M rather than 0.3M) produced a distribution of oligomers skewed toward the lighter products, after the same reaction time and temperature. The higher concentration meant that $AlEt_2$(butenyl) monomers would be more likely to encounter in solution and re-dimerise – this agrees with Wilke's experiments, performed using neat $AlEt_3$, where 1-butene was the only product seen. Further evidence for this theory has also been attained in the current study, with the crystallographic evidence discussed in Section 3.3.2 proving that the butenyl bridge

is a real feature of these structures. Notably, the crystal structure features a *cis*-arrangment at the bridging alkene, which is consistent with the post-insertion geometry predicted computationally.

It was of interest to model a variety of possible dimeric configurations, based on combinations of $AlEt_3$ and $AlEt_2$(butenyl), and to compare their energies (Figure 4-1). The energies reported are all for *cis* alkenyl groups, and compared to the respective *cis* monomers. The *trans* structures were also modelled, and all showed relative energies within 2 kJ/mol of the *cis* structures; the *trans* energies are given in parentheses. The dimers can be comprised of one of each monomer (**2** and **5**) or two of the same (**1** for $AlEt_3$; **3, 4** and **6** for $AlEt_2$(butenyl)). The results certainly support the notion of stronger bridging by the butenyl groups. Looking at relative energies, there seem to be three approximate energy levels based on the type of bridging ligand. When there are two ethyl bridges (**1-3**), the dimers are stabilised by between 38 and 29.9 kJ/mol, with an increase in terminal butenyl groups corresponding to lower stabilisation (**3 > 2 > 1**). One butenyl bridge (**4, 5**) lowers the relative energy by around 12 kJ/mol compared to two ethyl bridges; again, the dimer with a terminal butenyl group (**4**) is less stabilised than that with only terminal ethyl groups (**5**). The double butenyl bridged dimer (**6**) is yet a further ~18 kJ/mol lower in energy than one featuring a single butenyl bridge. The hexadienyl bridged structure **7** has a stabilisation energy closest to the butenyl-bridged dimer **6**, which is logical as they both feature two briding alkenyl moieties. Hence, it seems fair that the increased dissociation energy for the butenyl bridged dimers is indeed the major factor in impeding rapid successive insertions of acetylene in this system. The alkynyl-bridged species **8** shows a similar stabilisation energy, if slightly lower, than the doubly alkenyl-bridged dimers. This structure is of relevance to the chain transfer

discussions in Section 3.5, using high zirconocene loadings. The postulated mechanism invokes the formation of metal-acetylides, however growth is retarded in certain cases, thus the concept of a stable dimeric species was discussed in that case. The result here supports that proposition.

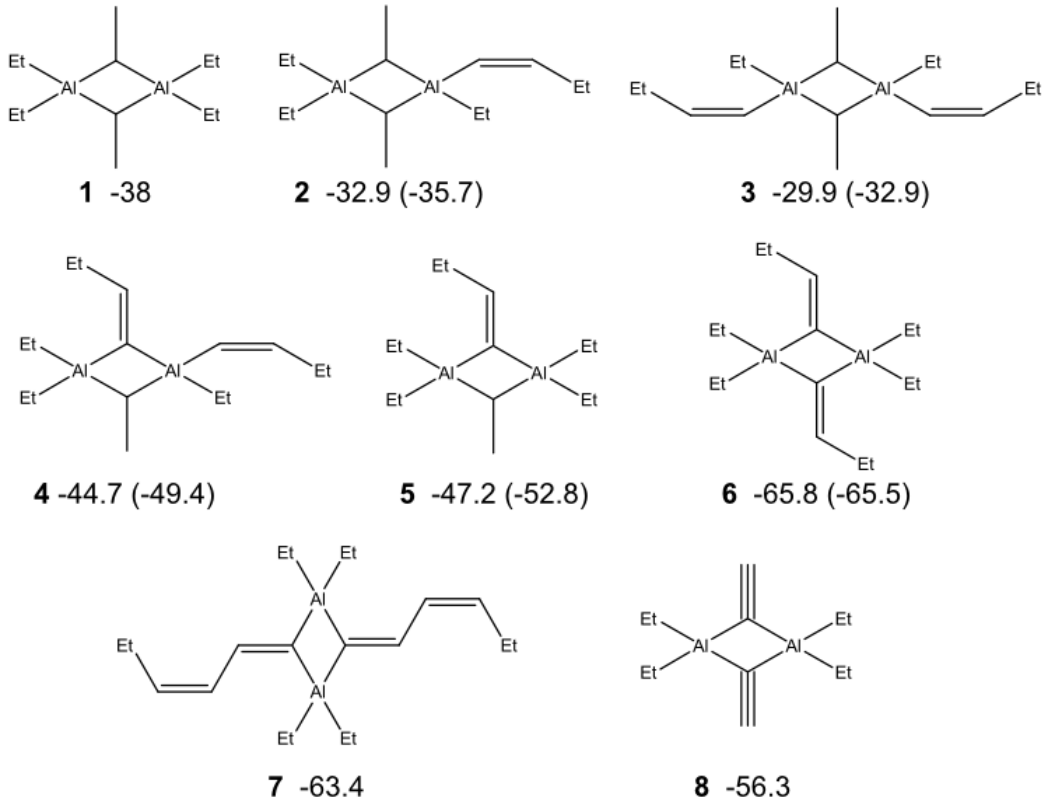

Figure 4-1. Relative Energies of Alkyl/alkenyl/alkynyl-bridged dimers (kJ/mol) Energies given are for the reaction $Et_2Al\text{-}R \rightarrow \frac{1}{2}Al_2Et_4(\mu\text{-}R)_2$

4.7 Diethylaluminiumchloride

The use of diethylaluminiumchloride was trialled as an activator of Cp_2MCl_n, and also on its own, during early oligomerisation trials. It was ineffective as an activator (although this may relate more to the poor performance of the metallocenes) and only slightly active alone: a long experiment at high temperature produced only a small amount of oligomeric product. In light of the results regarding strength of the butenyl bridged dimers, this system was modelled for the insertion of acetylene into an ethyl

group, beginning from a chloride bridged dimer (Scheme 4-6). The energy surface forms a now familiar profile leading, via transition state, to a very stable product. The barrier for dimer dissociation is 55.7 kJ/mol, supporting the notion of a strong chloride-bridged dimer. The energy requirement to proceed from **D** to **TS** is 94 kJ/mol, which is similar to that for the second insertion at $AlEt_2$(butenyl), although the 68.3 kJ/mol gap from **C** to **TS** is reminiscent of the more difficult insertions at a second ethyl group. Hence, this being only the first insertion of acetylene, it is perhaps understandable that this compound is relatively unreactive: the barrier from dimer to transition state is 20.9 kJ/mol higher than the first insertion of acetylene into triethylaluminium.

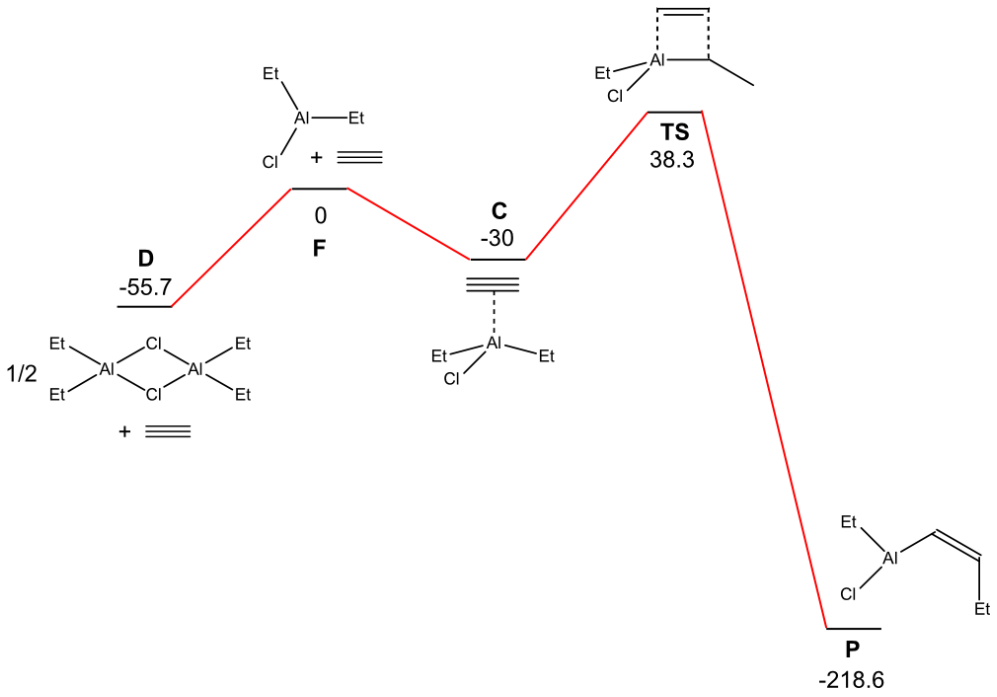

Scheme 4-6. Energy Surface for the Insertion of Acetylene at $AlEt_2Cl$ (kJ/mol)

4.8 Chain transfer with hydrogen

A number of experiments were performed with triethylaluminium using a mixture of acetylene and dihydrogen, the latter as a potential chain transfer agent (Section 3.4). It was found that a large amount of dihydrogen impeded the production of the longer

oligomers and solid polymer seen in comparable runs without dihydrogen. Some other results (GC-MS) suggested that chain transfer was indeed occurring to some extent, and it was postulated that this could result in a species such as $AlEt_2H$ – the dimer of which might be extremely strongly bound, and impede further reactions. The hydride bridged dimer (Figure 4-2) was modelled versus free $AlEt_2H$, and found to be 65.3 kJ/mol more stable – a fraction more so than the double butenyl bridged dimer. The literature reports that $AlEt_2H$ also exists as a hydride bridged trimer,[105] so this structure was modelled for comparison and found to be even more stable than the dimer at 80.2 kJ/mol below monomer (on a per-Al). Thus, it is very believable that these polymeric structures impede further reaction with acetylene.

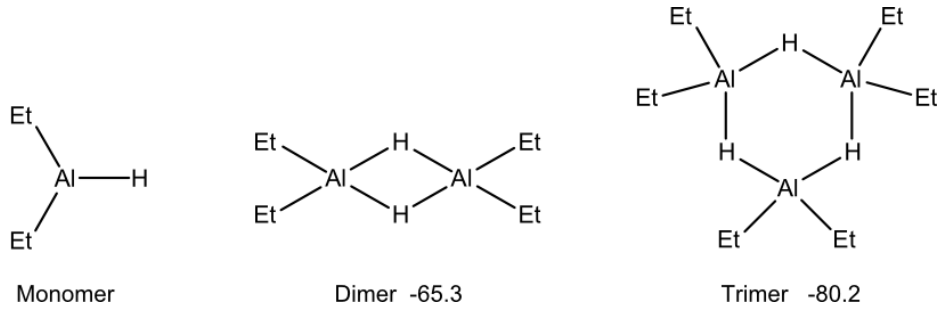

Figure 4-2. Relative Energies of Polymeric forms of $AlEt_2H$ (kJ/mol)
Energies are per mole of Al: $Et_2AlH \rightarrow 1/2\ Al_2Et_4(\mu\text{-}H)_2$ or $1/3\ Al_3Et_6(\mu\text{-}H)_3$

The chain transfer process itself was also of interest as a computational target. As mentioned, there is some evidence for chain transfer by dihydrogen in this system (discussed in Section 3.4), although a large amount of oligomeric product remained bound to metal after catalytic trials. This suggested that the chain transfer process was not exceptionally facile, and thus warranted further investigation. An energy surface was constructed beginning from $AlEt_2$(butenyl) whereby an incoming H_2 molecule facilitates cleavage of the Al-C bond, forming 1-butene and an aluminium hydride (Scheme 4-7). Even without the consideration of dimer dissociation, there is a barrier of 93.2 kJ/mol to the discovered transition state, which is higher in energy

than most of the discussed acetylene insertions *including* dissociation. The observation of non-deuterated oligomers in a D_2O quenched reaction solution, where hydrogen had been employed in the reaction, does confirm that this process is relevant. However the models presented here show the process not to be particularly facile and support the mediocre effect of hydrogen as a chain transfer agent, as observed in this system.

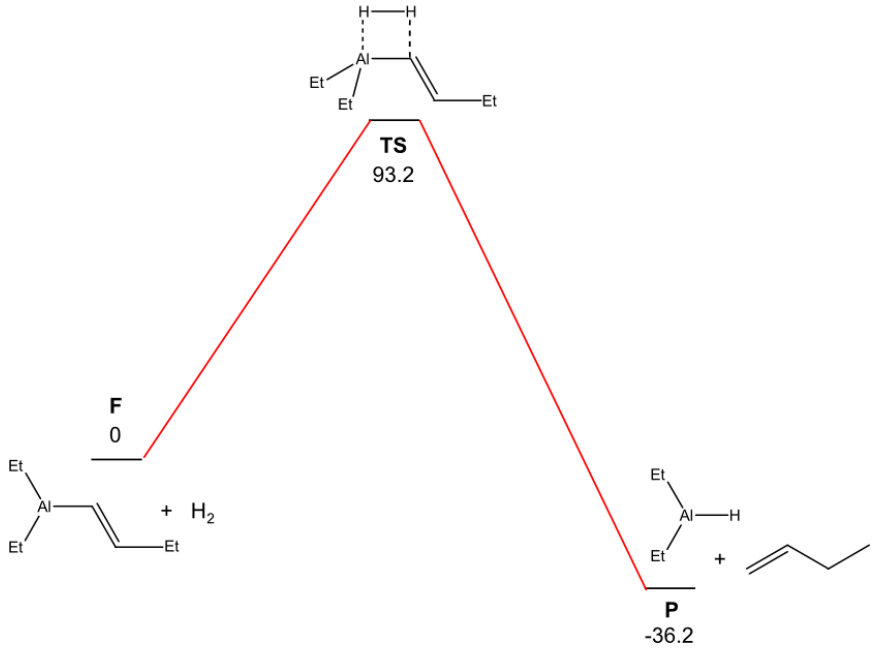

Scheme 4-7. Energy Surface for Hydrogen facilitated chain transfer at Al (kJ/mol)

4.9 Summary and Conclusions

The use of computational models has proven to be a useful tool when experimental evidence is lacking, or simply to reinforce the results of a study; in this case, it has been possible to do both. The proposed strength of a butenyl-bridged aluminium dimer, evidenced by crystallographic evidence, has been shown computationally to play a large role in impeding the reaction of acetylene with triethylaluminium beyond the first migratory insertion. Generation of energy profiles for these insertions, proceeding via four-centre transition states, has shown the process to be

relatively facile before consideration of aluminium dimers, leading to very thermodynamically favourable products, which goes even further toward underlining the retarding effect of the discussed dimeric species. A comparison of possible dimeric structures showed the stability of these structures to increase on the move from zero to one, then two butenyl bridges. Analogous dimers bridged by other groups support other experimental evidence such as the slowing of the reaction in the presence of chloride, hydrogen or acetylide bridges. The lacklustre result of using dihydrogen as a chain transfer agent was also confirmed by the presence of a particularly high barrier to Al-C bond cleavage by this reagent. Unfortunately, time constraints did not allow for a deeper investigation of mechanistic aspects, such as the mode of chain branching observed experimentally. Thus, further theoretical studies are required to fully understand growth in this system.

Chapter 5 Copolymerisation of Acetylene and Arenes

5.1 Introduction

As noted in Section 2.3, the first use of ethylaluminiumdichloride, as an activator for one of the metallocenes, led to an exothermic reaction in the presence of the aluminium alkyl alone. This quickly led to polymerisation and a large amount of dark solid was collected. It was a welcome surprise to note the rapid consumption of acetylene during this trial, however it was not expected that this would occur in the absence of a transition metal. The nature of this reaction and its products was investigated further, both in terms of oligomeric and polymeric products, and of the reaction itself. These results were different enough to the oligomerisation results discussed in Chapters 2 and 3, that it was felt they should be presented separately; hence they will be discussed here.

5.2 Investigation of the Reaction

The residual toluene phase from the initial polymerisation was analysed by GC-MS, searching for clues as to the nature of the reaction, and of the polymer. A number of soluble oligomers were identified, with molecular weights of 210, 236, 328, 354, and higher. Many of the observed molecular weights resolved as small clusters of peaks, suggesting a number of isomers for a given mass. The increase in molecular weight of these clusters appeared to follow pattern of alternating additions of toluene (92) and acetylene (26) units, which pointed to a copolymerisation of acetylene and the solvent. The reaction was trialled in petroleum spirits to test this theory, and no reaction was seen to occur, however the use of benzene as solvent did effect a similar formation of polymer. Analysis of the organic residue from this reaction showed

peaks of molecular weights 182, 208, 286 and higher, which follow a similar growth pattern to that seen for toluene, this time with alternating benzene (78) and acetylene units. The oligomer structures were not certain at this stage, but the available library spectra all pointed to combinations of arene and acetylene units.

Literature investigation revealed that a similar process was documented some years ago in the work of Cook and Chambers, who in 1921 reported on the condensation of benzene and acetylene in the presence of trichloroaluminium.[107] The major reported products of this reaction are 1,1-diphenylethane (from two benzenes and one acetylene) and 9,10-dihydro-9,10-dimethylanthracene (one further acetylene) (Figure 5-1), and a small amount of dark uncharacterised solid. Further studies by Nieuwland documented the results for the use of various aromatic compounds in this reaction, which were found to behave in a similar fashion.[108,109]

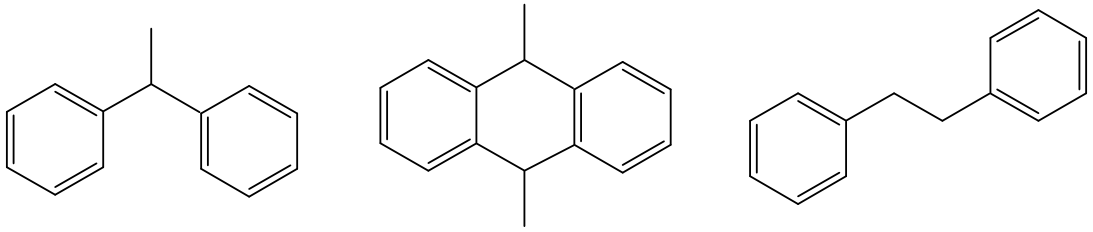

Figure 5-1. Possible condensation products of acetylene and benzene

It is clear that the recent results have produced a wider variety of products than those originally reported. This is to be expected, considering the use in this work of acetylene under pressure with vigorous stirring, whereas the early experimenters simply passed acetylene gas through the reaction solution. In the interest of gaining more information, the reactions with benzene and toluene were repeated in a controlled manner, and the oligomeric phase collected before the formation of

polymer. In terms of GC-MS evidence, the toluene-based oligomers were more difficult to interpret, owing to the multiple isomers at each molecular weight – presumably due to different positions of the toluene methyl group. The benzene-based oligomers, however, show only one peak for each of MW 182 and 286, and two for 208. The MS for the peak at 182 is a very close match for 1,1-diphenylethane, is in accordance with Cook's original report, and proton NMR of the mixture, although complex, showed signals attributable to the methine (quartet at 4.21 ppm) and methyl protons (doublet at 1.71 ppm) of this compound.[110] The higher peaks could not be definitively identified, although the peaks at MW 208 – the correct mass for the anthracene compound – have mass spectra that clearly rule out Cook's reported compound. The best matches of library mass spectra, all remarkably similar, still however suggest some arrangement of two benzene and two acetylene units. One possibility that was considered was bibenzyl (Figure 5-1), but there was no evidence of this compound by NMR. Styrene, a likely precursor to all these compounds, was neither detected by GC-MS or NMR, so presumably reacts quickly to form higher products. All in all, the evidence thus far has pointed to a Friedel-Crafts type addition of an arene to acetylene, catalysed by Lewis acidic ethylaluminiumdichloride, which continues to form higher oligomers and polymer following this initial addition (Scheme 5-1). This mechanism is consistent with that reported for the trichlorogallium catalysed vinylation of arenes by terminal acetylenes.[111]

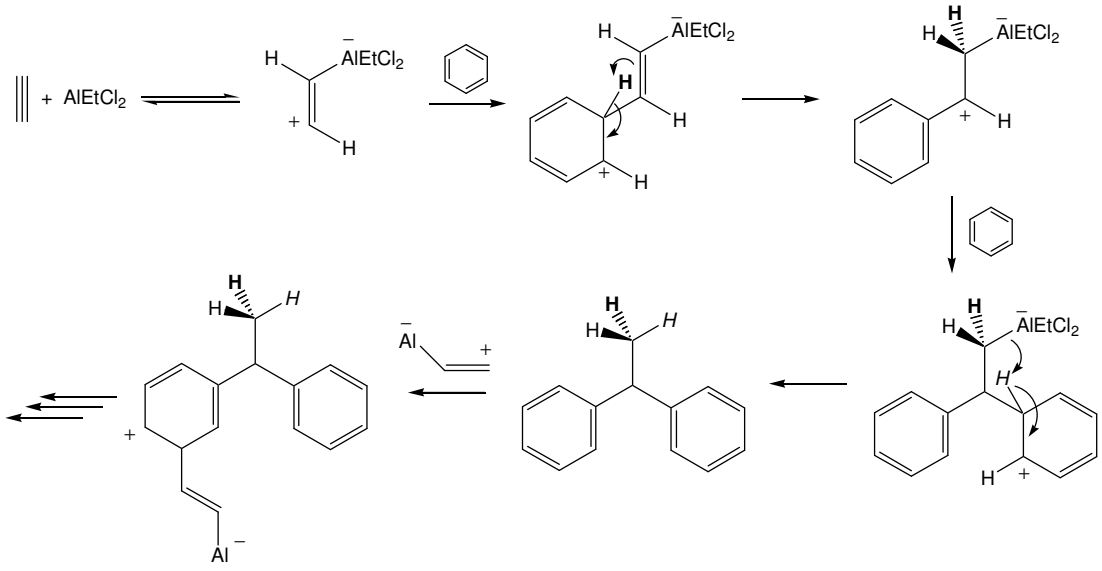

Scheme 5-1. Proposed Friedel-Crafts addition of acetylene to benzene

5.3 Nature of the Polymer

The black solid formed from this reaction was noted to fade to a yellow colour over time, and this process could be accelerated by an acid quench. Based on this colour change, it is believed that aluminium remains bound to the polymer after reaction, but is released on quenching. The polymer is extremely hydrophobic in nature, so quenching was performed in MeOH/HCl to yield a bright yellow solid that remains stable after months, kept in air. The use of the different arenes led to quite different activities over 15 minutes. There was 30.1 g of polymer produced per gram of Al for the toluene/acetylene mixture, but this dropped to 8.6 g polymer/g Al for benzene/acetylene; this is probably due to the more activated ring system in toluene, compared to benzene. The use of trichloroaluminium was also trialled as a comparison to ethylaluminiumdichloride, however both compounds were found to be just as active in facilitating this reaction. Some attempts were made to analyse the polymers, but were not particularly successful. Melting point determinations were performed in air, which led to charring by 350 ºC; the toluene polymer started to

darken around 160 ºC, while the benzene was unchanged until above 200 ºC. Solution studies were hampered by extreme insolubility, the polymers tended to do little more than swell in a number of different solvents – even trichlorobenzene at 130 ºC (commonly used to dissolve PE) – and as such it was not possible to analyse them by GPC or solution NMR. Solid-state ^{13}C NMR spectra were obtained, however, which showed the expected broad aromatic and aliphatic signals. Interestingly, for the benzene polymer, the methine or methylene resonance (~41 ppm) was much stronger than the methyl resonance (~20 ppm), which would tend to favour a structure similar to bibenzyl. While the evidence suggested that this structure did not form in the early stages of this reaction, it cannot be ruled out at higher molecular weights; neither can cross-linking between any reactive unsaturated groups in the polymer, to form a similar arrangement. Overall, the polymer may be a combination of various structural motifs, and it is difficult to be sure which are more favoured given the available data; some conceivable structural arrangements are depicted in Figure 5-2. It is unfortunate that more information could not be obtained about this material, but the equipment for polymer analysis was not available. Given the nature of this reaction and the required acid quench, however, preparation of the thin-film samples preferred for mechanical testing may not have been feasible, and the high polymer insolubility would make GPC analysis of the bulk solid difficult.

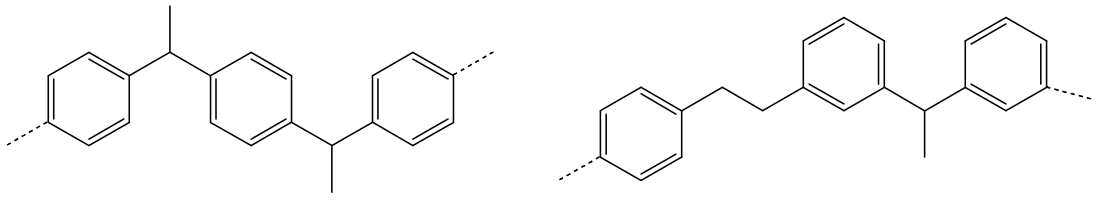

Figure 5-2. Possible polymer structures

5.4 Summary and Conclusions

The co-polymerisation of arenes and acetylene was observed, catalysed by ethylaluminiumdichloride and trichloroaluminium. This reaction quickly proceeds to a dark solid, which can be quenched to yield a bright yellow, hydrophobic, air-stable solid. Analysis suggests the alternating addition of arene and acetylene units to form higher structures as evidenced by GC-MS and NMR evidence, although the major binding mode for the bulk solid remains unclear. Testing of the mechanical properties of the polymer was not possible at this time.

Chapter 6 Bis(imino)pyridineiron(II) Catalysts

6.1 Introduction

A class of complex that has acquired much attention in the field of non-metallocene ethylene polymerisation is that featuring bis(imino)pyridine ligands. Of particular interest are iron complexes of these ligands, which have demonstrated excellent activity in ethylene polymerisation, in some cases greater than Group IV metallocenes under similar conditions.[63] They also allow for quite a degree of variability: within the same ligand framework, the properties of these catalysts can be altered significantly by varying substitution at the N-aryl rings. Two particular catalysts have been focussed on in the current studies, which exhibit quite different behaviours in their reactions with ethylene, and are shown in Figure 6-1. When activated with MAO the 2,6-diisopropylphenyl derivative ("2,6-*i*Pr") is a very active polymerisation catalyst, forming high molecular weight polyethylene (PE) (M_w > 600000) with a catalyst activity of 5340 g/mmol·h·bar.[112,113] The *ortho*-tolyl derivative ("*o*-tolyl") exhibits reasonable activity of 1300 g/mmol·h·bar, however forms primarily oligomeric products. The oligomers up to ~C_{30} follow a Schulz-Flory distribution, while a low molecular weight PE fraction is also obtained (M_w ~ 1500).[114] The ligand N-aryl rings of the two catalysts vary in steric bulk at the *ortho* positions, which has a marked effect on activity. The use of a 2,6-dimethyl substituted ligand, in comparison to the 2,6-diisopropyl system, increases catalyst activity but lowers polymer molecular weight. The difference in activity effected by these ligand modifications has been attributed to rotation around the N-aryl bonds.[114,115] For bulkier 2,6-diisopropyl substitution, rotation is a high energy barrier, and it has been suggested that this locks the catalyst into one conformation,

disfavouring β-H elimination and leading to high molecular weight PE. For 2,6-dimethyl substitution the barrier is less, and for the *o*-tolyl catalyst even more so, such that other catalytic processes impeded by steric bulk are possible; the rate of β-H elimination is increased, for example, leading to lower molecular weight products. Hence, this class of complex demonstrates a great deal of flexibility in producing oligomeric and polymeric products.

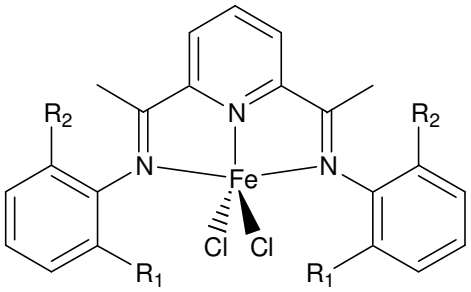

2,6-Bis-[1-(alkylphenylimino)ethyl]pyridineiron(II) dichloride
R_1, R_2 = 2,6-*i*Pr; R_1 = Me, R_2 = H

Figure 6-1. Notable Bis(imino)pyridineiron(II) complexes

What makes the 2,6-*i*Pr catalyst particularly interesting, however, is its behaviour in the presence of metal alkyls. An initial report showed that in the presence of diethylzinc, the properties of the polymer produced by this catalyst changed dramatically.[116] The more equivalents of the zinc reagent that were added, the lower was the molecular weight of PE produced and the narrower the polydispersity, without a significant loss of activity. In a sample run that was stopped before polymer had formed, GC analysis showed that a Poisson distribution of paraffins had formed, the average chain length of which was directly related to the reaction time. This was a remarkable change in behaviour from the standard system, and a series of investigations in more depth revealed that diethylzinc undergoes rapid and reversible chain transfer with the iron catalyst. So rapid is this exchange (thought to be in excess of 100 times faster than insertion at the iron centre),[117] that all polymer chains

present in the system, each starting from insertion into an ethyl group, grow at the same rate. This regulates chain growth, and leads to the observed distribution. The overall process is termed "catalysed chain growth on zinc," as the chains appear to grow at zinc centres, although actual ethylene insertion occurs at iron (Scheme 6-1). It should be noted that chain growth in this system is ultimately not a catalytic process with respect to $ZnEt_2$, as the oligomer chains remain bound to zinc. Chains can be released by reaction with $Ni(acac)_2$ in the presence of ethylene, regenerating diethylzinc, or could be released following an acid quench. In light of these initial investigations, a number of metal alkyls were investigated for analogous behaviour, including a range of aluminium and zinc alkyls, *n*BuLi, $(n\text{Bu})_2\text{Mg}$, BEt_3, $SnMe_4$, $PbEt_4$ and $GaMe_3$, however diethylzinc remained the best choice in terms of controlling chain growth in this system.[117] A separate study examined a number of other transition metal catalysts for their behaviour toward ethylene in the presence of diethylzinc, and found the 2,6-*i*Pr iron complex to be the best match for the chain transfer agent.[118]

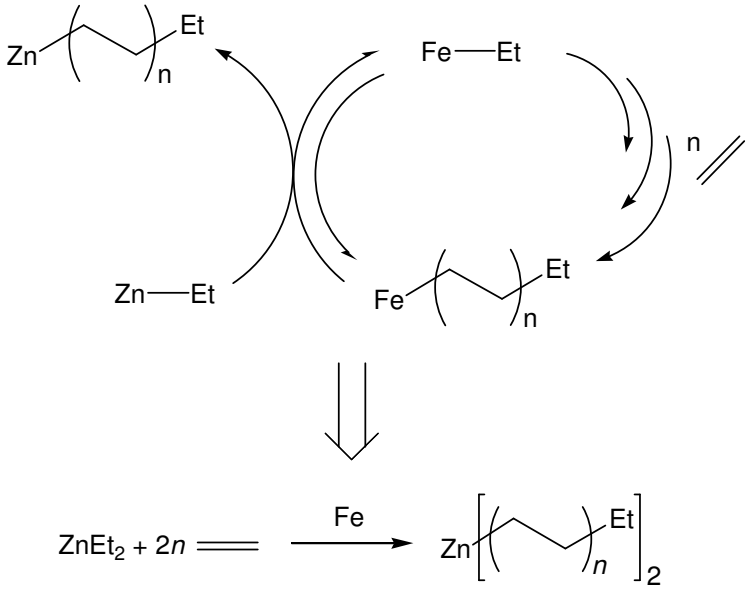

Scheme 6-1. Iron catalysed chain growth on Zinc

It has been suggested that the reaction of this iron catalyst with phenylacetylene showed traces of a dimer.[119] Given this and the ability of diethylzinc to control chain growth with ethylene, this system seemed an ideal target to test for acetylene oligomerisation. This work was commenced at Imperial College London during a research exchange visit with Dr. George Britovsek.

6.2 The 2,6-*i*Pr Catalyst

6.2.1 Initial Oligomerisation Trials

Initial catalytic trials with the 2,6-*i*Pr complex were performed using 1-hexyne as monomer. The reason for this was that the supply of acetylene was uncontrollably delayed upon commencement at Imperial College, thus the use of 1-hexyne served as a probe for general reactivity of this catalyst toward alkynes. Owing to the high reported activity of this complex with ethylene, only 5 μmol was used per trial. Standard conditions for the system were 100 equivalents of MAO and 500 of diethylzinc, in 50 mL of toluene. The addition of 2000 equivalents of 1-hexyne led to an initial darkening of the solution, however this did not develop further over 30 minutes. GC-FID and GC-MS analysis of the quenched solution showed evidence of several oligomeric products. Most prominent was a large peak for 3-octene, which could form via a single hexyne insertion into an ethyl group derived from diethylzinc. There were three minor unidentified products: two of molecular weight 194 and one of 276, which were not definitively identified, but are the correct masses for two and three hexyne insertions into an ethyl group. Some cyclotrimerisation was evident based on the presence of small amounts of 1,2,4- and 1,3,5-tributylbenzene, and overall around half of the unreacted monomer remained. An increase in temperature to 60 ºC had little effect on product output, or overall conversion of

1-hexyne. The use of neat $ZnEt_2$ failed to generate any oligomeric products, even after stirring for 20 hours, highlighting the role of the iron catalyst. The cobalt and manganese analogues of the iron catalyst were trialled under these conditions (100 eq. MAO, 500 eq. $ZnEt_2$), but did not produce the oligomers seen for the iron catalyst. This result is compatible with the previously reported greater reactivity of the iron catalyst.[118] So, initial screenings showed the iron catalyst to be reactive toward alkynes, although the major product suggests just a single linear insertion, and total monomer conversion was not achieved. The presence of cyclotrimers is interesting, as these structures cannot form via linear insertions into an ethyl group, and suggests that another parallel growth process may be occurring.

Before screening the iron catalyst with acetylene, the reactivity of this monomer with neat diethylzinc was tested. Given the results when triethylaluminium was used as an activator (see Chapter 3), it seemed sensible to test the metal alkyl alone at the onset. The reactivity observed for triethylaluminium was not, however, seen for diethylzinc. At room temperature the reaction solution developed a blue colour over 30 minutes, while at 60 ºC a darker purple hue evolved. GC analysis revealed the presence of only a trace of 1-butene (less than 1 mol% of the diethylzinc added), even at the higher temperature, and no higher oligomers. This was only a minute output compared to that of triethylaluminium with acetylene, so was not considered to be an issue.

The mild reactivity of the iron catalyst toward 1-hexyne was not the best indication of things to come. When the Fe/MAO/$ZnEt_2$ system was exposed to 1 barg of acetylene, a rapid reaction occurred and a bright red colour quickly formed (ca. seconds). This was accompanied by an initial exotherm to almost 50 ºC, which

was controlled using an external ice bath and the temperature kept around 20 ºC from then on. Interestingly, the initial flurry of activity did not continue throughout a 30 minute run, although the red solution did thicken noticeably after around 10 minutes. A slower acetylene uptake and a milder exotherm were noted, but these seemed to cease after around 15 minutes. Work-up yielded almost 2 g of bright red polymer, which darkened to black over time when left in air. GC analysis of the yellow organic phase confirmed the presence of 1-butene, 1,3-hexadiene and several isomers of octatriene, as well as showing evidence for some higher oligomers. These polyenes are consistent with linear acetylene insertion into an ethyl group; a small amount of benzene above the solvent background was also detected. Thus, there was evidence that this system was producing oligomeric products, and although the bulk of the product at this stage was solid polymer, this catalyst was certainly worth investigating further. During these initial experiments, the cobalt analogue tested with 1-hexyne was trialled, but showed only a mild reactivity toward acetylene. Given this and the similar results of the cobalt and manganese complexes with 1-hexyne, the manganese analogue was not trialled with acetylene.

It was useful to benchmark the reactivity of the iron catalyst without diethylzinc present, simply activated by MAO, to see if the metal alkyl was having an obvious effect. The difference between the two reactions was striking. Exposure of the activated iron catalyst to acetylene effected an almost instantaneous evolution of a dark purple colour in solution, after which no further activity was observed. The purple solid that resulted was jelly-like and weighed over 16 g when wet, however after sitting in a beaker in the fume hood overnight, only 250 mg of solid remained. It appears that polymer production resulted in the formation of a polymer/solvent gel, holding the majority of the reaction solvent, but which later evaporated. Attempts to

swell the polymer again by soaking it in toluene were not successful. It did seem curious that such a seemingly active catalyst would deactivate so quickly – the catalyst in the presence of diethylzinc also seemed to slow after its initial flurry of activity, but not in such a drastic way. This catalyst deactivation is discussed later, as is the nature of the polymer (see Sections 6.2.4 and 6.2.5).

6.2.2 Optimisation for Oligomer Production

Clearly we were dealing with a very active catalyst system – perhaps too active in the context of acetylene oligomerisation, given the rapid formation of solid product. This differs from the known activity with ethylene, as solid polymer does not begin to form immediately, and not for several minutes in the presence of diethylzinc where oligomer length can be tuned by adjusting the run-time. Evidently this catalyst is initially much more reactive toward acetylene than ethylene, so much so that even with the chain transfer agent present, polymer formation occurs in seconds. However, the metal alkyl definitely seemed to slow the reaction somewhat, compared to the system without zinc, so this system was explored in greater depth to see if product output could be directed towards the oligomeric contingent. A number of catalytic trials were performed, varying the concentrations of diethylzinc and the iron catalyst itself, and are summarised in Table 6-1.

The oligomer yield is based on GC-FID and GC-MS quantification versus an *n*-alkane internal standard. As was the case for the triethylaluminium studies, a large number of oligomeric products were identified above C_8, which made exact quantification difficult. So, ranges of the GC trace containing the same molecular ion were integrated, with each range corresponding to likely growth products: butene (56), hexadiene (82), octatriene (108), C_{10} (134), and so on. The oligomer weights

presented here are the sum of all oligomers, including produced benzene. More detailed work has been done toward identifying these products, and this is discussed later (see Section 6.2.3).

Table 6-1. Summary of Product Output from Trials of 2,6-*i*Pr Fe Catalyst[a]

Fe (µmol)	MR_x	Equivalents	Oligomer (g)	Polymer (g)	Total Mass (g)	% Oligomer
5	$ZnEt_2$	500	0.11	2.34	2.45	4.6
5	$ZnEt_2$	1000	0.27	2.66	2.93	9.1
5	$ZnEt_2$	5000	1.30	0.39	1.69	76.9
5	$ZnEt_2$	10000	1.75	0.09	1.84	95.2
20	$ZnEt_2$	500	0.87	4.48	5.35	16.2
50	$ZnEt_2$	500	1.34	1.96	3.30	41.0
5	$AlEt_3$	500	0.01	1.45	1.46	0.7
5	$GaMe_3$	500	0.50	1.30	1.80	27.7
5[b]	$ZnEt_2$	500	0.22	1.05	1.27	17
50[b]	$ZnEt_2$	500	1.43	Trace	1.43	100

[a] Conditions: room temperature, 50 mL toluene, 30 minutes, 1 barg acetylene
[b] Reaction performed under Acetylene/H_2 (2 bar:9 bar)

Broadly speaking, an increase in diethylzinc concentration led to a greater proportion of oligomeric product. What also happened at higher concentrations, however, is that the overall product mass decreased, and the oligomer distribution was pushed toward the earliest growth products. For 500 and 1000 equivalents only a small change in distribution was observed, though the oligomer output did double, whereas the use of 5000 and 10000 equivalents all but stopped polymer formation. The use of a higher concentration of diethylzinc could be expected to increase the rate of chain transfer, and the greater number of possible chains (2 per zinc) would mean that each chain would take longer to grow on average. Hence, the progression to solid polymer would be slowed, although chain growth would be expected to continue throughout a trial. However, the use of 5000 and, particularly, 10000 equivalents of diethylzinc had a very severe effect on the progress of this reaction. In both trials the characteristic red colour appeared with an accompanying exotherm, but the thickness

of solution seen for lower zinc concentrations never developed. These solutions remained quite fluid throughout, particularly for the highest zinc concentration. There was only minimal acetylene uptake noticeable after the initial period, which is at odds with the premise that chain growth should continue. Rather, these high zinc concentrations seemed to inhibit chain growth beyond an initial point, which is particularly noticeable when considering the oligomer distribution (Figure 6-2).

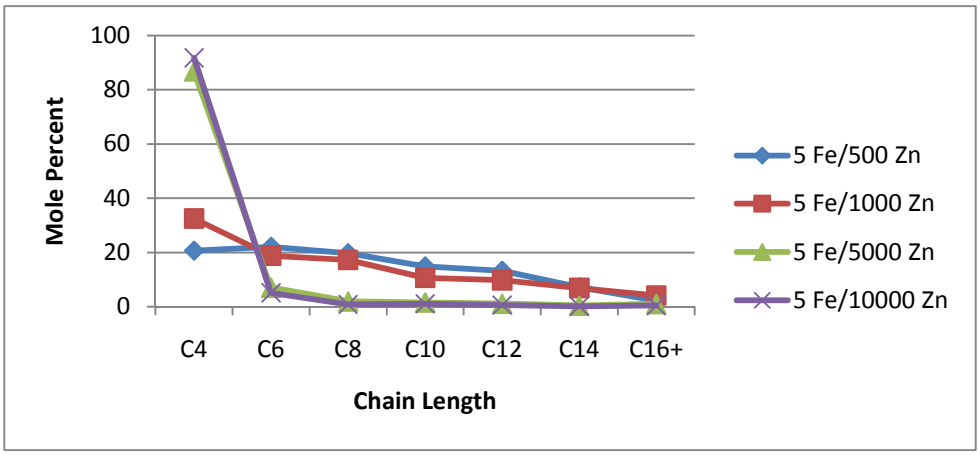

Figure 6-2. Mole% of Linear Oligomers from runs varying [Zn]

The use of greater concentrations of the iron catalyst and diethylzinc together would also be expected to increase the rate of chain transfer, so this might help to reduce polymer formation. Trials with 20 and 50 µmol of the catalyst (500 eq. $ZnEt_2$) confirm this, with higher concentrations producing a greater proportion of oligomers. There was a corresponding large increase in polymer yield when 20 µmol of Fe was used, though the overall yield dropped for 50 µmol of Fe. The oligomer distribution for 20 µmol of Fe stayed much the same as the 5 µmol run, however the use of 50 µmol pushed the distribution toward the lighter products, as shown in Figure 6-3. Again, this is consistent with a higher rate of chain transfer between Fe and Zn. Another way of thinking about this is to consider the much higher concentration of ethyl groups present at higher Fe and Zn loadings, relative to the concentration of

acetylene. As such, chain growth occurs at more oligomer chains, and the net result would be a greater number of shorter chains.

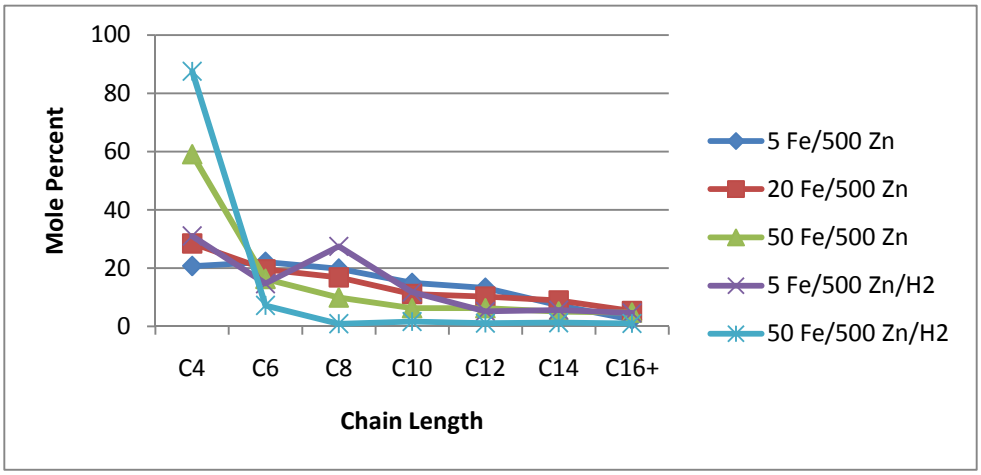

Figure 6-3. Mole% of Linear Oligomers for runs varying [Fe]

All runs with this catalyst produced a small amount of benzene above the solvent background, as was noted in the first trial. This amount seemed to be proportional to the amount of iron catalyst present, but did not vary when the zinc concentration was changed; this benzene was produced even in the absence of diethylzinc. As the benzene is a relatively minor product, and its formation likely unrelated to that of the linear products, it was excluded from the oligomer distributions. A trial run using the iron catalyst, diethylzinc and no MAO failed to produce any benzene, but did produce the characteristic polymer and oligomers in reduced quantities, so benzene production must be related to catalyst activation by MAO. The production of benzene, and the cyclotrimers formed with 1-hexyne, suggests a different mode of catalyst action or perhaps another active species in solution, as these arenes cannot form beginning from an ethyl group, while the observed linear oligomers must. While linear growth would appear to be the major process in this system, the mechanism is unclear: these products might form via a metallocycle mechanism or

by a Cossee-type process. Beginning from M-Et, the Cossee-type pathway could explain the linear growth products, by successive acetylene insertions into an ethyl group (Scheme 6-2). The absence of ethyl groups in the cyclotrimer products might be better explained, however, by a metallocyclic mechanism. This could occur via the oxidative addition of two acetylenes to a low-valency iron(I) species, followed by further addition and reductive elimination of an arene from an iron(III) species (Scheme 6-2); other redox couples may also be possible, such as iron(II)/iron(IV), or iron(0)/iron(II). This theory is in favour of a secondary active species in solution, different to that which facilitates linear growth. (These reaction mechanisms have been investigated further in the context of the *o*-tolyl catalyst, and are discussed in Section 6.3.2).

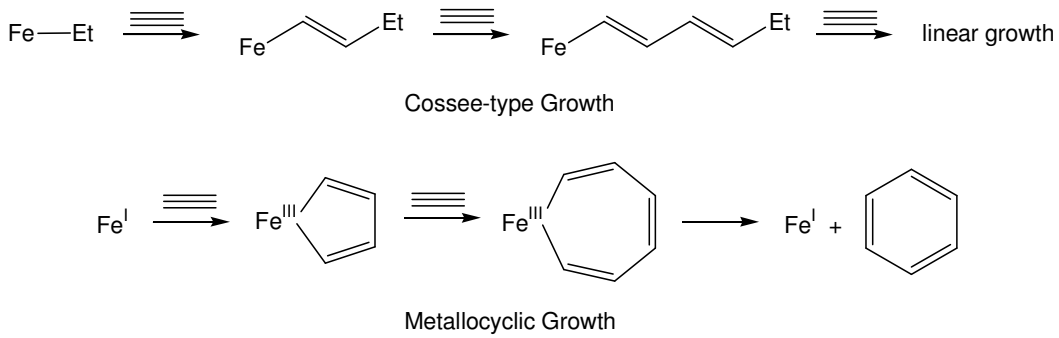

Scheme 6-2. Metallocyclic formation of benzene at Fe

In the context of a redox metallocycle mechanisms, an iron(I) amidinate complex was trialled, without the presence of an activator, to see if the low oxidation state was able to facilitate oligomerisation or polymerisation. Depicted in Figure 6-4, this compound was part of a series developed as analogues to β-diketiminate complexes, which are known for their role in dinitrogen fixation.[120] Unfortunately there was no reaction to be seen between this complex (50 μmol) and acetylene, with no observation of exotherm, colour change or acetylene uptake.

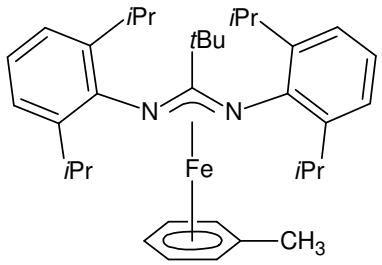

Figure 6-4. N,N'-diarylamidinateiron(I) complex

It was of interest to investigate if the 2,6-*i*Pr system was truly catalytic, and whether it released the oligomeric products during runs. A D_2O quench of the standard system was analysed by GC-MS, which showed primarily [D_1]-oligomer to have formed, meaning that the product chains remained bound to metal at the end of the trial. This was not ideal, so the use of H_2 as a chain transfer agent was trialled in the standard system, combining 10 bars of H_2 with 2 bars of acetylene as the reaction gas. This did have the effect of generating a greater proportion of oligomers, but at the cost of a significant reduction in overall yield (Table 6-1). Hydrogen was also trialled with a higher loading (50 μmol) of the iron catalyst, and this completely suppressed polymer production. It was also clear from this run that the oligomer distribution was pushed toward the lighter products – much more so that the respective trial *sans* hydrogen (see Figure 6-3). While the trial with 50 μmol of Fe produced basically all oligomers, this was only an ideal outcome if chain transfer was occurring, such that the system was truly catalytic. A D_2O quench of this revealed not a hint of [D_0]-oligomer, meaning that all of the growth products still remained bound to metal, and no chain transfer was occurring. This reduction in product output suggests, then, that hydrogen must be inhibiting the reaction in some way, but the available data was not sufficient to suggest how this might be occurring.

In the published trials of this catalyst with ethylene, a large number of metal alkyls were tested as chain transfer agents. While diethylzinc was by far the best match for this catalyst, several others also showed good results.[117] Thus, it was of interest to test the reactivity of some other metal alkyls in the place of diethylzinc. The use of triethylaluminium in the Fe/MAO system yielded a small amount of dark polymer, as was seen for the same system without diethylzinc. Oligomer analysis showed a significant amount of 1-butene and a trace of 1,3-hexadiene, which is consistent with the reactions of triethylaluminium discussed in Chapter 3; in short, $AlEt_3$ did not seem to interact with the iron catalyst. When trimethylgallium was used, there was some red polymer formed, much like that in the presence of diethylzinc. There were small amounts of odd-numbered oligomers detected by GC-MS – likely growth products from acetylene insertion into a methyl group – and a significant amount of benzene. The oligomer fraction represented a much higher proportion of the total product than that from the same concentration of diethylzinc, however 98% of the oligomer in this case was benzene. Overall, this suggested that trimethylgallium was not useful for targeting linear oligomers.

6.2.3 Identification of Oligomers

As already mentioned, GC quantification was performed based on groups of peaks with molecular weights corresponding to likely growth products. While there is only a single peak for each of C_4 (1-butene) and C_6 (1,3-hexadiene), the higher products feature a number of overlapping peaks for each molecular weight (see Figure 6-5), and mass spectra that are not easily identified against a reference library. More information was needed to get an idea of what products are formed here, and the underlying mechanisms. One interesting observation noted early in this analysis

related to the oligomer molecular weights. After hexadiene (MW 82), sequential addition of acetylene should increase each mass by 26, giving C_8 (108), C_{10} (134), C_{12} (160), C_{14} (186) and so on. This pattern was consistent until C_{12}, where the most commonly observed ion had a molecular weight of 164 and only a trace of 160 could be detected. This is unexpected, as it suggests growth by some path other than acetylene addition; an increase of 30 is consistent with the addition of an ethyl group. A D_2O quench revealed further information: while the majority of pre-C_{12} oligomer peaks were [D_1]-products suggesting one point of attachment to metal, the C_{12} peaks buck this trend, showing primarily [D_2]-substitution. This indicates a second point of attachment to metal prior to quench, and could suggest a metallocyclic or bimetallic structure.

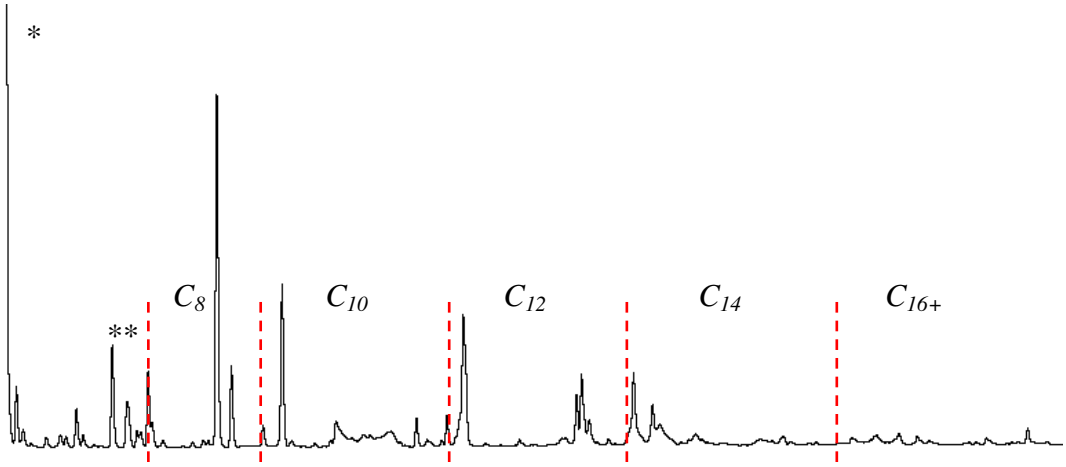

Figure 6-5. GC of oligomers C_8 and above
* Toluene ** Xylenes in Toluene

To further aid in mechanistic elucidation, a sample was hydrogenated to simplify the GC trace. Even with saturation removed the chromatogram still showed a multitude of peaks for compounds above C_8, however a number of these were now well enough resolved to be identified (Figure 6-6). From C_8 and above there are major peaks corresponding to the even-numbered *n*-alkanes, which suggests that linear growth plays a large role in this system; on the face of it, these paraffins look not unlike a

Poisson distribution, centred around C_{14}. Smaller peaks representing the odd-numbered *n*-alkanes can be seen between the evens; these likely begin from MAO-derived methyl groups, and are necessarily smaller due to the ratio of reagents used.

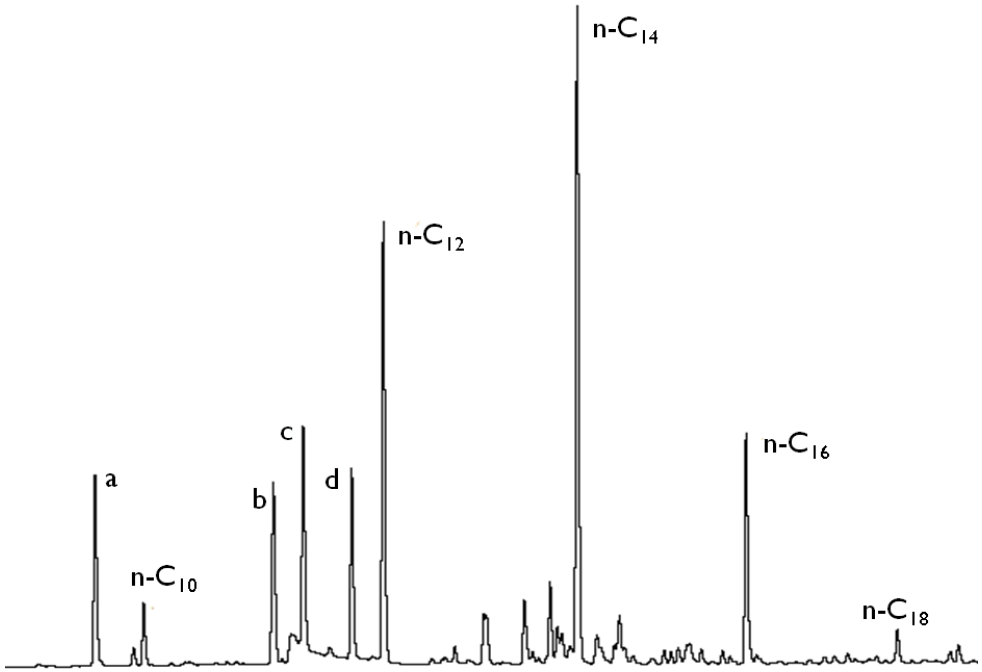

Figure 6-6. GC of hydrogenated C_{10+} oligomers
[a] 3-ethyloctane, [b] ethylcyclooctane, [c,d] branched C_{12s}

There are other large peaks, particularly around the C_{10} and C_{12} regions, representing non-linear backbone structures. These extra peaks continue to occur throughout the range visible by GC, but the C_{10} and C_{12} compounds will be focused on, owing to their relatively large abundance. For C_{10}, we see 4 peaks: the smallest is a minor branched isomer, with linear n-decane the next largest. The two major C_{10} peaks respectively fall some way before and after the n-alkane, the latter eluting just before n-C_{11}. The early eluting peak was confirmed as 3-ethyloctane by MS comparison and coelution. The later peak caused some confusion because it occurred so much later on the GC timescale, and branching typically leads to earlier eluting peaks. The molecular weight was also odd: 140 post-hydrogenation is 2 protons short of a fully saturated alkane, suggesting a cyclic structure. Library spectra and Kovats indices

suggested a structure like ethylcyclooctane, and this identity was confirmed by co-elution with a genuine sample. So, at this point, product growth definitely seemed to be more complicated than initially imagined, with branched, cyclic and linear C_{10} products all observed. Less success was achieved in fully identifying the C_{12} compounds. Two large peaks together are as abundant as n-C_{12} itself; in this case the linear product was the most significant. Library mass spectra very much suggested simple branched structures for both compounds, such as 4-ethyldecane and 3,4-dimethyldecane, and their earlier elution times relative to n-C_{12} would support this. Unfortunately the library spectra and Kovats indices available for this range of compounds were not adequate to fully assign the structures. Significant, later eluting ions at MW 168 also suggested that a cyclic structure was present for C_{12}, perhaps analogous to the ethylcyclooctane backbone observed for C_{10}. Although not everything remains clear in this analysis, the observations discussed thus far have allowed for the development of a mechanistic proposal for the formation of these compounds. The simplest linear structures could form by successive acetylene insertions into an ethyl group, which would seem to be the main pathway until C_{10}. At this point, while the molecular weight has increased by the amount expected for acetylene addition, three distinct products types are formed: linear, branched and cyclic. The branching in 3-ethyloctane can be explained by an intramolecular sigma-bond metathesis, as proposed for the branching seen with triethylaluminium (Section 3.3.1), followed by acetylene insertion (Scheme 6-3). The formation of a cyclooctane ring could then occur at this stage via intramolecular insertion of the furthest olefin on the chain into the metal-carbon bond, creating the necessary backbone. The same cyclic structure might also occur following the back-biting at of a longer C_{10} chain, however, without the sigma-bond metathesis step. As mentioned, D_2O quenching

yields primarily [D_1]-oligomer for the pre-hydrogenated C_{10} compounds which is consistent with these proposals (Scheme 6-3).

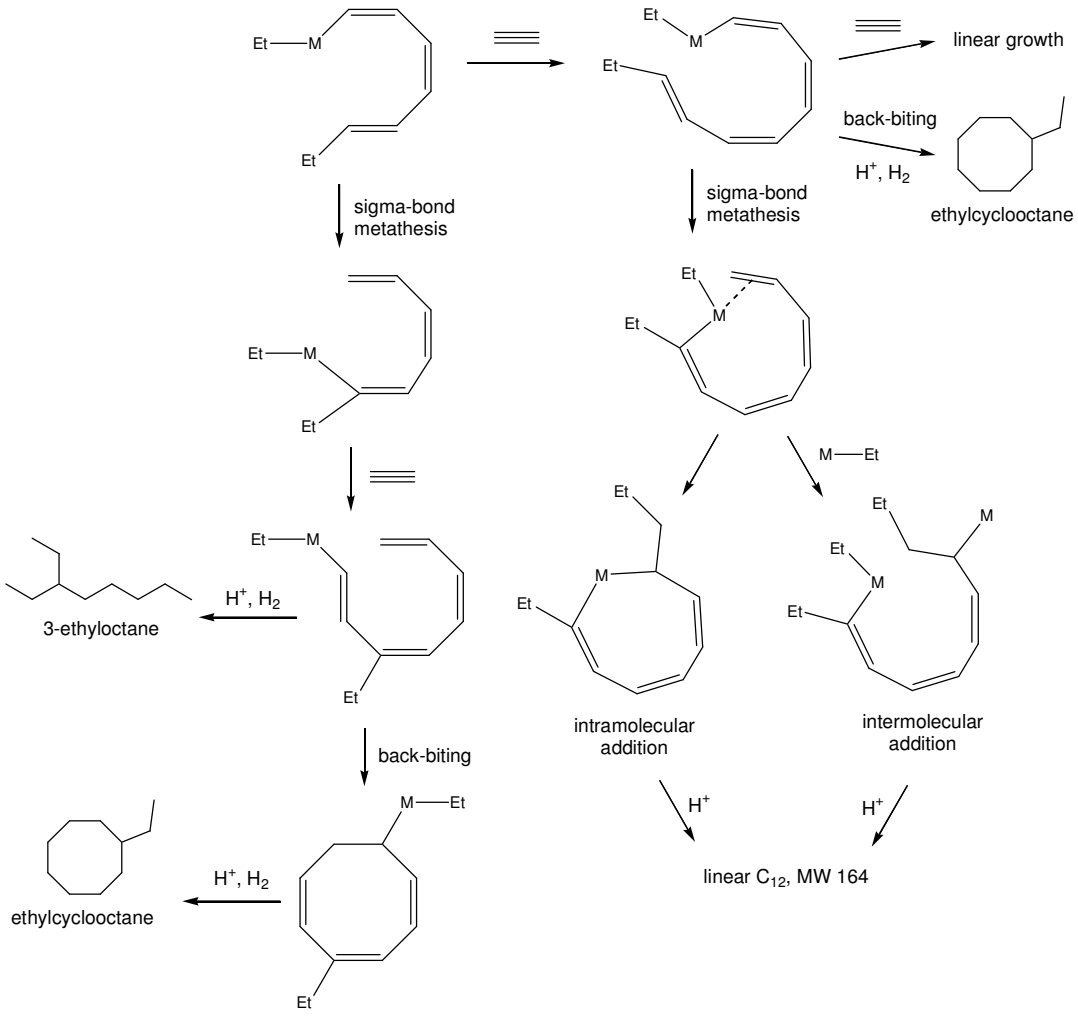

Scheme 6-3. Formation of C_{10} and C_{12} oligomeric products

Next come the C_{12} compounds: the major linear peak and two significant branched products. The situation here is more complicated due to the higher-than-expected molecular weight of 164, and the [D_2]-oligomers seen after a D_2O quench support the addition of another ethyl group attached to metal as the primary growth process (Scheme 6-3). A range of branched isomers can be envisaged by such an addition of M-Et, including a linear chain; the problem is growth after this point. The GC-MS shows n-C_{14} to be even more abundant than n-C_{12}, but the proposed mechanisms involving two points of attachment to metal cannot facilitate growth without

branching after this point. Growth by normal acetylene addition could of course give the linear structures, but this requires a molecular weight of 160 (C_{12}) prior to C_{14}, and at first these ions were not clear on the chromatogram. Closer inspection revealed a small cluster of 160 ions, eluting in a position quite far from where they would be expected – well after n-C_{14}. An examination of Kovats indices in the literature suggests that conjugated polyenes can elute quite a long time after the parent n-alkane, depending on the stationary phase used, and that this shift increases with greater conjugation – this is consistent with what is being seen here. For example, 1,3-hexadiene has a Kovats index of 619 on non-polar SE-30,[121] (E,E)-1,3,5-heptatriene elutes at 781 on HP-5MS,[122] and (E,E)-1,3,5-octatriene arrives at 920 on a DB-1701 column.[123] There are few references available featuring simple linear chains with more than 3 conjugated double bonds. The 160 cluster also presented itself as a [D_1]-oligomer after a D_2O quench which suggests that linear growth remains relevant for the higher oligomers. The major C_{14} ions pre-hydrogenation are 190, which is also higher than expected for normal acetylene addition, and the D-quenched products are [D_2]-oligomers like the C_{12} ones. Thus, while these structures could form by acetylene addition to the MW 164 C_{12} compounds, it is also possible they form following an analogous addition of M-Et to a growing oligomer chain, as proposed for the formation of the C_{12} species, simply at a later stage. In this fashion, a contribution to the linear C_{14} products can be made. The presence of the normal linear growth ion for C_{14} of MW 186 can also be detected in the GC-MS chromatogram, far later than the other C_{14} compounds, and also converting to [D_1]-oligomer with a D_2O quench. This pattern also appears to repeat for C_{16}, although the MS data is much less abundant in that region. One possible explanation is that the bimetallic intermediates suggested here, and

supported by the presence of [D_2]-oligomers, are in fact quite stable and resist further rapid growth. Linear growth may still be occurring, leading primarily to higher molecular weight products; evidence for this pathway is in the presence of the expected oligomer ions (C_{12} 160, C_{14} 186) in small amounts. The addition of a second ethyl group must be quite favourable, but perhaps not as fast as linear growth, so this addition could occur at different chain lengths, creating a range of different sized linear and branched structures; the absence of this strange growth pattern before C_{12} suggests that C_{10} is the shortest chain length at which the process is possible. Hence, we see an accumulation of these various higher oligomers, C_{12} and above, linear and otherwise, with only a small presence of the normal linear growth products. If linear growth is fast enough, less of the linear chains would remain at these shorter, soluble lengths, such that if they are not trapped by the formation of bimetallics or metallocycles, they quickly grow to insoluble lengths. Unfortunately, as noted, there is less data available after around C_{16} to support this claim, as the quantities of oligomer reduce, and all of these unsaturated compounds become insoluble after around C_{20}. In any case, growth in this system is clearly very complicated, with a number of processes likely contributing to the array of observed products. These proposed mechanisms necessarily remain highly speculative, however they do offer an explanation for the major identified products.

6.2.4 Polymer Investigations

The two polymers formed by this catalyst, with and without the presence of diethylzinc, are very different to look at when freshly prepared. With zinc present we see a powdery red solid, the smallest particles able to pass through basic filtration apparatus. With no zinc, the polymer is dark purple and film like with a lustrous,

metallic sheen. It was important to determine the nature of the polymers, and confirm if they were PA. The standard workup for these trials is to quench with dilute acid in air, which is not ideal for the preservation of reactive compounds. These polymers darken to black over time in air, which shows they are not entirely stable. For the purpose of analysis, two normal runs were performed in Schlenk flasks, with and without diethylzinc, and the reactions worked up by filtering and vacuum drying under inert conditions, avoiding air and acid (see Section 8.13). Owing to its extreme insolubility, infrared spectroscopy is the analysis of choice for PA, so the dried polymer samples were investigated in this fashion. Both polymers were identified as PA based on the presence of characteristic bands.[28,124] The two samples clearly have different properties, and this could be related to chain transfer with diethylzinc. Given the ability of the metal alkyl to regulate chain length in ethylene polymerisation, this could lead to a larger number of shorter polymer chains, each attached to zinc, rather than a smaller number of very long polymer chains for the iron catalyst alone. Colour variation in conjugated polymers has been related to factors such as backbone conformation and the extent of conjugation, and their effect on electronic transitions within the polymer.[125] Thus, the differences observed for these samples would suggest a great deal of variation in chain length and polymer structure. The nature of the polymers was not investigated in any further detail.

6.2.5 Catalyst Deactivation

The dramatic slowing of catalytic activity as observed in a number of trials could be attributed to factors such as poisoning of the catalyst by oxygen, although a great deal of care was taken to ensure oxygen was not present. The presence of oxygen would also be expected to poison the catalyst from the start, such that catalysis would

not commence, rather than lead to deactivation of an active catalyst. Another possibility is rapid degradation of the active catalyst to an inactive species. Yet another idea centred on the formation of polymer: as PA is notoriously insoluble, it will precipitate from solution upon formation. If the catalyst remains bound to the product, as D_2O quenching results would suggest is the case, the catalyst may become inaccessible to acetylene, encapsulated within a highly insoluble polymer structure. A longer polymer chain should be less soluble than a short one, and would result in more pronounced deactivation, which may be why this system appears to deactivate more rapidly when no diethylzinc is present to regulate chain length. In any case, it was necessary to obtain more information to confirm this theory. The same polymer samples prepared for IR were sputter-coated with gold, and analysed using a scanning electron microscope with an ultra-thin window energy dispersive x-ray spectrometer (see Section 8.1). This made it possible to view the polymer at high magnification (Figure 6-7), and to obtain an elemental analysis of the surface being examined by detection of x-ray emissions. This predictably showed large amounts of carbon and aluminium (from MAO), as well as zinc for the polymer made with diethylzinc present. There was no sign of iron at the surface of either sample, although this was always going to be a faint signal given the quantity of catalyst used. While the zinc-free polymer was being examined, a crack in the polymer was focused on under a higher magnification, and the elemental scan repeated. This now showed a positive (if small) response for iron (highlighted in Figure 6-8), suggesting the catalyst may indeed be encapsulated inside the polymer. A satisfactory iron signal could not be detected in a similar fashion for the zinc-containing polymer, so at the least, this result suggested that the encapsulation theory may be relevant for the zinc-free system.

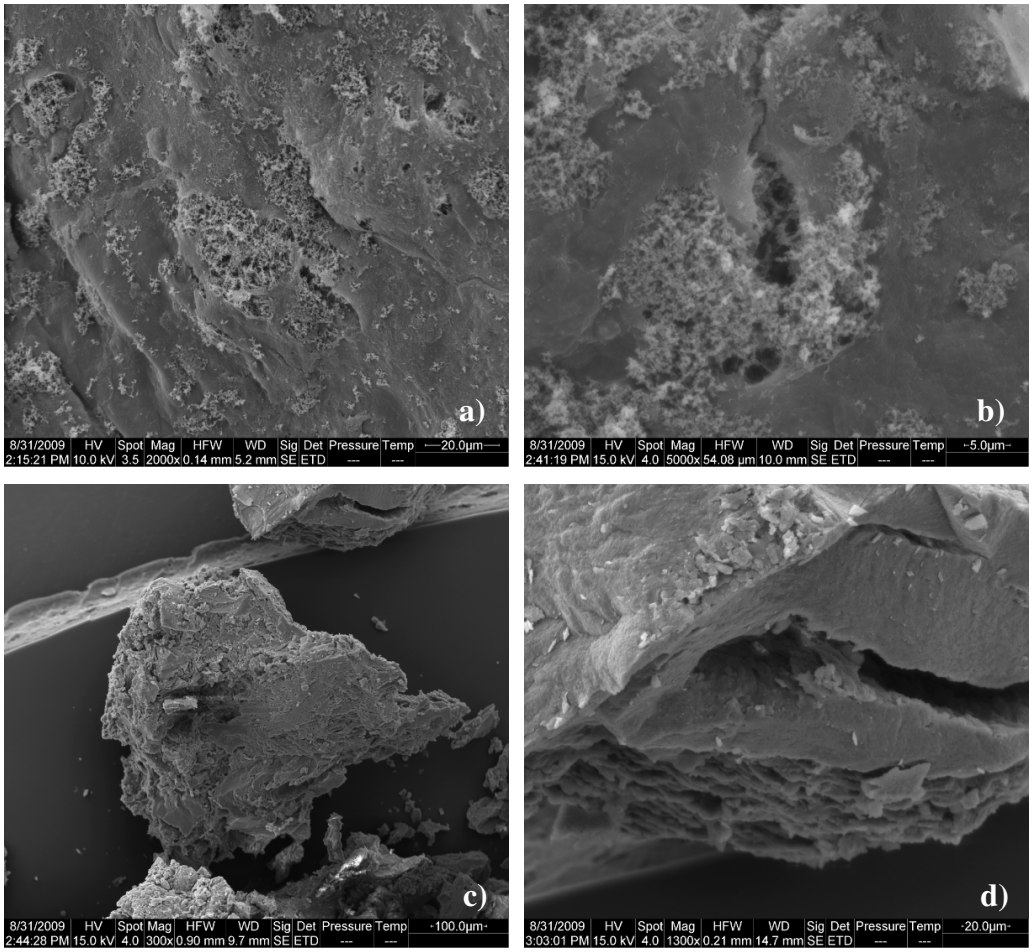

Figure 6-7. SEM images of polyacetylene samples
a) No zinc b) No zinc, zoom c) With zinc d) With zinc, zoom

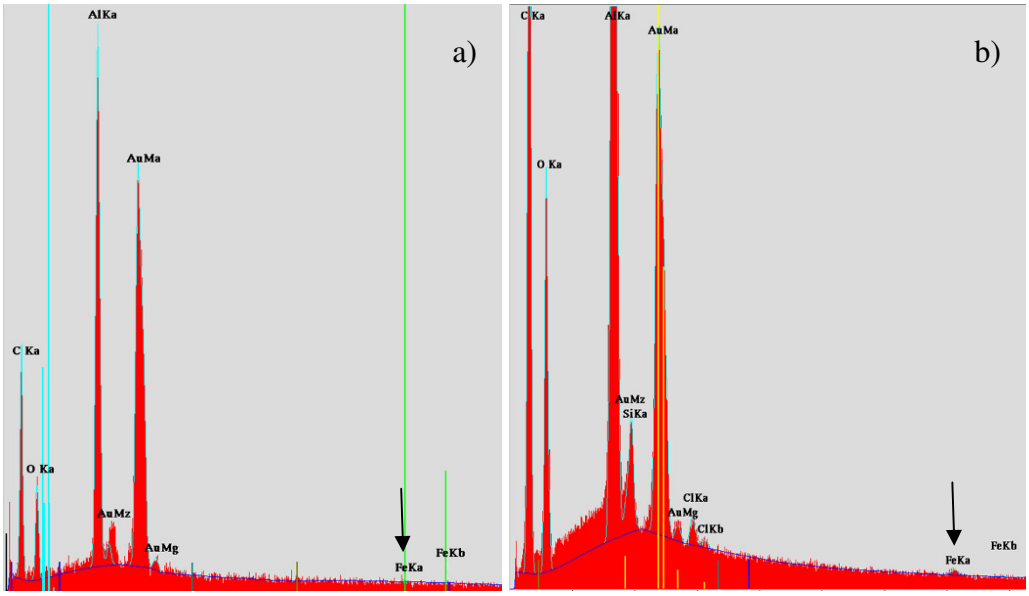

Figure 6-8. Elemental analysis of zinc-free polymer by x-ray detection
a) Initial View b) Zoom of crack in polymer

The SEM analysis, while indicative, was not conclusive evidence as to the fate of the catalyst. Thus, it was decided to use ICP-MS as a highly sensitive technique for trace metal analysis, searching for the presence of iron. The particular instrument used (see Section 8.1) overcomes problems often faced in ICP-MS analysis of iron due to the overlap of ^{56}Fe with ArO species formed in the plasma, and is able to correctly resolve iron.[126] Two fresh samples of the zinc-free and zinc-containing polymers were prepared, ashed in a high-temperature furnace and the residues digested in aqua regia (see Section 8.14); the final solutions were diluted and analysed by ICP-MS. For the zinc-free polymer, this revealed that 92% of the initially added iron was present in the polymer, along with the correct ratio of aluminium from the MAO, which very much supports the theory of encapsulation. For the zinc-containing polymer, only 44% of the initial iron concentration remained, which is still significant, but not such a clear-cut result. As mentioned, however, the system with diethylzinc does not deactivate in such a dramatic fashion as the zinc-free system.

A final point to corroborate the theory is an observation made while preparing these polymers in Schlenk flasks. The iron catalyst was activated with MAO in toluene, and at first exposed to acetylene for only a second. The characteristic purple polymer formed quickly, but only in small amounts. The solution was filtered into a Schlenk flask and again exposed to acetylene – 90 minutes after the initial exposure – and the catalyst was still found to be as active as before. After stirring under acetylene for several minutes, a larger quantity of polymer was formed. The solution was again filtered into a new Schlenk flask, and this time not a trace of polymer formed on exposure to acetylene. These results are consistent with the catalyst being encapsulated in the extremely insoluble polymer and not undergoing some kind of poisoning or other deactivation pathway. The brief first acetylene exposure only

developed a small amount of polymer, not enough to fully lock up the catalyst, which was still very active after 90 minutes. Another way of testing this would be to analyse the final solution filtered from the polymer for trace metals, as this should indicate that no iron remains after maximum polymer formation. Together, these experiments have confirmed the fate of the catalyst in the zinc-free system. The same explanation likely has significance in the zinc-containing system, but the result in that case is less black and white, and other factors may be at play. This is especially pertinent considering that system deactivation occurs when 10000 equivalents of diethylzinc are used, as only trace polymer is formed in that case. This may relate to the observations for triethylaluminium and acetylene (Section 3.3.2), where relatively stable bimetallics form once alkene double bonds are included in a growing polymer chain. If, for example, a similar alkene-bridged zinc dimer formed that slowed further growth, it follows that a greater inhibitory effect would be noted at a higher zinc concentration.

6.2.6 Co-polymerisation of Acetylene and Ethylene

Given the known reactivity of this system with ethylene and now acetylene, it was of interest to investigate the formation of a copolymer of the two monomers. Biodegradable polymers are of interest because of their ease of decomposition,[127] and in the context of PE, the incorporation of double bonds into the polymer structure may help to facilitate degradation. Such copolymers featuring longer conjugated sections have potential as conductive polymers without the stability and handling issues of PA, while the presence of double bonds might allow for further functionalisation and tuning of polymer properties. Some reports of the production of such polymers have been presented.[124,128,129]

A number of trials were performed using the 2,6-*i*Pr catalyst with various pre-mixed ratios of acetylene and ethylene. The gas mixtures were prepared in a ballast vessel under pressure, as the equipment for continuous-flow dual-gas supply was not available. As acetylene has shown itself to be far more reactive than ethylene in this system, only a small percentage of acetylene was used, with the first trial using just 5%. It quickly became apparent that even 5% acetylene was too high to allow novel polymer formation, as runs at 1 barg pressure (no diethylzinc) effected the formation of only minimal polymer and showed the same quick deactivation seen in normal acetylene runs. A trial at 4 barg pressure produced a larger amount of polymer that was not homogeneous in colour, but featured white streaks seen running through dark purple regions. Reducing the acetylene proportion to 1% and 0.1% allowed for the generation of a range of polymers, with and without diethylzinc, and the yield increased with the reduction in acetylene concentration (Table 6-2). The range of polymers produced is shown in Figure 6-9, and the fading of colour with a decrease in acetylene concentration is consistent with a reduction in overall polyconjugation. Similar colour gradients have been reported for the copolymerisation of different acetylene/ethylene ratios by Ziegler-Natta catalysts.[128,129]

Table 6-2. Yields and Properties of Polymers from C_2H_2/C_2H_4 mixtures

Sample	% C_2H_2	$ZnEt_2$ Used?	Mass (g)	Colour
1	5	Y	0.045	Purple
2	5	N	0.060	Light Red
3	1	Y	1.905	Light Purple
4	1	N	2.364	Dusky Pink
5	0.1	Y	3.809	Off-white
6	0.1	N	6.292	White

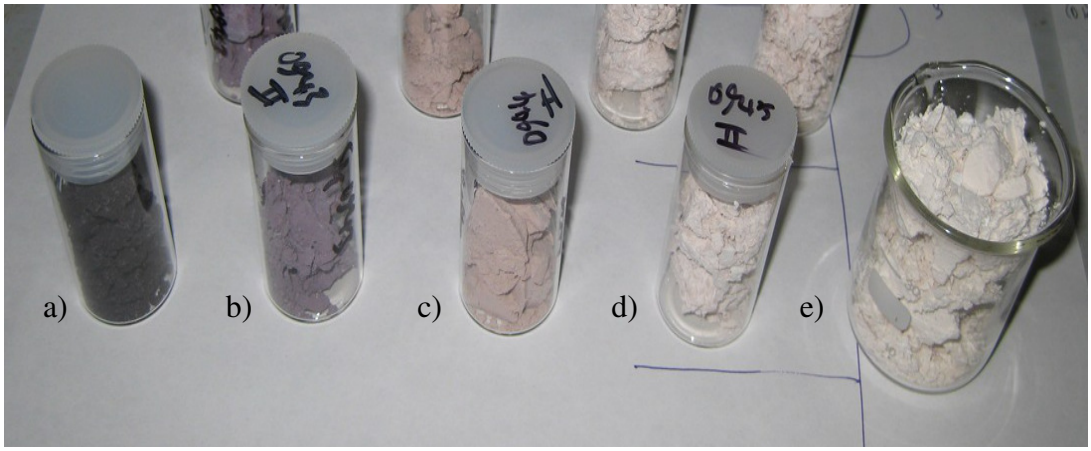

Figure 6-9. Polymers produced using C_2H_2/C_2H_4, with and without $ZnEt_2$ C_2H_2 content: a) 5% b) 1% c) 1% + Zn d) 0.1% e) 0.1% + Zn

So, while a variety of products had been produced, at this stage it was not known if they were true copolymers. Several samples were analysed by NMR, looking for evidence of double-bond inclusion in the polymer chains. While PA is effectively insoluble, PE can be dissolved in trichlorobenzene above 140 ºC, allowing for the acquisition of NMR spectra. It was noted that, while the majority of the added solid dissolved, some traces of dark colour were seen suspended in solution. The ^1H NMR showed characteristic signals for PE, representing methylene chain protons and methyl tail groups. No clear olefinic signals could be detected which, given the insoluble dark colour seen in the NMR tube, suggested that a mixture of polymers had been formed, rather than a true co-polymer. Infrared analysis showed no evidence of alkene signals, which is expected given the low proportions of acetylene used.

It was unfortunate that flow-through apparatus was not available, as this would have allowed a constant stream of the same gas mixture to be fed to the reactor. As it was, given the apparent higher reactivity of acetylene, this monomer was likely consumed first, and the ethylene more slowly. Even with the reactor pressure kept at a constant level, the acetylene proportion would slowly decrease, leading overall to a

disproportionate content of PE. The reactor was typically bled and backfilled several times during these runs, refreshing the acetylene content, and a quick darkening of colour was always noted at these times as the acetylene was consumed. So, while not the ideal setup, these results still serve as a guide to the behaviour of these gas concentrations. One trial run was performed with a slightly open reactor port, which effectively led to a flow-through setup, and the polymer appearance and yield did not change markedly.

The observations from NMR analysis suggest that a small amount of PA is formed separately to PE, and that the polymers end up as a mixture. The large difference between the reactivity of acetylene and ethylene with this catalyst, coupled with the catalyst deactivation observed for this system with pure acetylene, makes it believable that the acetylene is quickly consumed, forming PA which precipitates. In the meantime, PE grows more slowly in the surrounding solution, eventually making up the bulk of the product. Thus, very little acetylene would ever be included into the bulk of the produced PE. As seen for the trials with pure acetylene, the results in the presence of diethylzinc are less clear-cut, with the formation of insoluble polymer not so rapid, and the catalyst deactivation less pronounced.

Examination of the soluble oligomers formed in the presence of diethylzinc provided more information as to the products of this system. For a 5% acetylene gas mixture, the predominant oligomers were n-alkanes, however a significant amount of unsaturated product was also noted at each even chain-length (Figure 6-10). There were at least two peaks with mass spectra suggesting one double bond, for each chain-length – with one always the major – and some smaller peaks hinting at further unsaturation.

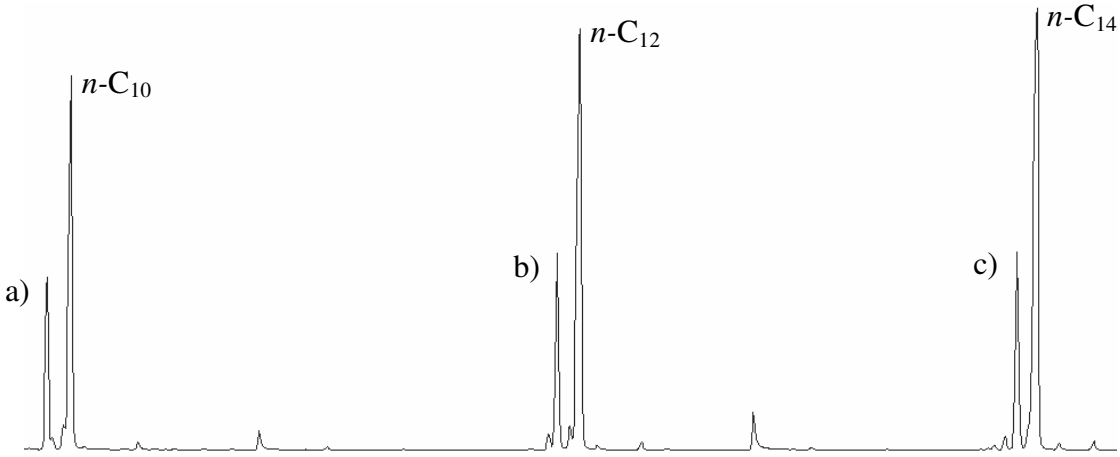

Figure 6-10. GC of Co-oligomers (5% acetylene w/ $ZnEt_2$)
a) 1-decene b) 1-dodecene c) 1-tetradecene

As mass spectra and Kovats indices for the various alkene positions (i.e 1-alkene, 2-alkene) do not vary greatly, the sample was treated with bromine in an attempt to clarify the alkene position in the major peaks. Using hexene as a model the only possible structures, assuming an ethyl tail group, are 1-hexene and 3-hexene, which would lead to 1,2- or 3,4-dibromohexane after bromination. Kovats for these dibrominated compounds are quite different, and the peak seen in the experimental GC here matched the reference value for 1,2- substitution. A linear series, derived from the retention times of the major dibrominated peaks eluting throughout the chromatogram, confirmed that the major alkenes were indeed α-olefins. Investigation of the GC from a trial run of this system with pure ethylene in the presence of diethylzinc also showed the presence of α-olefins as well as the *n*-alkanes, which could mean that a small amount of β-hydrogen transfer occurs in the original system. The proportion of olefins in the mixed gas system was much higher, however, and a D_2O quench in the 5% acetylene/ethylene system confirmed the presence of 94% [D_1]-oligomer across the board. So while chain elimination might play a tiny role, the majority of olefins seen here appear to arise from acetylene insertion, and the oligomers primarily remain bound to metal after the reaction is complete. It would

appear, then, that very little acetylene is making its way into the oligomers, which may simply represent the small proportion available in the reaction gas. Based on the oligomers observed from the reaction with diethylzinc present, only 1 olefin per chain seems to be included most of the time. Predictably, a lower proportion of olefin was observed for lower acetylene/ethylene ratios. The observation that the alkenes produced in this case are primarily α-olefins might suggest that the inclusion of an acetylene unit is the final stage in the formation of these oligomers. This might hint again at the formation of stable structures that slow further growth, with the bimetallic alkene-bridged structures observed for triethylaluminium in mind (see Section 3.3.2). Overall, the evidence all suggests that this approach did not lead to true copolymerization of acetylene and ethylene.

6.3 The *o*-tolyl Catalyst

6.3.1 Initial Trials

The *o*-tolyl analogue of the 2,6-*i*Pr catalyst, as mentioned earlier, varies structurally only in N-aryl substitution, however leads to the production of primarily soluble oligomers when reacted with ethylene. How it reacted toward acetylene would surely be of interest, then, given the current results for the 2,6-*i*Pr catalyst. A first trial using 6 μmol (100 equivalents MAO) produced only a trace of solid product, and no detectable oligomer. Not to be discouraged, the catalyst loading was scaled up to 60 μmol and the run repeated. Here an interesting thing was seen: while there was no major initial exotherm as noted for the 2,6-*i*Pr system, some mild heat development was observed which continued throughout a 30 minute period. Still only a trace of solid product was collected, but GC analysis revealed an extremely large peak for benzene. This was most interesting, as while the 2,6-*i*Pr catalyst does

generate a small amount of benzene (a 20 μmol loading yields 0.2 g benzene), a 30 minute run using the *o*-tolyl catalyst produced over 2.4 g of benzene. A closer look by GC-MS showed a few higher molecular weight peaks, at 104 and 130, and around 500 mg of a dark red polymer was collected. The MW 104 oligomer was confirmed as cyclooctatetraene by mass spectra and co-elution; there were no likely mass spectra matching the heavier compound, but the molecular weight is one acetylene unit above cyclooctatetraene, perhaps suggesting a cyclic C_{10} polyene structure. Either way, these higher peaks were only small, with benzene comprising over 99 mole% of the oligomeric output. Clearly this system behaves in a very different mechanistic fashion to the 2,6-*i*Pr catalyst and so, given the comparatively simple product output, it was considered that further studies might more easily shed light on the nature of this process.

6.3.2 Deuterium Labelling Studies

The formation of benzene in the *o*-tolyl system is intriguing, so it was of interest to try and establish by what mechanism cyclotrimerisation proceeded; the result of this might also be of relevance to benzene formation by the 2,6-*i*Pr catalyst. Two processes that could lead to this would be a Cossee-type or a metallocycle mechanism. In ethylene oligomerisation, metallocycle and Cossee mechanisms are differentiated between using an approach developed by Bercaw.[130] By using a mixture of normal and [D_4]-ethylene and analysing the deuterium content of product oligomers by MS, it is possible to deduce if H/D scrambling has occurred during reaction. The difference is that a metallocycle mechanism does not allow H/D scrambling, so only even-numbered D-substitutions will be found on the product oligomers. The Cossee, however, begins from a metal hydride, and product release

occurs through β-hydride elimination, so an avenue exists for H/D exchange and the formation of odd-numbered D-substitutions. The metallocycle mechanism was illustrated and discussed in Section 6.2.2 (Scheme 6-2), while a linear growth, or Cossee-type route to benzene requires further explanation. A possible route is shown in Scheme 6-4, and involves three acetylene insertions into an Fe-hydride, yielding an Fe-hexatrienyl complex. At this point, interaction of the chain-end unsaturation with Fe is possible, and concomitant cyclisation and hydrogen transfer could produce benzene and regenerate the active Fe-hydride.

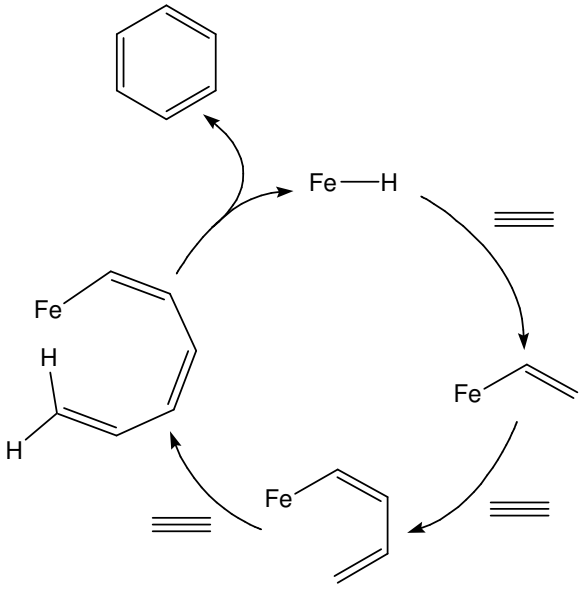

Scheme 6-4. Proposed Cossee-type Pathway to Benzene

The same D-labelling approach should be relevant here if a mixture of normal and $[D_2]$-acetylene were used, as a metallocycle mechanism would produce only $[D_0]$-, $[D_2]$-, $[D_4]$- and $[D_6]$-benzene, while the proposed Cossee-type mechanism would produce these as well as $[D_1]$-, $[D_3]$- and $[D_5]$-benzene. The ratio of these products was calculated assuming a 1:1 mixture of C_2H_2:C_2D_2, and some model distributions were produced. The ratios were based on all possible combinations of the two acetylenes, and the total deuterium count from each combination. So for a

metallocycle, only one combination leads to each of C_6H_6 and C_6D_6, however three combinations each lead to $C_6H_4D_2$ and $C_6H_2D_4$. The same idea was applied to the Cossee-type mechanism, which is complicated as it also involves a metal hydride starting point (Fe-D or Fe-H) and elimination, which can occur with the loss of either of two tail protons. These ratios (Table 6-3) allow for the formation of the model distributions. For each isomer, the contribution to major ions was determined based on the natural ion abundance for benzene, as detected on the GC-MS instrument used for these analyses: 24% 77, 100% 78 and 8.9% 79 (standardised). The calculated ratios were applied to each isomer, and the contributions to each ion summed to form the final model.

Table 6-3. D-benzene isomer ratios for model distributions

Model	D_0	D_1	D_2	D_3	D_4	D_5	D_6
Metallocycle	1	0	3	0	3	0	1
Cossee-type	3	2	9	4	9	2	3

The experiment was performed in a Schlenk according to the general procedure (see Section 8.9). Acetylene-d_2 was prepared by quenching calcium carbide with D_2O and dried (see Section 8.1), then mixed in a 1:1 ratio with normal acetylene. The first experiment was run was for 30 minutes, carefully quenched, and analysed by GC-MS. The observed distribution (see Figure 6-11) did not match either of the model scenarios perfectly, although the presence of odd-numbered [D_n]-benzenes suggested that the Cossee-type mechanism might be likely, as the metallocycle mechanism does not allow their formation. The GC-MS molecular ion distribution would, of course, contain odd-numbered ions even in the absence of odd-numbered [D_n] products, however their abundance and the time offsets observed for these ion peaks confirmed that genuine odd-numbered [D_n] compounds were present.

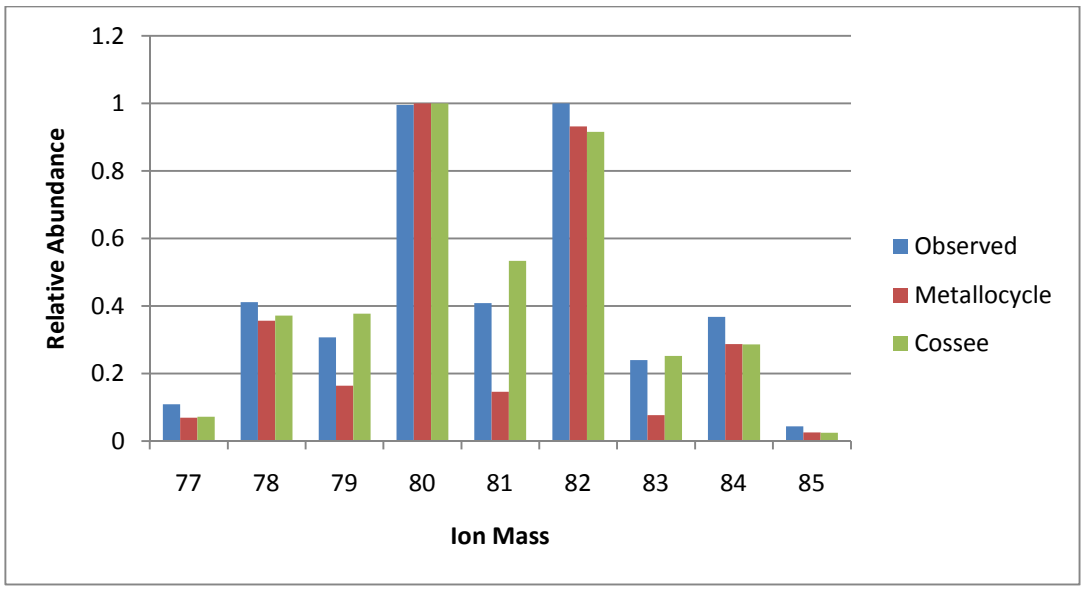

Figure 6-11. First Observed Distribution vs Metallocycle and Cossee-type Models

Another factor that came into play was possible H/D exchange between the normal and deuterated acetylenes, as there was a significant amount of C_2HD detected in the reaction solution. A report discussing the oxidation reactions of acetylene utilised C_2H_2 and C_2D_2 mixtures for mechanistic studies, and suggests that H/D exchange between the two monomers is indeed significant, proceeding via a radical exchange mechanism.[131] Given that the two gases had been mixed several hours before reaction with the iron catalyst, and the length of the reaction, a significant amount of C_2HD may have in fact been present. The presence of C_2HD could explain the presence of odd-numbered $[D_n]$-benzenes forming via a metallocycle mechanism, and meant that the experiment had thus far proved nothing. Hence, the run was repeated, but this time the two acetylenes were not mixed until immediately before reaction; the reagents were only exposed to the gas for 2 minutes, then quickly quenched and analysed. This approach minimised the available time for H/D exchange between the two gases; the literature report mentioned above suggests that C_2HD should account for less than 3% of the gas mixture after this time. However,

the second run was not hugely different from the first, if anything making the choice between metallocycle or Cossee-type less clear. As a follow-up, a sample of the unmixed C_2D_2 was analysed by high-resolution MS, which revealed that 8.7% of this gas was in fact C_2HD prior to the addition of C_2H_2. This might be attributed to the presence of the decomposition product $Ca(OH)_2$ in the calcium carbide, which might rapidly exchange with D_2O or C_2D_2 itself, producing this initial concentration of C_2HD. Alternatively, drying of the produced C_2D_2 by passage through molecular sieves could provide an explanation: while these were activated prior to use, trace remaining H_2O could exchange with C_2D_2, particularly at acidic zeolite sites. In terms of H/D exchange between acetylenes, the same gas sample was analysed some hours after mixing with normal acetylene and showed a much higher proportion of the exchanged gas, confirming that this mode of H/D scrambling was also relevant. Once the initial C_2HD content of the C_2D_2 was factored into the models, the observed distribution (from the trial with minimal C_2D_2/C_2H_2 mixing time) became a much closer fit to the predicted metallocycle distribution, with the Cossee-type distribution clearly incorrect (see Figure 6-12). The predicted large abundance of the MW 81 peak representing $[D_3]$-benzene, in particular, is not supportive of the Cossee-type approach. A similar experiment has in fact been reported, analysing benzene formation over a heterogeneous palladium catalyst.[132] The authors also noted a 10% C_2HD impurity in their C_2D_2, and their benzene isomer distribution is very close to that observed in the current experiment. Their experimental data is said to fit a mechanism involving no C-H bond cleavage, although it is not made clear exactly what mechanism is proposed. A metallocycle mechanism seems to be the best explanation.

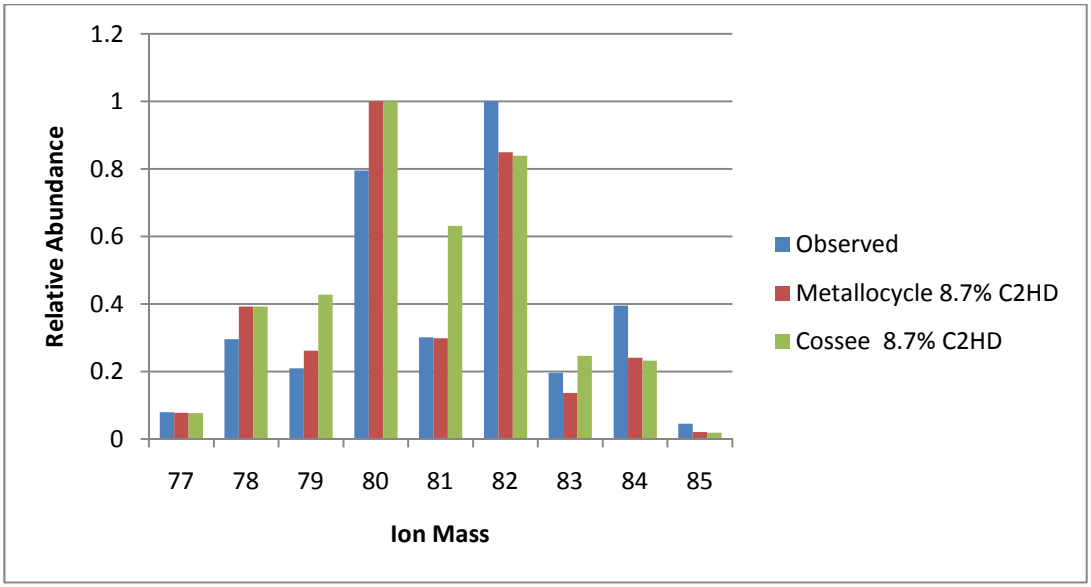

Figure 6-12. Second Observed Distribution vs Metallocycle and Cossee-type Models The 8.7% C_2HD content of the C_2D_2 is factored into these models

The current investigation has shown that a metallocycle mechanism for benzene formation by the *o*-tolyl catalyst is a reasonable explanation. This process is also likely to be relevant to chain growth in the 2,6-*i*Pr catalyst system where benzene formation, though minor, could be expected to follow the same mechanistic pathway as the *o*-tolyl catalyst. As has been mentioned, this may represent a different active species to that which produces primarily solid polymer. It is interesting to muse whether the major pathway in the 2,6-*i*Pr system also follows a metallocycle mechanism, or if a Cossee-type process is more likely. It is possible that a metallocycle mechanism leads to polymer, which is interfered with by rapid chain transfer in the presence of diethylzinc, leading to the observed range of oligomers incorporating ethyl groups. A metallocyclic mechanism should also produce higher cyclics such as cyclooctatetraene which are not observed for the 2,6-*i*Pr catalyst, with or without zinc, while a Cossee-type process has relevance when considering the range of branched products discussed earlier (Section 6.2.3). This mechanism may also be favoured by the increased ligand bulk in this catalyst, which could hinder the

coordination of an incoming acetylene monomer and thus further metallocyclic growth, while a two-site migratory insertion process would not be so impeded (Figure 6-13).

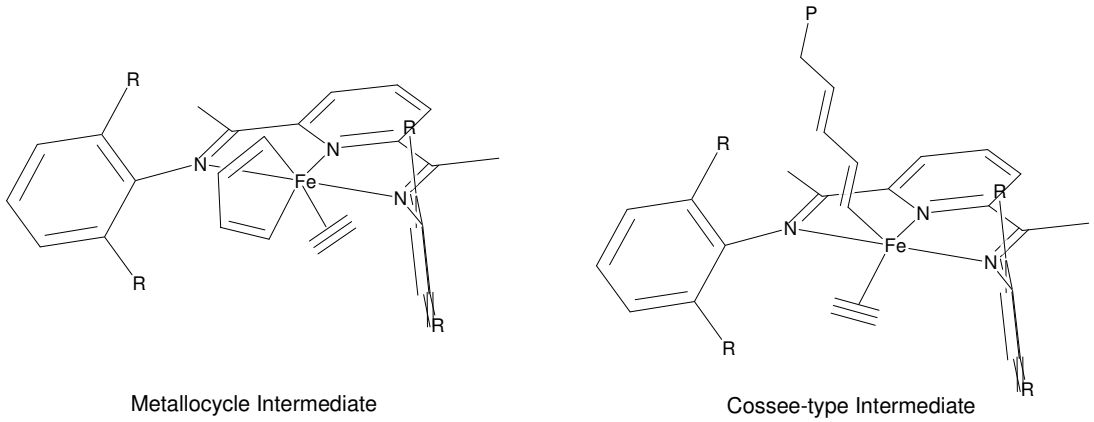

Figure 6-13. Metallocycle vs Cossee-type Mechanism: Possible Intermediates

6.3.3 Further Experiments using $ZnEt_2$ and H_2

It was of interest to trial the effect of chain transfer agents with this catalyst. As diethylzinc has such a marked effect in the 2,6-*i*Pr system it was also trialled for the *o*-tolyl catalyst, although previous studies have shown the metal alkyl to have no effect in the *o*-tolyl system with ethylene.[118] The addition of zinc did, in fact, have the curious effect of ceasing benzene formation, and the system now produced a range of oligomers. More curious was the oligomer distribution, as this showed a very different distribution of the known products. There was almost no 1-butene present, despite care taken not to lose volatiles when working up the reaction. Rather, 75 mol% of the oligomer was 1,3-hexadiene, representing about 50% of the total $ZnEt_2$ added to the reaction. Higher compounds were present, but in reduced proportions. Running for 60 minutes rather than 30 did not change the oligomer distribution much, producing a little more of the C_{14}+ compounds. Several repeat runs produced around 2 g of oligomeric product and only a trace of polymer, which

is good in terms of targeting soluble compounds. The preference for hexadiene is curious, as it suggests two acetylene additions to an ethyl group. Two additions, of course, is one short of the three required for cyclotrimerisation, which the presence of diethylzinc is clearly interrupting, although it is unclear exactly how this is happening. To gather more information about this, the run was repeated in a Schlenk, and analysed by NMR. Given the large proportion of hexadiene present, it was thought that some clue may be evident regarding its prominence in the oligomer spread. The spectrum showed a number of broad signals in the olefinic region from 5.2-6.2 ppm. The broadness is typical for paramagnetic compounds, so indicates that iron is still present, however the spectrum did not allow for structural assignment.

The current observation of hexadiene formation can be explained in the context of a metallocyclic mechanism, whereby chain transfer to zinc interrupts the normal growth process, leaving zinc tethered to iron via a butadienyl chain. Reductive elimination from iron would yield a zinc-hexadienyl moiety and regenerate the active iron centre for further reaction, as shown in Scheme 6-5. This can explain the absence of 1-butene, as the first intermediate that forms in a metallocyclic mechanism is the metallacyclopentadiene. This means that hexadiene is the shortest oligomer than can form via the proposed mechanism, so goes a long way to explaining its abundance. Further to this, the interruption of metallocyclic growth would prevent the formation of greater cyclic structures, including benzene, which are absent from the product distribution. Finally, the *o*-tolyl catalyst is around a quarter as active towards ethylene as the 2,6-*i*Pr catalyst, so this could help explain the low abundance of oligomers beyond C_6.

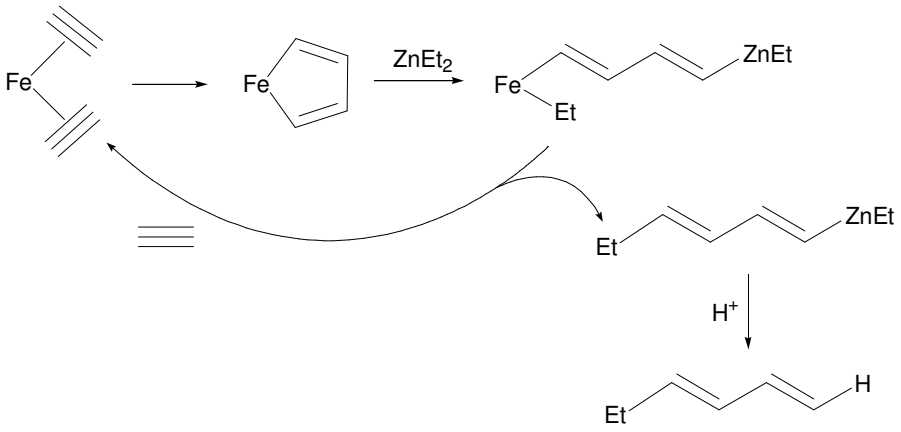

Scheme 6-5. Proposed formation of hexadiene by *o*-tolyl/$ZnEt_2$ system

Another possibility comes back to the idea of stable alkene-bridged bimetallics, and is supported by the fact that only around half of the added zinc was converted to higher oligomers. Indeed, the lack of activity toward ethylene noted for this catalyst in the presence of diethylzinc has been attributed to the formation of stable hetero-bimetallic complexes between iron and zinc.[118]

It was of interest to benchmark the use of an acetylene/H_2 gas mixture towards this catalyst, without the use of diethylzinc. The reaction output was greatly reduced, with only 260 mg of benzene detected, and none of the higher oligomers seen. The polymer production actually rose to 900 mg, and had a more pale red appearance, but still appeared to decompose over time in air. The use of hydrogen was not pursued any further.

6.4 Summary and Conclusions

The reactivity of acetylene toward bis(imino)pyridineiron(II) catalysts was explored with the goal of oligomerisation in mind. The 2,6-*i*Pr catalyst is initially extremely active, leading to polyacetylene formation and a quick catalyst deactivation. Addition of diethylzinc as a chain transfer agent effects different polymer properties and the

formation of a complicated range of soluble oligomers. Varying the amount of diethylzinc was able to drive production toward oligomers, but at the cost of overall output, showing that an excess of this reagent impedes growth. The oligomers were partially identified with the aid of hydrogenation, GC-FID and GC-MS, and a mechanism for the production of the base structures was proposed, though the complexity meant that much remained unclear. The polymer was investigated by IR, SEM and ICP-MS, which led to the conclusion that catalyst encapsulation by insoluble PA was the primary cause of deactivation. The 2,6-*i*Pr catalyst was trialled for the copolymerisation of acetylene and ethylene, however analysis showed that a mixture of polymers was the best approximation of the products formed; the relatively high reaction rate of acetylene versus ethylene was not thought to be helpful in this case. Trial of the *o*-tolyl catalyst led primarily to benzene production, with mechanistic studies pointing toward metallocyclic growth. Although this result was not definitive, it enabled further discussion of polymerisation in the 2,6-*i*Pr system which may have otherwise been unattainable given the raft of complicated compounds produced in reaction with acetylene. Ultimately the 2,6-*i*Pr does not undergo chain termination, which makes it unsuitable for acetylene oligomerisation at this stage. While chain transfer to zinc allows for some oligomer formation, polymer is still a significant part of the product yield. The process is not catalytic in zinc, as no chain termination from this metal is observed. The *o*-tolyl catalyst does undergo rapid chain transfer, however mainly leading to the formation of cyclotrimer. Overall, some light has hopefully been shed on the pathways by which these catalysts do facilitate the growth of unsaturated products from acetylene.

Chapter 7 Conclusions

7.1 General Summary

This research project has tested a wide range of well known ethylene polymerisation catalysts for their reactivity towards acetylene, in the context of generating fuel-range oligomeric products. Broadly speaking, a great majority of trialled catalysts have been ineffective in this context, which is surprising given their known high activities toward ethylene, and the similarities between the two monomers. There was reactivity to be found, however – certainly in places unexpected – which has allowed for the production of a range of oligomeric and polymeric products. The different stages of this project will now be summarised in turn.

7.2 Metallocenes and Other Transition Metal Complexes

The Group III-V metallocenes were ultimately a disappointment, and proved ineffective as acetylene oligomerisation catalysts for all the trialled activators. It is possible that other activators might render some of these precatalysts active toward acetylene and there are indeed a great range, such as the perfluoroarylborates, that were not investigated in this research. The reactivity of certain metallocenes toward acetylene has been noted in the literature, such as the Group III and lanthanide alkyls.[47,48,51,53] It is possible that these alkylated species may serve as useful catalysts in their own right, without the need for an activating species, and this chemistry might have potential to be pursued in the current context, although the literature examples show extremely low TONs. It should be noted in this context that dimethylzirconocene did not show any noticeable reactivity toward acetylene. As for the metallocenes, the majority of non-metallocene catalysts trialled also did not

prove useful for acetylene oligomerisation. There was evidence for linear oligomer formation in some of the chromium systems, and benzene was detected in other cases, but none of these products were at all significant.

7.3 Triethylaluminium

Reaction with triethylaluminium was interesting for several reasons. One is the oddity of the quick first insertion followed by slower growth thereafter, which was eventually explained in terms of strongly-bound dimers. The strange oligomer growth was also of note, with a clear absence of C_8 compounds, but plenty of compounds C_{10} and above. The branching introduced at this stage is also fascinating, and highlights the fact that a range of growth processes much be in action. Unfortunately the relatively slow nature of this growth, even at high temperature, leaves much to be desired in terms of a productive system. More pertinently, the ineffectiveness of the trialled chain transfer agents meant that oligomer growth ultimately remained stoichiometric in Al. It is possible that there exists a more suitable chain transfer agent which would render this system catalytic, and further investigation may uncover such a reagent.

7.4 Computational Investigations

The theoretical work undertaken here has provided data to both supplement and reinforce the experimental findings from the triethylaluminium studies. The relative energies for the calculated potential reaction surfaces certainly agreed with the overall premise that acetylene insertion at triethylaluminium is initially facile, but impeded after the first reaction by the strength of alkenyl-bridged dimers. This work also shed light on other aspects of growth facilitated by aluminium, such as further strongly-bound dimeric species, and the process of chain transfer by hydrogen at Al,

which was found to have a quite high energy requirement. The mechanisms leading to branching and the strange carbon number distribution in this system were never definitively described, and the insight of theory in this context would certainly be a worthwhile future pursuance.

7.5 Copolymeristaion of Acetylene and Arenes

The use of this $AlEtCl_2$ as an activator was interesting, as its Lewis acidity was adequate to initiate a Friedel-Crafts type reaction between acetylene and arenes. Inadvertently reviving some 1920s chemistry, it was possible to form extremely stable, hydrophobic polymers that were not easily characterised due to their insolubility. Some clues were given by NMR, GC-FID and GC-MS of the soluble oligomeric fractions. It would be of interest to determine if the polymer has any useful mechanical properties, as these could not be investigated in the course of this project.

7.6 Bis(imino)pyridineiron(II) Catalysts

It was a welcome change after the metallocenes to find the iron catalysts to be extremely active toward acetylene. This high activity, of course, brings problems of its own with the rapid progression to insoluble PA. Even with the aid of diethylzinc as chain transfer agent, it was not possible to satisfactorily optimise product output toward oligomer without the loss of overall activity. More work still needs to be done toward determining the mechanisms of growth in this system, which are certainly very complex, and this again may be aided by theoretical calculations. It is unlikely that a better metal alkyl chain transfer agent, more suited to the reaction with acetylene, will be discovered, as these were extensively investigated in the initial work with ethylene and found diethylzinc to be the best match for the iron catlyst.[117]

The results from deuterium labelling studies with the *ortho*-tolyl catalyst are certainly interesting in providing mechanistic insight, although the model metallocycle distribution does not perfectly match the observed data. So, while the current results are quite indicative, it remains to conclusively show the mechanism of cyclotrimerisation.

7.7 Final Remarks

The use of acetylene to generate linear hydrocarbons is always likely to be plagued by difficulties. The inherent reactivity of the C=C double bonds that are present in the produced oligomer chains leaves the door open for further reactions, both inter- and intramolecular. This is evident in the range of branched and cyclic structures deduced for products of this study. The cyclotrimerisation of acetylene is a well known and highly energetically favourable process, however it is not one that contributes to the goals set out here. There are, of course, systems that will generate predominantly linear products from acetylene, and there has been evidence for these in this project. What remains the biggest challenge, however, is controlling this chain growth and rendering a system truly catalytic.

The choice of catalyst is always a difficult one, with so many combinations devised and discussed in the literature, and the use of ethylene polymerisation catalysts seemed a fair bet at the outset. However the lacklustre results for the majority of trialled catalysts only goes to show just how important the right choice of ligand and metal are in developing an active system, and just how different the truth can be from what is envisaged *a priori*. There is certainly potential for this chemistry, and it would seem to depend on finding the right combination of chain growth activity, coupled with a mechanism for chain transfer at the appropriate stage. The use of

dihydrogen in this context would be ideal, given its production in the methane pyrolysis process, however it was unfortunately not found to be effective in the trials carried out in this project. While some chain transfer with dihydrogen was observed with triethylaluminium – the system less active for growth – it came at the cost of reduced catalyst activity, and the highly active 2,6-*i*Pr catalyst did not respond to the chain transfer agent at all.

In the context of fuel production, given the wealth of knowledge available regarding ethylene oligomerisation, a more sensible approach may indeed be the partial hydrogenation of acetylene to ethylene and further reaction of this monomer. The relative unreactivity of saturated chains could certainly remove some of the complications encountered for chain growth with acetylene, which can be attributed to the reactivity of C=C double bonds in the products; while the presence of a degree of chain branching is favourable in fuel, cyclic and aromatic structures are not.

Ultimately, while there may be an ideal system for GTL conversion via acetylene, it was not possible to uncover such a process during this research. However, there has been progress made in understanding the complex growth observed for triethylaluminium and the iron catalysts in the presence of acetylene, and the stage has certainly been set for further research in this area.

Chapter 8 Experimental

8.1 General Details

Unless noted otherwise, all manipulations were performed under an argon atmosphere using standard Schlenk techniques, or in a nitrogen glovebox. Solvents were purified by passage through an Innovative Technologies solvent purification system and, where appropriate, stored over a sodium mirror. Acetylene (99.0%) was purified by passage through a column of activated molecular sieves (3Å) and alumina. Ultra-high purity H_2 (99.999%) was used as supplied. $[Cp_2ScCl]_n$ and $[Cp_2YCl]_n$ were prepared via a general method.[66,67] $Cp^*_2YCl{\cdot}THF$ and $[Cp^*_2CeCl]_n$ were likewise prepared according to methods reported in the literature.[68] The complex 2,6-bis-[1-(2,6-diisopropylphenylimino)ethyl]pyridineiron(II) chloride was prepared according to the literature.[133] The ligand 2,6-bis-[1-(2,6-diisopropylphenylimino)ethyl]pyridine, the cobalt and manganese complexes of this, the *ortho*-tolyl analogue of the iron complex, the bis(imino)pyridinechromium(III) complex and the bis(benzimidazole)pyridinechromium(III) complex were sourced from glove boxes at Imperial College London. The NHC-chromium complex was donated by Dr Dave McGuinness, and the iron(I) amidinate complex was donated by Professor Cameron Jones. The ligand glyoxal-bis(2,6-dimethylphenylimine) was prepared according to the literature,[74] as was the dibromonickel(II) complex of this.[72] Acetylene-d_2 was prepared by reaction of CaC_2 with degassed D_2O under argon, dried by passage through activated molecular sieves (3Å) and collected in a pre-dried ballast vessel. All other reagents were purchased from commercial sources and used as received. ^1H and ^{13}C NMR spectra were recorded on a Varian Mercury Plus NMR spectrometer

operating at 300 MHz and 75 MHz respectively, while solid-state ^{13}C NMR at 75 MHz were recorded by CSIRO at Clayton South, Melbourne. Microanalysis, GC-MS, MS, IR, ICPMS and SEM were performed at the Central Science Laboratory at the University of Tasmania. IR spectra were recorded on a Bruker Vertex 70 unit with a ZnSe Single Reflection ATR crystal, with an Extended ATR correction applied. Microanalysis was performed by Dr Thomas Rodemann using a ThermoFinnigan FlashEA 1112 Series Elemental Analyser. GC-MS and MS were performed by A/Prof. Noel Davies as described below. SEM was performed by Dr Karsten Gömann using an FEI Quanto 600 scanning electron microscope with an EDAX Sapphier ultra-thin window energy dispersive x-ray spectrometer. ICPMS was performed by Dr Ashley Townsend using an ELEMENT High-Resolution ICP-MS operation at medium resolution mode (3000 $m/\Delta m$).

8.2 GC-FID, GC-MS and MS Analysis

Oligomer quantification was carried out by GC-FID on an HP 5890 chromatograph fitted with an HP1 column (25 m × 0.32 mm internal diameter and 0.52 μm film). The carrier gas was nitrogen with a flow rate of 3.0 mL per min. The column oven was held at 40 ºC for 4 min then ramped to 300 °C at 20 °C per min. Identification of the oligomers, both before and after hydrogenation, was carried out by GC-MS. Analyses were carried out on a Varian 3800 GC coupled to Varian 1200 triple quadrupole mass spectrometer in single quadrupole mode. The column was a Varian 'Factor Four' VF-5 ms (30 m x 0.25 mm internal diameter and 0.25 micron film). Injections of 1 microlitre of diluted samples were made using a Varian CP-8400 autosampler and a Varian 1177 split/splitless injector at 240 °C with a split ratio of 25:1. The ion source was at 220 ºC, and the transfer line at 290 ºC. The carrier gas

was helium at 1.2 mL minute using constant flow mode. For separation of C_4 and C_6 components the column oven was held at –30 ºC for 2 minutes then ramped to 250 ºC at 15 °C per min. For all other separations the column oven was held at 50 ºC for 2 minutes then ramped to 290 ºC at 8 °C per minute. The range from *m/z* 35 to 450 was scanned 4 times per second. Oligomers were identified by their characteristic electron ionisation spectra, supported by Kovats' retention indices relative to published data. 3-ethyloctane, 4-ethyloctane, 3-methylnonane, 3-ethylheptane, cyclooctatetraene and ethylcyclooctane were further identified by comparison of GC retention times and mass spectra with authentic samples. High resolution MS chromatograms were recorded on a Kratos Concept High-Resolution Mass Spectrometer with a GC inlet, or using a Finnigan LCQ with directly coupled HPLC.

8.3 Collection and Treatment of X-ray Crystallographic Data

Data were collected at 100(2) K for crystals of Glyoxal-bis(2,6-dimethylphenylimino)palladium(II) chloride, $Al_4Et_4(OPh)_8$ and $Al_2Et_2(C_4H_7)(OC_6H_3Ph_2)_3$ mounted on Hampton Scientific cryoloops at the MX1 or MX2 beamlines of the Australian Synchrotron (λ = ca. 0.65-0.77 Å, varied with experiment, details in cif). Data reduction used BluIce[134] software. The structures were solved by direct methods with SHELXS-97, refined using full-matrix least squares routines against F^2 with SHELXL-97,[135] and visualised using X-SEED.[136] Details of the refinements appear in the cif files, but standard procedure was all non-hydrogen atoms being refined anisotropically and hydrogen atoms were placed in calculated positions and refined using a riding model with fixed C-H distances of 0.95 Å (sp^2C-H) and 0.98 Å (CH_3), and $U_{iso}(H) = 1.2U_{eq}(C)$ (sp^2) and

1.5U_{eq}(C) (sp^3). A summary of crystallographic data of the structures are given with the experimental data for each compound, and the full CIF data files are contained on the accompanying CD-ROM. All data collection and refinement was performed by Dr Michael Gardiner (and helpers) from the University of Tasmania.

8.4 Theoretical Considerations

All calculations were performed using Gaussian03[93] or Gaussian09 software,[94] utilising hardware from the Australian Partnership for Advanced Computing Program (APAC), or National Computational Infrastructure. The B3LYP[95-98] functional was used in all cases, with a $C_6 \cdot R^{-6}$ dispersion correction added to give B3LYP-D.[104] The 6-31G(d) basis set[99,100] was used for geometry optimisations, and 6-311+G(2d,p)[101,102] for single point energies. All XYZ coordinates for modelled structures can be found on the accompanying CD-ROM.

8.5 Preparation of Glyoxal-bis(2,6-dimethylphenylimino)palladium(II) chloride

This preparation was based on those of analogous compounds described by Brookhart.[72] Bis(benzonitrile)palladium(II) chloride (314 mg, 0.82 mmol) was added to a Schlenk under argon along with 20 mL of dry DCM, forming a dark red/brown solution. Glyoxal-bis(2,6-dimethylphenylimine) (219 mg, ~1.01 eq.) was added to the flask under a stream of argon. The solution quickly changed to a lighter orange/brown colour, and was stirred overnight. This was then cannula filtered, leaving a small amount of solid. The murky filtrate was left to settle, then filtered again, leaving a clear solution and orange solid. A second small crop was obtained by the addition of 10 mL dry petrol to the solution with cooling. Yield 123 mg, 34%.

Crystals suitable for x-ray diffraction were obtained by slow evaporation from a CH_3NO_2 solution.

^{1}H NMR in DMSO-d$_6$: δ 8.29 (s, 2H, N=C<u>H</u>), 7.13 (m, 6H, Ar-<u>H</u>), 2.32 (s, 12H, Ar-C<u>H</u>$_3$)

^{13}C NMR in DMSO-d$_6$: δ 173.45 (N=<u>C</u>H), 164.32 (*ipso*-Ar), 146.30 (*o*-Ar), 130.50 (*p*-Ar), 128.21 (*m*-Ar), 18.69 (Ar-<u>C</u>H$_3$)

EA: Calculated for $C_{18}H_{20}N_2PdCl_2$: C 48.95%, H 4.56%, N 6.34%. Found: C 48.75%, H 4.53%, N 6.31%

MS: Calculated isotope distribution for $C_{18}H_{20}N_2PdCl_2+H^+$: 439 23.55%, 440 50.01%, 441 79.98%, 442 44.83%, 443 100%, 444 24.71%, 445 67.78%, 446 13.70%, 447 22.55%. Found for $C_{18}H_{20}N_2PdCl_2+Na^+$: 461 24.6%, 462 50.9%, 463 75%, 464, 44.3%, 465 100%, 466 23.7%, 467 65.6%, 468 14.5%, 469, 25.1%.

Crystal Data*:* $C_{39}H_{49}Cl_4N_7O_6Pd_2$, M = 1066.45, prism orange, 0.02 × 0.01 × 0.01 mm^3, monoclinic, space group *Cc* (No. 9), a = 23.305(4), b = 10.662(3), c = 18.889(3) Å, β = 93.578(4)°, V = 4684.4(16) Å^3, Z = 4, D_c = 1.512 g/cm^3, F_{000} = 2160, 3-ID1 Australian Synchrotron, Synchrotron radiation, λ = 0.65253 Å, T = 100(2)K, $2\theta_{max}$ = 54.0º, 21717 reflections collected, 10495 unique (R_{int} = 0.0361). Final *GooF* = 1.065, *R1* = 0.0421, *wR2* = 0.1025, R indices based on 10234 reflections with I >2sigma(I) (refinement on F^2), 534 parameters, 2 restraints. Lp and absorption corrections applied, μ = 1.045 mm^{-1}. Absolute structure parameter = 0.11(3).[137]

8.6 Preparation of $AlEt_2(C_4H_7)$

To a Schlenk flask under argon was added 20 mL of a 1.9M solution of $AlEt_3$ in toluene. The solution was heated in an oil bath around 50 ºC with stirring, then the flask exposed to 1 barg of acetylene and flushed 4-5 times. Stirring continued for 1 hour, then the acetylene was purged with argon and the flask left to cool. GC analysis of a quenched sample at this stage showed the solution to contain primarily ethane and 1-butene, and no higher oligomers. The solvent was removed under vacuum over around 6 hours, reducing the volume by ~40% and yielding a yellow liquid. The liquid is viscous and very pyrophoric. NMR showed the yield to be quantitative. ^{1}H and ^{13}C NMR signals were assigned with the aid of HSQC.

^{1}H NMR in C_6D_6: δ 7.45 (m, 1H, Al-CH=C<u>H</u>-Et), 5.54 (d, 1H, Al-C<u>H</u>=CH-Et), 2.15 (m, 2H, Al-CH=CH-C<u>H</u>$_2$-CH$_3$), 1.17 (t, 6H, Al-CH$_2$-C<u>H</u>$_3$), 0.84 (t, 3H, Al-CH=CH-CH$_2$-C<u>H</u>$_3$), 0.16 (q, 4H, Al-C<u>H</u>$_2$-CH$_3$)

^{13}C NMR in C_6D_6: δ 187.70 (Al-CH=<u>C</u>H-Et), 122.86 (Al-<u>C</u>H=CH-Et), 32.48 (Al-CH=CH-<u>C</u>H$_2$-CH$_3$), 12.35 (Al-CH=CH-CH$_2$-<u>C</u>H$_3$), 8.96 (Al-CH$_2$-<u>C</u>H$_3$), 1.92 (Al-<u>C</u>H$_2$-CH$_3$)

8.7 Preparation of $Al_4Et_4(OPh)_8$

To a Schlenk flask under argon was added 840 mg (6 mmol) of $AlEt_2(C_4H_7)$. In a separate Schlenk, 1.131g of phenol (12 mmol, 2 eq.) was dissolved in 3 mL of dry toluene. The aluminium containing flask was cooled to -10 ºC in an ice bath, then the phenol solution added dropwise over 40 minutes, stirring slowly; this addition was noticeably very reactive for the first 1 mL of solution used. The solution was warmed

to room temperature while gently stirring, then placed in the freezer at -20 ºC overnight. This yielded a white crystalline solid, which was suitable for the acquisition of an x-ray crystal structure. GC analysis of an acid-quenched sample showed an ethane:butene ratio of around 30:1. ^{1}H NMR showed a mixture of compounds to be present.

Crystal Data: $C_{56}H_{60}Al_4O_8$, M = 968.96, colourless prism, 0.08 × 0.08 × 0.05 mm^3, monoclinic, space group $P2_1/n$ (No. 14), a = 12.819(3), b = 15.4020(9), c = 13.3430(9) Å, β = 92.923(2)°, V = 2631.0(6) Å^3, Z = 2, D_c = 1.223 g/cm^3, F_{000} = 1024, 3-BM1 Australian Synchrotron, Synchrotron radiation, λ = 0.77500 Å, T = 100(2)K, $2\theta_{max}$ = 48.5º, 27961 reflections collected, 4077 unique (R_{int} = 0.0937). Final *GooF* = 1.049, *R1* = 0.0698, *wR2* = 0.1869, *R* indices based on 3502 reflections with I >2sigma(I) (refinement on F^2), 356 parameters, 0 restraints. Lp and absorption corrections applied, μ = 0.141 mm^{-1}.

8.8 Preparation of $Al_2Et_2(C_4H_7)(OC_6H_3Ph_2)_3$

To a Schlenk flask under argon was added 431 mg (3 mmol) of $AlEt_2(C_4H_7)$. In a separate Schlenk, 2,6-diphenylphenol (765 mg, 1.01 eq.) was dissolved in 4 mL of dry toluene. The aluminium containing flask was submerged in an ice bath at -12 ºC, and the alcohol added dropwise over 15 minutes with stirring. The yellow solution was warmed to room temperature then placed in the freezer at -20 ºC. This failed to precipitate any solid product, so the solution was concentrated under vacuum to an oily consistency and replaced in the freezer. White crystals now slowly formed, which were suitable for x-ray diffraction. A GC quench of the solid showed an ethane:butene ratio of around 3:1. The apparent disproportionation that occurs in this

reaction (see Section 3.3.2) meant that clean NMR and microanalysis could not be obtained for this product, as it evidently contains a mixture of compounds.

Crystal Data: $C_{62}H_{56}Al_2O_3$, M = 903.03, colourless prism, 0.06 × 0.03 × 0.03 mm^3, triclinic, space group P-1 (No. 2), a = 9.961(3), b = 11.907(3), c = 20.919(5) Å, α = 78.717(3), β = 88.993(11), γ = 81.797(16)°, V = 2408.1(12) Å^3, Z = 2, D_c = 1.245 g/cm^3, F_{000} = 956, 3-BM1 Australian Synchrotron, Synchrotron radiation, λ = 0.77500 Å, T = 100(2)K, $2\theta_{max}$ = 52.9º, 26394 reflections collected, 6908 unique (R_{int} = 0.0910). Final *GooF* = 1.032, *R1* = 0.0674, *wR2* = 0.1723, *R* indices based on 5509 reflections with I >2sigma(I) (refinement on F^2), 656 parameters, 0 restraints. Lp and absorption corrections applied, μ = 0.108 mm^{-1}.

8.9 Oligomerisation and Polymerisation Trials

In a typical run, an oven dried glass reaction vessel was attached to a Lab-Crest reactor head, and purged for 30 minutes with argon. The solvent and other reagents were added under a flow of argon, either individually or after mixing in a Schlenk flask, and the solution heated to the desired internal temperature using an oil bath. Once at temperature, the solution was exposed to acetylene (1 bar gauge), and flushed several times to purge the remaining argon. The solution was stirred for the desired time with the acetylene supply open. Following this, acetylene flow was stopped and the solution cooled with an ice bath to around 5 °C, then excess gas pressure released. An *n*-alkane standard (*n*-nonane or *n*-heptane) was weighed and injected into the reactor. The solution was then carefully quenched with 10% HCl, keeping the solution cool to avoid loss of low molecular weight compounds. A large excess of acid was necessary to dissolve all metals (aluminium, zinc, catalyst

complexes) present in the organic phase. A sample of the organic phase was filtered through Celite and Na_2CO_3 and analysed by GC-FID and GC-MS as described above. The bulk solution was vacuum filtered through a glass frit; any solid residue was collected, dried and weighed. Particularly fine polymer was separated from the solution by centrifuging the solution for 15 minutes.

Some of these oligomerisation and polymerisation reactions were also performed in Schott-top Schlenk flasks when other investigations were necessary (eg NMR experiments, further reactions of AlR_n, preparation of polymers), so that the reaction could be manipulated under inert conditions. Experiments using a mixture of gases at pressures above 4 bar gauge, for example acetylene (2 bars) and hydrogen (9.5 bars), were performed in a Parr reactor.

8.10 Hydrogenation of Oligomer Samples

The sample for hydrogenation was added to a glass autoclave flask, along with a stirrer bar and the catalyst (ca. 100 mg of 5% Pd/C or ca. 10 mg of PtO_2). The solution was degassed with argon for several minutes and the flask placed inside the autoclave which had been flushed with argon. Upon sealing, the autoclave was purged with H_2 then filled to a pressure of 10 bar. The reactor was heated in a sand or oil bath at 80 °C and the mixture stirred for 24 hours. The H_2 cylinder was then detached and the mixture allowed to cool; any remaining pressure was then released. A sample could be taken for GC using a needle and filtered through Celite, with a positive argon pressure flowing through the autoclave. If further reaction was needed the process could be resumed, otherwise the solution was removed and filtered for storage. Where only a small amount of sample was available, the procedure was performed in a Schlenk flask. In this case, the reaction flask was

purged with hydrogen, then stirred for 48 hours under 1 bar gauge of hydrogen without heating. The use of an H-Cube hydrogenation apparatus was also trialled for an $AlEt_3$/acetylene oligomer sample, using 80 bar of online-generated H_2 at 80 °C, for an oligomer sample diluted to 1:10, at a 1 mL/min flow rate.

8.11 Oxygen Quench

Following acetylene oligomerisation with triethylaluminium as described above, but prior to quenching, a mixture of dry N_2/O_2 (5% O_2) was bubbled through the rapidly stirred solution with cooling in an ice bath. After approximately 40 L of the mixed gas had been bubbled through over 30 minutes, the solution had turned into a viscous oil. An equal volume of dry toluene was added to reduce the viscosity, and the gas was switched to pure oxygen for a further ca. 30 min. Following this, the solution was quenched with 10% HCl and both the organic phase and the aqueous phase were analysed for ethanol.

8.12 Isolation and Characterization of Higher Oligomers (C_{10}+)

The reaction solution from a 2 hr oligomerisation run with $AlEt_3$ was washed twice with water and dried over $MgSO_4$. After filtration, the volatiles were removed under vacuum to leave a yellow liquid. The chromatogram of this fraction is showed prominent peaks for C_{10}, C_{14} and C_{18} oligomers. The NMR data reported in the text are of this oligomer mixture in C_6D_6. The presence of terminal alkyne functionality in this product was confirmed by reaction with Tollens' reagent (ammoniacal silver nitrate), which produced a fine precipitate. Further confirmation came from reaction of the higher oligomers with dilute CuCl in aqueous ammonia, which slowly produced a red-brown precipitate, indicative of the formation of copper acetylide

complexes.

8.13 Preparation of Polyacetylene Samples for IR and SEM Analysis

Two polymer samples were prepared under inert conditions in Schlenk flasks, using the 2,6-*i*Pr catalyst with and without diethylzinc, and following the general procedure in Section 8.9. After reaction with acetylene, the flasks were put under argon and the reaction solutions cannula filtered into clean Schlenks, then these solutions exposed to acetylene a second time. This process repeated until no further polymer formed. The filtered polymer samples were dried under vacuum overnight, and the fractions combined to give final yield. These samples were used as-is for IR analysis, and were sputter-coated with gold for SEM analysis.

Characteristic IR: 3011, 1795, 1327, 1011, 735 cm^{-1}

8.14 Preparation of Polyacetylene Samples for ICP-MS Analysis

Two polymer samples were prepared in pre-weighed Schlenk flasks as described in Section 8.13, except the diethylzinc containing solution was exposed to acetylene only once. The lids, taps and stirrer bars were carefully removed from the flasks without loss of polymer, and the flasks placed in a furnace oven along with 2 empty flasks. A furnace program was run accordingly: ramped at 300 ºC/hour to 500 ºC, held for 2 hours, cooled to room temperature. After this, both polymers had decomposed: the zinc polymer less so, with the flask still holding some dark coloured solid; the other flask held a white solid believed to be Al_2O_3. To each flask (blanks included) was added 1 mL of concentrated HNO_3 and 2 mL of concentrated HCl. These were stirred at 100 ºC for 2 hours to digest the residues as best as possible, the left to cool. Milli-Q water was added to each flask so the total content

of each flask was 25 g. The samples were diluted 1:100 before ICP-MS analysis, with an additional filtration step added to remove some dark precipitate from the zinc-containing flask. The final iron concentrations were compared to the maximum possible concentration given the quantity of catalyst added (13.2 ppm), subtracting the blank background. The zinc-containing solution held 5.8 ppm iron, the zinc-free 12.1 ppm.

8.15 Copolymerisation of Ethylene/Acetylene

Following the general procedure in Section 8.9, these were prepared using acetylene/ethylene gas mixtures from a separate ballast vessel to feed the reactor. Polymers were placed on top of the oven and dried to constant weight.

NMR in $C_7D_8/C_6H_3Cl_3$: δ 1.32 (broad *s*, -C<u>H</u>$_2$-), 0.89 (broad *t*, -C<u>H</u>$_3$)

IR: 2915, 2848, 1473, 1462, 731, 717 cm^{-1}

8.16 Bromination of Oligomers

To a glass tube was added 1.5 mL of an ethylene/acetylene co-oligomer solution in toluene. A 10 wt% (approx) solution of bromine in DCM was added with stirring, and the dark colour seen to disappear over 1-2 mins. The addition of bromine with stirring was continued until the brown colour ceased to fade quickly. The solution was left in the fumehood to evaporate excess bromine and DCM, then filtered through Na_2CO_3 and Celite. The pale brown solution was submitted for GC-MS analysis.

8.17 Copolymerisation of Acetylene/Arene

Following the general procedure in Section 8.9, the runs to produce large amounts of

polymer were performed using 50 mL the appropriate solvent (benzene or toluene) and 15 mmol of aluminium reagent ($AlEtCl_2$ or $AlCl_3$). Upon exposure to acetylene, a rapid colour change of yellow, through orange and dark red to almost black was observed. After 15 mins, 10% HCl was added to the reactor and the slurry stirred for 10-20 minutes until the majority of the dark colour had vanished, to be replaced by a yellow solid. The mixture was filtered and the extremely hydrophobic solid put into a beaker, with 100 mL of 10% HCl in methylated spirits. This suspension was stirred for 90 minutes to remove the last of the dark colour. The solid was filtered and collected with Büchner apparatus, then dried under vacuum at 70 °C for 3 days to remove all moisture. Solid-state ^{13}C NMR of the polymers were recorded for the benzene and toluene samples.

^{13}C NMR: δ 143 (*ipso*-Ar), 126 (*o,m,p*-Ar), 41 (Ar-$\underline{C}H_n$-), 20 (-CH_n-$\underline{C}H_3$)

To investigate the lower, soluble oligomers formed in this process, 5 mmol of $AlEtCl_2$ was added to 17 mL of benzene or toluene in a Schlenk flask under argon. This was cooled in an ice bath, then exposed to acetylene for around 10 seconds: enough to effect a colour change to a dark orange over around 30 seconds of further stirring. The gas pressure was released and the solution quenched with 10% HCl. A sample was taken for GC, then the organic phase was separated and the solvent removed under vacuum to yield ~1 mL of a yellow oil. This was taken up in $CDCl_3$ and ^1H NMR recorded, showing a complex mixture of signals, which are discussed in text (Chapter 5).

Chapter 9 References

1. Stewart, L. *Oilfield Review* **2003**, *Autumn*, 32-37.

2. Hall, K. R.; Akgerman, A.; Anthony, R. G.; Eubank, P. T.; Bullin, J. A.; Cantrell, J. G.; Weber, B. R.; Betsill, J. *Appea J.* **2002**, 59-63.

3. Hall, K. R. *Catalysis Today* **2005**, *106*, 243-6.

4. Alkhawaldeh, A.; Wu, X.; Anthony, R. G. *Catal. Today* **2003**, *84*, 43-9.

5. Trimm, D.; Liu, I.; Cant, N. *Stud. Surf. Sci. Catal.* **2007**, *172*, 309-12.

6. Trimm, D. L.; Liu, I. O. Y.; Cant, N. W. *J. Molec. Catal. A* **2008**, *288*, 63-74.

7. Dibdin, W. J. *Public Lighting by Gas and Electricity*; Sanitary Pub. Co.: London, 1902.

8. Groth, L. A. *Welding And Cutting Metals By Aid Of Gases Or Electricity*; D. Van Nostrand Company, 1909.

9. Kauffman, G. B.; Chooljian, S. H. *Chem. Educ.* **2001**, *6*, 121-33.

10. Myers, R. L. *The 100 most important chemical compounds: a reference guide*; Greenwood Press: Westport, 2007.

11. Pässler, P.; Hefner, W.; Buckl, K.; Meinass, H.; Meiswinkel, A.; Wernicke, H.-J.; Ebersberg, G.; Müller, R.; Bässler, J.; Behringer, H.; Mayer, D. In *Ullmann's Encyclopedia of Industrial Chemistry*; Wiley VCH: Weinheim, 2008.

12. Tedeschi, R. J. *Acetylene-based chemicals from coal and other natural resources*; Marcel Dekker Inc.: New York, 1982.

13. Chauser, M. G.; Rodionov, Y. M.; Misin, V. M.; Cherkashin, M. I. *Russ. Chem. Rev.* **1976**, *45*, 348-74.

14. Nieuwland, J. A.; Calcott, W. S.; Downing, F. B.; Carter, A. S. *J. Am. Chem. Soc.* **1931**, *53*, 4197-202.

15. Carothers, W. H.; Williams, I.; Collins, A. M.; Kirby, J. E. *J. Am. Chem. Soc.* **1931**, *53*, 4203-25.

16. Weissermel, K.; Arpe, H.-J. *Industrial Organic Chemistry*; 3 ed.; Wiley VCH: Weinheim, 1997.

17. Reppe, W.; Schlichting, O.; Klager, K.; Toepel, T. *Liebigs Ann. Chem.* **1948**, *560*, 1-92.

18. Reppe, W.; Sweckendiek, W. J. *Liebigs Ann. Chem.* **1948**, *560*, 104-16.

19. Winter, M. J. In *The chemistry of the metal-carbon bond*; Hartley, F. R., Patai, S., Eds.; Wiley & Sons: Chichester, 1985; Vol. 3, p 259-94.

20. Natta, G.; Mazzanti, G.; Corradini, P. *Atti accad. nazl. Lincei Rend. Classe sci. fis. mat. e nat.* **1958**, *25*, 3-12.

21. Ito, T.; Shirakawa, H.; Ikeda, S. *J. Polym. Sci., Polym. Chem. Ed.* **1974**, *12*, 11-20.

22. Stang, P. J.; Diederich, F. *Modern Acetylene Chemistry*; Weinheim; VCH: New York, 1995.

23. Shirakawa, H.; Louis, E. J.; MacDiarmid, A. G.; Chiang, C. K.; Heeger, A. J. *J. Chem. Soc., Chem. Commun.* **1977**, 578-80.

24. Shirakawa, H. *Angew. Chem., Int. Ed.* **2001**, *40*, 2575-80.

25. Matnishyan, A. A.; Kobryanskii, V. M. *Russ. Chem. Rev.* **1983**, *52*, 751-6.

26. Katz, T. J.; Lee, S. J. *J. Am. Chem. Soc.* **1980**, *102*, 422-4.

27. Takagi, Y.; Saeki, N.; Tsubouchi, A.; Murakami, H.; Kumagai, Y.; Takeda, T. *J. Polym. Sci., Part A: Polym. Chem.* **2002**, *40*, 2663-9.

28. Ohff, A.; Burlakov, V. V.; Rosenthal, U. *J. Mol. Catal. A* **1996**, *108*, 119-23.

29. Schlund, R.; Schrock, R. R.; Crowe, W. E. *J. Am. Chem. Soc.* **1989**, *111*, 8004-6.

30. Keim, W.; Behr, A.; Röper, M. In *Comprehensive Organometallic Chemistry: the synthesis, reactions, and structures of organometallic compounds*; Wilkinson, G., Ed.; Pergamon: New York, 1982; Vol. 8, p 371-454.

31. Meriwether, L. S.; Colthup, E. C.; Kennerly, G. W.; Reusch, R. N. *J. Org. Chem.* **1961**, *26*, 5155-63.

32. Meriwether, L. S.; Leto, M. F.; Colthup, E. C.; Kennerly, G. W. *J. Org. Chem.* **1962**, *27*, 3930-41.

33. Vollhardt, K. P. C. *Acc. Chem. Res.* **1977**, *10*, 1-8.

34. Famili, A.; Farona, M. F. *Poly. Bull.* **1980**, *2*, 289-91.

35. Thanedar, S.; Farona, M. F. *Poly. Bull.* **1982**, *8*, 429-35.

36. Farona, M. F.; Thanedar, S.; Famili, A. *J. Polym. Sci. A., Polym. Chem.* **1986**, *24*, 3529-40.

37. Orian, L.; Van Stralen, J. N. P.; Bickelhaupt, F. M. *Organometallics* **2007**, *26*, 3816-30.

38. Dachs, A.; Osuna, S.; Roglans, A.; Sola, M. *Organometallics* **2010**, *29*, 562-9.

39. Koga, T.; Otsuka, H.; Takahara, A. *Bull. Chem. Soc. Jpn.* **2005**, *78*, 1691-8.

40. Kirchner, K.; Calhorda, M. J.; Schmid, R.; Veiros, L. F. *J. Am. Chem. Soc.* **2003**, *125*, 11721-9.

41. Masuda, T.; Deng, Y. X.; Higashimura, T. *Bull. Chem. Soc. Jpn.* **1983**, *56*, 2798-801.

42. Masuda, T.; Mouri, T.; Higashimura, T. *Bull. Chem. Soc. Jpn.* **1980**, *53*, 1152-5.

43. Yur'eva, L. P. *Russ. Chem. Rev.* **1974**, *43*, 48-68.

44. Cossee, P. *J. Catal.* **1964**, *3*, 80-8.

45. Daniels, W. E. *J. Org. Chem.* **1964**, *29*, 2936-8.

46. Clarke, T. C.; Yannoni, C. S.; Katz, T. J. *J. Am. Chem. Soc.* **1983**, *105*, 7787-9.

47. Straub, T.; Haskel, A.; Eisen, M. S. *J. Am. Chem. Soc.* **1995**, *117*, 6364-5.

48. Haskel, A.; Straub, T.; Dash, A. K.; Eisen, M. S. *J. Am. Chem. Soc.* **1999**, *121*, 3014-24.

49. Haskel, A.; Wang, J. Q.; Straub, T.; Neyroud, T. G.; Eisen, M. S. *J. Am. Chem. Soc.* **1999**, *121*, 3025-34.

50. Wang, J. Q.; Eisen, M. S. *J. Organomet. Chem* **2003**, *670*, 97-107.

51. Heeres, H. J.; Teuben, J. H. *Organometallics* **1991**, *10*, 1980-6.

52. Duchateau, R.; van Wee, C. T.; Meetsma, A.; Teuben, J. H. *J. Am. Chem. Soc.* **1993**, *115*, 4931-2.

53. St. Clair, M.; Schaefer, W. P.; Bercaw, J. E. *Organometallics* **1991**, *10*, 525-7.

54. Thompson, M. E.; Baxter, S. M.; Bulls, A. R.; Burger, B. J.; Nolan, M. C.; Santarsiero, B. D.; Schaefer, W. P.; Bercaw, J. E. *J. Am. Chem. Soc.* **1987**, *109*, 203-19.

55. Tsonis, C. P. *React. Kinet. Catal.Lett.* **1992**, *46*, 359-64.

56. Masuda, T.; Hasegawa, K.; Higashimura, T. *Macromolecules* **1974**, *7*, 728-31.

57. Masuda, T.; Thieu, K.-Q.; Sasaki, N.; Higashimura, T. *Macromolecules* **1976**, *9*, 661-4.

58. Yokokawa, K.; Azuma, K. *Bull. Chem. Soc. Jpn.* **1965**, *38*, 859-60.

59. Tsumura, R.; Hagihara, N. *Bull. Chem. Soc. Jpn.* **1964**, *37*, 1889-90.

60. Böhm, L. L. *Angew. Chem. Int. Ed.* **2003**, *42*, 5010-30.

61. Kaminsky, W. *J. Chem. Soc., Dalton Trans.* **1998**, 1413-8.

62. Chen, E. Y.-X.; Marks, T. J. *Chem. Rev.* **2000**, *100*, 1391-434.

63. Britovsek, G. J. P.; Gibson, V. C.; Wass, D. F. *Angew. Chem. Int. Ed.* **1999**, *38*, 428-47.

64. Gibson, V. C.; Spitzmesser, S. K. *Chem. Rev.* **2003**, *103*, 283-315.

65. Karpiniec, S. S.; McGuinness, D. S.; Patel, J.; Davies, N. W. *Organometallics* **2009**, *28*, 5722-32.

66. Maginn, R. E.; Manastyrskyj, S.; Dubeck, M. *J. Am. Chem. Soc.* **1963**, *85*, 672-6.

67. Evans, W. J.; Meadows, J. H.; Wayda, A. L.; Hunter, W. E.; Atwood, J. L. *J. Am. Chem. Soc.* **1982**, *104*, 2008-14.

68. Herrmann, W. A. *Synthetic Methods of Organometallic and Inorganic Chemistry*; Georg Thieme Verlag: New York, 1997; Vol. 6.

69. den Haan, K. H.; de Boer, J. L.; Teuben, J. H. *Organometallics* **1986**, *5*, 1726-33.

70. Heeres, H. J.; Renkema, J.; Booij, M.; Meetsma, A.; Teuben, J. H. *Organometallics* **1988**, *7*, 2495-502.

71. Alt, H. G.; Engelhardt, H. E.; Rausch, M. D.; Kool, L. B. *J. Organomet. Chem.* **1987**, *329*, 61-7.

72. Johnson, L. K.; Killian, C. M.; Brookhart, M. *J. Am. Chem. Soc.* **1995**, *117*, 6414-5.

73. Svoboda, M.; Tom Dieck, H. *J. Organomet. Chem* **1980**, *191*, 321-8.

74. Tom Dieck, H.; Svoboda, M.; Greiser, T. *Zeitschrift fuer Naturforschung, Teil B: Anorganische Chemie, Organische Chemie* **1981**, *36B*, 823-32.

75. Comerlato, N. M.; Crossetti, G. L.; Howie, R. A.; Tibultino, P. C. D.; Wardell, J. L. *Acta. Cryst.* **2001**, *E57*, m295-7.

76. Tomov, A. K.; Chirinos, J. J.; Jones, D. J.; Long, R. J.; Gibson, V. C. *J. Am. Chem. Soc.* **2005**, *127*, 10166-7.

77. McGuinness, D. S.; Gibson, V. C.; Wass, D. F.; Steed, J. W. *J. Am. Chem. Soc.* **2003**, *125*, 12716-7.

78. Esteruelas, M. A.; López, A. M.; Méndez, L.; Oliván, M.; Oñate, E. *Organometallics* **2003**, *22*, 395-406.

79. Wilke, G.; Muller, H. *Liebigs Ann. Chem.* **1960**, *629*, 222-40.

80. Ziegler, K. *Angew. Chem.* **1952**, *64*, 323-350.

81. Karpiniec, S.; McGuinness, D.; Patel, J.; Davies, N. *Chem. Eur. J.* **2009**, *15*, 1082-5.

82. Rylander, P. N. *Catalytic Hydrogenation in Organic Synthesis*; Academic Press: New York, 1979.

83. Laubengayer, A. W.; Gilliam, W. F. *J. Am. Chem. Soc.* **1941**, *63*, 477-9.

84. Malone, J. F.; McDonald, W. S. *Dalton Trans.* **1972**, 2649-52.

85. Takeda, S.; Tarao, R. *Bull. Chem. Soc. Jpn.* **1965**, *38*, 1567-75.

86. Davidson, N.; Brown, H. C. *J. Am. Chem. Soc.* **1942**, *64*, 316-24.

87. Gardiner, M. G.; Raston, C. L.; Skelton, B. W.; White, A. H. *Inorg. Chem.* **1997**, *36*, 2795-803.

88. Budzelaar, P. H. M., Talarico, G. *Insertion and β-hydrogen transfer at aluminium*; Springer-Verlag: Berlin, 2003; Vol. 105.

89. Heeres, H. J.; Heeres, A.; Teuben, J. H. *Organometallics* **1990**, *9*, 1508-10.

90. Negishi, E.-i.; Kondakov, D. Y.; Choueiry, D.; Kasai, K.; Takahashi, T. *J. Am. Chem. Soc.* **1996**, *118*, 9577-88.

91. Thomas, D.; Peulecke, N.; Burlakov, V. V.; Heller, B.; Baumann, W.; Spannenberg, A.; Kempe, R.; Rosenthal, U.; Beckhaus, R. *Z. Anorg. Allg. Chem.* **1998**, *624*, 919-24.

92. Stucky, G. D.; McPherson, A. M.; Rhine, W. E.; Eisch, J. J.; Considine, J. L. *J. Am. Chem. Soc.* **1974**, *1974*, 1941-2.

93. Frisch, M. J.; Trucks, G. W.; Schlegel, H. B.; Scuseria, G. E.; Robb, M. A.; Cheeseman, J. R.; Montgomery, J., J. A.; Vreven, T.; Kudin, K. N.; Burant, J. C.et al; Revision E.01 ed.; Gaussian, Inc: Wallingford CT, 2004.

94. Frisch, M. J.; Trucks, G. W.; Schlegel, H. B.; Scuseria, G. E.; Robb, M. A.; Cheeseman, J. R.; Scalmani, G.; Barone, V.; Mennucci, B.; Petersson, G. A.et al; Revision A.02 ed.; Gaussian, Inc.: Wallingford CT, 2009.

95. Becke, A. D. *Phys. Rev. A.* **1988**, *38*, 3098-3100.

96. Becke, A. D. *J. Chem. Phys.* **1993**, *98*, 5648-5652.

97. Lee, C.; Yang, W.; Parr, R. G. *Phys. Rev. B.* **1988**, *37*, 785-789.

98. Stephens, P. J.; Devlin, F. J.; Chabalowski, C. F.; Frisch, M. J. *J. Phys. Chem.* **1994**, *98*, 11623-11627.

99. Hehre, W. J.; Ditchfield, R.; Pople, J. A. *J. Chem. Phys.* **1972**, *56*, 2257-61.

100. Francl, M. M.; Pietro, W. J.; Hehre, W. J.; Binkley, J. S.; Gordon, M. S.; DeFrees, D. J.; Pople, J. A. *J. Chem. Phys.* **1982**, *77*, 3654-65.

101. Krishnan, R.; Binkley, J. S.; Seeger, R.; Pople, J. A. *J. Chem. Phys.* **1980**, *72*, 650-4.

102. McLean, A. D.; Chandler, G. S. *J. Chem. Phys.* **1980**, *72*, 5639-48.

103. Shamov, G. A.; Budzelaar, P. H. M.; Schreckenbach, G. *J. Chem. Theory Comput.* **2010**, *6*, 477-90.

104. Grimme, S. *J. Comput. Chem.* **2006**, *27*, 1787-99.

105. Hay, J. N.; Hooper, P. G.; Robb, J. C. *Journal of Organometallic Chemistry* **1971**, *28*, 193-204.

106. Sakai, S. *Journal of Physical Chemistry* **1991**, *95*, 7089-7093.

107. Cook, O. W.; Chambers, V. J. *J. Am. Chem. Soc.* **1921**, *43*, 334-40.

108. Reichart, J. S.; Nieuwland, J. A. *J. Am. Chem. Soc.* **1923**, *45*.

109. Reilly, J. A.; Nieuwland, J. A. *J. Am. Chem. Soc.* **1928**, *50*.

110. Gal, J.-F.; Maria, P.-C.; Mó, O.; Yáñez, M.; Kuck, D. *Chem. Eur. J.* **2006**, *12*, 7676-83.

111. Yamaguchi, M.; Kido, Y.; Hayashi, A.; Hirama, M. *Angew. Chem. Int. Ed.* **1997**, *36*, 1313-5.

112. Britovsek, G. J. P.; Gibson, V. C.; Kimberley, B. S.; Maddox, P. J.; McTavish, S. J.; Solan, G. A.; White, A. J. P.; Williams, D. J. *Chem. Commun.* **1998**, 849-50.

113. Britovsek, G. J. P.; Bruce, M.; Gibson, V. C.; Kimberley, B. S.; Maddox, P. J.; Mastroianni, S.; McTavish, S. J.; Redshaw, C.; Solan, G. A.; Strömberg, S.; White, A. J. P.; Williams, D. J. *J. Am. Chem. Soc.* **1999**, *121*, 8728-40.

114. Britovsek, G. J. P.; Mastroianni, S.; Solan, G. A.; Baugh, S. P. D.; Redshaw, C.; Gibson, V. C.; White, A. J. P.; WIlliams, D. J.; Elsegood, M. R. J. *Chem. Eur. J.* **2000**, *6*, 2221-31.

115. Small, B. L.; Brookhart, M. *Macromolecules* **1999**, *32*, 2120-30.

116. Britovsek, G. J. P.; Cohen, S. A.; Gibson, V. C.; Maddox, P. J.; Van Meurs, M. *Angew. Chem. Int. Ed.* **2002**, *41*, 489-91.

117. Britovsek, G. J. P.; Cohen, S. A.; Gibson, V. C.; van Meurs, M. *J. Am. Chem. Soc.* **2004**, *126*, 10701-12.

118. Van Meurs, M.; Britovsek, G. J. P.; Gibson, V. C.; Cohen, S. A. *J. Am. Chem. Soc.* **2005**, *127*, 9913-23.

119. Britovsek, G. J. P., Personal Communication, 2008.

120. Rose, R. P.; Jones, C.; Schulten, C.; Aldridge, S.; Stasch, A. *Chem. Eur. J.* **2008**, *14*, 8477-80.

121. Bredael, P. *J. Hi. Res. Chromatogr. & Chromatogr. Comm.* **1982**, *5*, 325-8.

122. Pino, J. A.; Mesa, J.; Munoz, Y.; Marti, M. P.; Marbot, R. *J. Agric. Food Chem.* **2005**, *53*, 2213-23.

123. Venkateshwarlu, G.; Let, M. B.; Meyer, A. S.; Jacobsen, C. *J. Agric. Food Chem.* **2004**, *52*, 311-7.

124. Kvashina, E. F.; Petrova, G. N.; Belov, G. P.; Roshchupkina, O. S.; Efimov, O. N. *Russ. Chem. Bull., Intl. Ed.* **2002**, *51*, 817-9.

125. Batchelder, D. N. *Contemp. Phys.* **1988**, *29*, 3-31.

126. Townsend, A. T. *J. Anal. At. Spectrom.* **2000**, *15*, 307-14.

127. Molanty, A. K.; Misra, M.; Hinrichsen, G. *Macromol. Mater. Eng.* **2000**, *276/277*, 1-24.

128. Noskova, V. N.; Russiyan, L. N.; Matkovskii, P. Y. *Polimery* **1998**, *43*, 155-60.

129. Aleshin, A. N.; Guk, E. G.; Marikhin, V. A.; Myasnikova, L. P.; Belov, G. P.; Belov, D. G. *Poly. Sci. Ser. A.* **1995**, *37*, 1179-83.

130. Agapie, T.; Schofer, S. J.; Labinger, J. A.; Bercaw, J. E. *J. Am. Chem. Soc.* **2004**, *126*, 1304-5.

131. Hay, J. M.; Lyon, D. *Proc. Roy. Soc. Lon. A.* **1970**, *317*, 1-20.

132. Patterson, C. H.; Lambert, R. M. *J. Phys. Chem.* **1988**, *92*, 1266-70.

133. Small, B. L.; Brookhart, M.; Bennett, A. M. A. *J. Am. Chem. Soc.* **1998**, *120*, 4049-50.

134. McPhillips, T. M.; McPhillips, S. E.; Chiu, H. J.; Cohen, A. E.; Deacon, A. M.; Ellis, P. J.; Garman, E.; Gonzalez, A.; Sauter, N. K.; Phizackerley, R. P.; Soltis, S. M.; Kuhn, P. *J. Synchrotron Rad.* **2002**, *2002*, 401-6.

135. Sheldrick, G. M. *SHELX97 Programs for Crystal Structure Analysis*; Universität Göttingen, Germany, 1998.

136. Barbour, L. J. J. *J. Supramol. Chem.* **2001**, *1*, 189-91.

137. Flack, H. D. *Acta Cryst.* **1983**, *A39*, 876-81.